

# Analysis of the nuclear egress complex of mouse cytomegalovirus



Dissertation zur Erlangung des Doktorgrades der  
Naturwissenschaften  
der Fakultät für Biologie  
der Ludwig-Maximilians-Universität München

vorgelegt von  
**Mark Lötzerich**  
München, 2007

Dissertation eingereicht am: 28.03.2007

Erstgutachterin: PD Dr. Bettina Kempkes

Zweitgutachter: Prof. Dr. Heinrich Leonhardt

Sondergutachter: Prof. Dr. Ulrich H. Koszinowski

Tag der mündlichen Prüfung: 19.12.2007

## Table of contents

---

<b>A. Summary .....</b>	<b>1</b>
<b>B. Introduction.....</b>	<b>2</b>
1. The cytomegaloviruses as family members of the herpesviruses .....	2
1.1 Biology of CMV infection and host immune defense .....	3
1.2 Transmission and clinical relevance of human cytomegalovirus (HCMV) ....	4
1.3 Mouse cytomegalovirus (MCMV) as animal model for HCMV infection .....	5
2. Structure of cytomegaloviruses .....	5
3. Replication of cytomegaloviruses .....	7
4. The nuclear envelope.....	9
4.1 The lamin proteins.....	11
4.2 Proteins and protein complexes interacting with lamins .....	12
4.2.1 The lamin B receptor-complex (LBR or p58) .....	12
4.2.2 LEM-domain proteins and BAF complexes.....	14
5. The egress of herpesvirus capsids from the nucleus .....	15
5.1 The nuclear egress complex (NEC) .....	17
6. Aims and concepts.....	20
<b>C. Material and methods.....</b>	<b>22</b>
1. Material .....	22
1.1 Devices .....	22
1.2 Consumables .....	23
1.3 Reagents.....	23
1.4 Commercial kits.....	25
1.5 Oligonucleotide-peptides.....	26
1.6 Plasmids.....	26
1.6.1 Commercially available and published plasmids .....	26
1.6.2 Plasmids constructed over the project .....	27
1.6.2.1 M53/p38 expression plasmids.....	27
1.6.2.2 pOriR6k-zeo-ie derived plasmids .....	27

## Table of contents

---

1.6.2.3 Plasmid with temperature sensitive origin of replication ( $T_s$ ) .....	29
1.6.2.4 MCMV-BACs.....	29
1.7 Bacterial strains.....	31
1.8 Cells .....	31
1.8.1 Cell culture reagents.....	31
1.8.1.1 Basal media .....	31
1.8.1.2 Supplements and sera .....	31
1.9 Viruses .....	32
1.10 Antibodies .....	32
1.10.1 Primary antibodies .....	32
1.10.1.1 Rabbit polyclonal antisera .....	32
1.10.1.2 Rabbit monoclonal antibodies .....	32
1.10.1.3 Mouse monoclonal antibodies.....	32
1.10.1.4 Rat polyclonal antisera.....	32
1.10.1.5 Goat polyclonal antisera.....	33
1.10.2 Secondary antibodies .....	33
1.10.2.1 FITC-conjugates .....	33
1.10.2.2 Texas-Red-conjugates .....	33
1.10.2.3 Alexa-488-conjugates .....	33
1.10.2.4 Alexa-633-conjugates .....	33
1.10.2.5 Peroxidase (Pox)-conjugates .....	34
2. Methods .....	34
2.1 Isolation and purification of nucleic acids .....	34
2.1.1 Small scale isolation of plasmid DNA .....	34
2.1.2 Large scale isolation of plasmid DNA .....	36
2.1.3 Small scale isolation of BAC-DNA .....	37
2.1.4 Large scale isolation of BAC-DNA.....	38
2.1.5 Determination of DNA concentration and purity of the isolated DNA ...	39
2.2 Analysis and cloning of DNA .....	40
2.2.1 Restriction digest of DNA.....	40
2.2.2 Dephosphorylation of DNA .....	40
2.2.3 Amplification of DNA by Polymerase Chain Reaction (PCR).....	41
2.2.3 Agarose gel electrophoresis .....	43

## Table of contents

---

2.2.4 Isolation of DNA fragments from agarose-gels .....	44
2.2.5 Annealing of synthetic oligonucleotides .....	44
2.2.6 Ligation of DNA fragments.....	44
2.2.7 Transformation of recombinant DNA .....	45
2.2.7.1 Preparation of electro-competent bacteria .....	45
2.2.7.2 Transformation of electrocompetent bacteria.....	45
2.2.8 Linker scanning mutagenesis of the M53 ORF .....	46
2.3 Cells and viruses .....	48
2.3.1 Tissue culture .....	48
2.3.1.1 Cultivation of cells .....	48
2.3.1.2 Freezing and thawing of eukaryotic cells .....	48
2.3.2 Working with MCMV .....	49
2.3.2.1 Generation of recombinant MCMV-BACs .....	49
2.3.2.2 Reconstitution of recombinant MCMV-BACs to virus.....	50
2.3.2.3 MCMV virus stock preparation .....	51
2.3.2.4 Growth curves.....	52
2.3.2.5 MCMV titer determination by plaque assay.....	52
2.4 Analysis of proteins .....	53
2.4.1 Transfection of eukaryotic cells using calciumphosphate-precipitation	53
2.4.2 Transfection of eukaryotic cells using Superfect <sup>®</sup> transfection reagent	54
2.4.3 Protein extraction from eukaryotic cells .....	54
2.4.3.1 Protein extraction from eukaryotic cells using total lysis buffer .....	54
2.4.3.2 Protein extraction from eukaryotic cells using IP lysis buffer.....	55
2.4.3.3 Protein extraction from eukaryotic cells using high salt lysis buffer	55
2.4.3.4 Preparation of nuclear extracts .....	56
2.4.4 Metabolic labeling of proteins and co-immunoprecipitation .....	57
2.4.5 Strep-tag pull down assay .....	58
2.4.6 HA-tag pull down assay .....	60
2.4.7 Flag-tag pull down assay .....	61
2.4.8 SDS-PAGE .....	61
2.4.9 Western Blot .....	63
2.4.9.1 Sandwich construction .....	64
2.4.9.2 Detection of blotted proteins .....	64

## Table of contents

---

2.4.10 Silver-staining .....	65
2.4.11 Confocal laser scanning microscopy .....	66
<b>D. Results.....</b>	<b>68</b>
1. M53/p38 is expressed with late kinetics and is essential for MCMV replication .....	68
1.1 Optimization of M53/p38 detection by Western-blot analysis .....	68
1.2 Determination of the expression kinetics of M53/p38 .....	69
1.3 M50/p35 and M53/p38 co-locate to the nuclear membrane .....	71
1.4 M50/p35 directly binds to M53/p38 .....	72
1.5 The M53 ORF is essential for viral growth and infectivity can be reconstituted by ectopic re-insertion of the wild-type M53 gene into the M53 deletion genome.....	75
1.5.1 Deletion of endogenous M53/p38 leads to loss of functionality of MCMV-infection .....	75
1.5.2 Ectopic expression of M53 reverts the null-phenotype of the $\Delta$ M53-MCMV-BAC .....	76
2. Construction of an insertion mutant library of the M53 ORF and analysis of the mutants in the context of the MCMV genome .....	78
3. Alignment of the aa-sequence of a total of 36 members of the UL31 family indicates conserved and not-conserved regions .....	83
4. Ability of the selected M53-mutant set to rescue the M53 null phenotype: Confirmation of the in silico predicted sequence homology.....	84
5. The N-terminal 1/3 of M53/p38 contains a nuclear localization signal.....	85
6. The M50/p35 binding site of M53/p38 .....	87
6.1 Using M53-stop and N-terminal deletion mutants the M50/p35 binding site of M53/p38 can be located to CR1 of M53/p38 .....	87
6.2 Using M53 insertion mutants the M50/p35 binding can be located to the beginning of CR1 and the most important residues are probably represented by aa 115 to 131 of the M53/p38 protein.....	93
7. Characterization of the M50/p35 binding site of M53/p38 .....	95

## Table of contents

---

7.1 Distinct M53-point mutants lost to some extent the ability to localize to M50/p35 .....	95
7.2 Distinct M53/p38 point mutants showed reduced binding to M50/p35 and resulting viruses were strongly attenuated .....	97
7.3 Exchange of only two aminoacids abolishes M50-M53 interaction and rescue of the M53 null phenotype .....	99
8. Homo-oligomerization of M53/p38 .....	101
9. Cellular interaction partners of M53/p38 and M50/p35.....	102
9.1 Identification of the M50/p35-M53/p38 complex in post nuclear fractions	103
9.2 Cellular lamins and M53/p38 are retained in a salt resistant compartment of the cell: the nuclear matrix .....	104
10. The lamin B receptor complex (LBR) interacts with STM50 alone or STM50 complexed with M53/p38.....	106
11. Both, Flag-tagged M53/p38 and HA-tagged M50/p35 can efficiently pull down LBR.....	107
12. Both M53/p38 and M50/p35 specifically interact with nuclear matrix proteins .....	111
13. Proteomics on the MCMV NEC.....	114
<b>E. Discussion.....</b>	<b>118</b>
1. The UL31- and UL34 homologues and their function during virus replication .....	118
2. M53/p38, an essential MCMV protein, which is expressed by late kinetics	118
3. Exploring M53/p38 by transposon mutagenesis of the M53 ORF .....	119
4. Analysis of M53/p38 mutants .....	121
4.1. The N-terminal part of M53/p38 harbors a NLS as functional element....	122
4.2. The interaction of M50/p35 and M53/p38.....	122
4.3. The C-terminal 2/3 of M53/p38 bears essential MCMV functions .....	124
5. Homo-oligomerization of M53/p38 .....	125
6. Interaction of M53/p38 and M50/p35 with nuclear matrix proteins .....	125
7. Basic proteomics to identify MCMV- and cellular NEC proteins .....	131

Table of contents

---

<b>F. References.....</b>	<b>132</b>
<b>G. Supplementary information.....</b>	<b>151</b>
1. Abbreviations .....	151
2. List of figures.....	155
3. List of tables .....	156
4. Primers used in this study .....	157
5. Publications.....	160
6. Posters and oral presentations.....	161
7. Acknowledgements .....	162
8. Ehrenwörtliche Versicherung .....	163
9. Curriculum vitae .....	164



## A. Summary

Herpesvirus infections are usually asymptomatic or associated with mild symptoms. Fatal diseases are seen in immune suppressed and immune incompetent individuals. Although herpesviruses are of emerging medical importance nowadays an infection only can be controlled by chemotherapeutics, which target viral DNA replication and cause negative side effects. Essential steps of herpesvirus morphogenesis might indicate new targets for interference.

The export of the 110 nm large herpesvirus nucleocapsid from the cell nucleus is a logistic problem, because such a cargo exceeds the size tolerated by the nuclear pore complex. Two conserved herpes simplex virus 1 proteins, UL31 and UL34, form a complex at the inner nuclear membrane and govern nuclear egress of herpesvirus nucleocapsids. In mouse cytomegalovirus (MCMV), a member of the beta-herpesvirus subfamily, the homologous proteins M53/p38 and M50/p35 form the nuclear egress complex (NEC). The interaction of these proteins is essential for the virus and might serve as a potential drug target.

Here we describe a saturating random mutagenesis procedure for the UL31 homologue M53/p38. From a total of 498 individual mutants 72 were reinserted into the genome to test virus complementation. The analysis revealed that the N- terminus of M53/p38 provides the nuclear localization signal (NLS). The M53/p38 binding site for the NEC partner M50/p35 was located to aa 112-137. No single aa exchange for alanine could destroy NEC formation but virus attenuation revealed a major role for the aa K128, Y129, and L130. Further, the lethal phenotype of several insertion and stop mutants indicated the functional importance of the C-terminus of the protein, which might serve to construct dominant negative mutants.

The interference of herpesvirus proteins with unknown cellular functions is of emerging interest. MCMV nucleocapsid formation is followed by a complex process of nucleocapsid transitions through cellular membrane barriers. The re-organization of the nuclear architecture by viral proteins probably involves the interaction with host cell proteins. Here, we found that the NEC of MCMV interacts with an important inner nuclear membrane protein complex, the lamin B receptor, which controls nuclear membrane stability. Thus, herpesviruses might target major cellular principles that govern nuclear integrity.

## **B. Introduction**

### **1. The cytomegaloviruses as family members of the herpesviruses**

Based on their structural and biological properties the cytomegaloviruses (CMV) form the  $\beta$ -subfamily of the herpesviridae. To date more than 120 herpesvirus species have been identified in mammals. Herpesviruses possess a large double stranded DNA-genome with high coordination capacity, which is surrounded by a capsid and an envelope. The genomes of herpesviruses differ in size and in GC-content. The GC-content varies between 32% in canine herpesvirus and 75% in herpesvirus simiae. Genome size varies between 125 kbp for Varicella Zoster Virus (VZV) and approximately 230 kbp for cytomegaloviruses (HCMV and MCMV, respectively) with a coding capacity of approximately 200 proteins (Chee, 1990; Rawlinson, 1996; Varnum, 2004; Tang, 2006). The ORFs code for structural components, virus-specific enzymes and factors, which are involved in nucleic acid synthesis and nucleotide metabolism (Roizman, 2001). Furthermore, a variable number of genes are involved in modulation of host defense.

A characteristic feature of all herpesviruses is the ability to persist lifelong in the infected host without inducing chronic symptoms. In this stage, called latency, the virus genome persists circular in the cell nucleus and gene expression is almost totally abrogated. Latent viruses usually remain undetectable by virological means until reactivation occurs. Then, lytic virus-replication is frequently accompanied by destruction of the host cell, which leads to symptomatic infection of susceptible hosts.

Based on host range, duration of replication cycle and cell tropism *Herpesviridae* can be further divided into the three subfamilies *alpha*herpesvirinae, *beta*herpesvirinae and *gamma*herpesvirinae. (Regenmortel,

## B. Introduction

---

2004). The  $\alpha$ -herpesviruses exhibit a broad host range, a short replication cycle and the capacity to establish latency in neuronal cells of sensory ganglia. The most prominent members of the  $\alpha$ -herpesvirus subfamily are herpes simplex virus type 1 and 2 (HSV-1; HSV-2) and varicella zoster-virus (VZV). The name of the whole virus family derived from the creeping skin lesions that are caused by HSV infection (Greek-herpein= creep). In contrast to the  $\alpha$ -herpesvirus subfamily the  $\beta$ -herpesviruses are characterized by their restricted host range (species specificity) and long replication cycle. The main representatives of this subfamily are the cytomegaloviruses which derives its name from its characteristic feature that infected cells frequently are enlarged (cytomegalia) and exhibit cytoplasmic and nuclear inclusion bodies (owl eyes). Besides murine cytomegalovirus (MCMV) and human cytomegalovirus (HCMV) the human herpesviruses 6 and 7 (HHV-6, HHV-7) can also be grouped into this subfamily. Like  $\beta$ -herpesviruses the  $\gamma$ -herpesviruses also have a restricted host range but exhibit replication cycles that vary by species. The  $\gamma$ -herpesviruses preferentially infect cells of the lymphatic system, like B- and T-lymphocytes. Prominent members of this subfamily are the Epstein-Barr virus (EBV) and the human herpesvirus 8 (HHV-8) (Mocarski, 2001; Roizman, 2001).

### 1.1 Biology of CMV infection and host immune defense

After infection of the host the virus spreads in the whole organism by blood transport with phagocytotic cells (Stoddart, 1994). CMV can replicate in epithelial- and endothelial cells of different organs (e.g. kidney, salivary glands, liver, cortex of adrenal glands, lung, intestines, heart, bone marrow and spleen). After a mostly asymptomatic primary acute infection CMV persists lifelong in the host. Reactivation can be induced by endo- and exogenous stress factors or immunosuppression (Krmptotic, 2003; Mocarski, 2001). Cells that carry latent virus genomes are presumably undifferentiated dendritic- and myeloid precursor cells of the monocyte-macrophage-system (Soderberg-Naucler, 1997; Hahn, 1998). During the latent phase of infection with the exception of CMV latency-associated transcripts (CLTs) no further viral genes are expressed within the

## B. Introduction

---

ie1/ie2- gene region (Kondo, 1996). This prevents exposition of viral antigens to the host immune defense. In the animal model it has been shown that MCMV infection is predominantly controlled by MHC-class-I restricted CD8<sup>+</sup> cytotoxic T-lymphocytes (CTLs) immune response (Jonjic; 1990; Reddehase, 1985, 1988). Until now several CMV-genes have been described interacting with the host immune system, thereby modulating and evading host defense (Wagner, 2002; Thale, 1995; Kleijnen, 1997; Ziegler, 1997; Reusch, 1999; Ziegler, 2000; Jones, 1996, 1997; Ahn, 1996, 1997; Hengel, 1999; Menard, 2003; Mocarski, 2002; Alcami, 2000; Arase, 2002; detailed overview: Koszinowski and Hengel, 2002; Krmpotic, 2003).

### **1.2 Transmission and clinical relevance of human cytomegalovirus (HCMV)**

Based on its strict species specificity HCMV only can infect humans. Depending on social status and geographic properties between 40-100 % of the adult population is infected with this virus (Britt and Alford, 1996; Landolfo, 2003). In developing countries these epidemiological numbers can peak up to 100 %. The virus can be spread by saliva and mother's milk but also by virus-contaminated blood or urine. Furthermore virus transmission by sexual contact is possible (Britt and Alford, 1996, Landolfo, 2003). In humans with an intact immune system the primary infection is usually asymptomatic although mononucleosis and hepatitis can occur. In contrast, HCMV can provoke fatal disease in immuno-suppressed-(e.g. AIDS-patients, bone marrow- and organ-transplanted individuals) and non-immuno-competent individuals (e.g. newborn) after primary infection or reactivation from latency (Landolfo, 2003; Mocarski, 2001). Here, CMV infection can cause retinitis, encephalitis, pneumonitis, hepatitis or colitis. During pregnancy intrauterine HCMV infection can cause damage to the fetus or abortion. Congenital infection can lead to damage of the central nerve system (microcephaly, chorioretinitis), deafness, thrombocytopenia, hemolytic anemia or hepatosplenomegaly (Stagno, 1982; 1986; Boppana, 1992). Congenital infection occurs in 1% of newborns and causes symptoms in 15% of infected children. So far, no effective vaccine

## B. Introduction

---

against HCMV is available. Almost all drugs used against HCMV are nucleoside analogues which target the DNA polymerase as a key enzyme for viral DNA replication (Coen, 2003).

### **1.3 Mouse cytomegalovirus (MCMV) as animal model for HCMV infection**

The strict species specificity of CMV prohibits analysis of HCMV infection in an animal model. Therefore, the analysis of the entire spectrum of HCMV infection biology needs closely related animal viruses that can serve as laboratory models. CMV in mice, rats or guinea pigs provide models. MCMV and HCMV are closely related concerning gene homology and both exhibit a high similarity of infection-biology and pathogenesis. Therefore, the most frequently used animal model to study HCMV infection in vivo is the MCMV infection of mice. As described for HCMV the infection with MCMV can be controlled and leads to virus-latency in immuno-competent mice (Hudson, 1979). In contrast, infection of immuno-suppressed mice results in lethal diseases like pneumonia, hepatitis or inflammation of the cortex of adrenal glands (Krpmotic, 2003; Mayo, 1977, Reddehase, 1985). Furthermore, it has been shown that MCMV can be reactivated from the latent stage (Reddehase, 1994; Krmpotic, 2003). Altogether, the MCMV model system enables, by analysis of MCMV-mutants in the biological context, the identification of unknown pathogenesis-mechanisms of HCMV-infection.

## **2. Structure of cytomegaloviruses**

All members of the herpesvirus family share morphological characteristics. Mature virions range between 120- and 300 nm in diameter and consist of four distinct elements: core, capsid, tegument and envelope (Fig. 1, Roizman, 2001). The viral core consists of linear, double stranded DNA, which is surrounded and most likely stabilized by a proteinaceous scaffolding matrix. The core is encased by a capsid, which is built from 12 pentameric- and 150 hexameric capsomers, arranged in a T=16 icosohedral lattice forming the protein shell and

## B. Introduction

ranges between 100-110 nm in diameter. Both, core and capsid form the nucleocapsid. Nucleocapsids are embedded into the tegument that consists of an amorphous electron-dense matrix of 20 to 30 different proteins. The tegument is presumed to be involved in early gene transcription after virus entry. Capsid and tegument are enveloped by a lipid bilayer that originates from the host cell. Virus encoded spike-like glycoproteins are embedded into the envelope. These allow virus attachment to host cell receptor structures and are responsible for virion-host cell membrane fusion during virus entry (Mocarski, 2006).

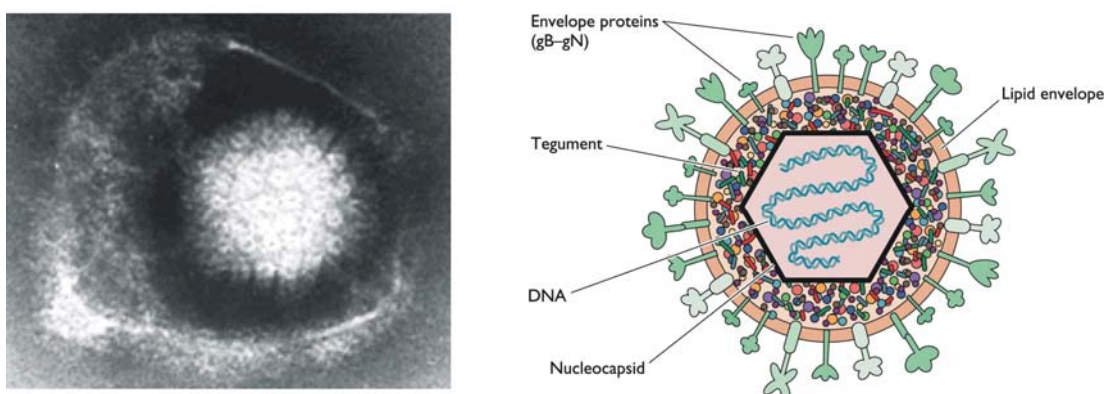


**Figure 1. Structure of a herpesvirus virion.** (Left) Electron micrograph of a herpes simple virus type 2 (HSV-2). The virion is approximately 180 nm in diameter. (Right) Schematic diagram of a herpesvirus virion showing the lipid envelope that is studded with at least 10 glycoproteins originating from virus. The tegument comprises at least 15 viral proteins and the linear double-stranded genome is encased by an icosahedral capsid. Adapted from Flint (Principles of virology), first edition, 2000.

During human CMV infection besides intact virions non-infectious virus particles are also built. These structures designated as “dense bodies” are located in the cytoplasm of the infected cell and possess neither viral DNA nor capsid but consist mainly of viral tegument protein pp65 (Irmiere, 1983). Furthermore, to a minor extent non infectious enveloped virus particles are built that possess a capsid but no viral genome. In contrast to HCMV the murine cytomegalovirus (MCMV) forms no “dense bodies” but virions with multiple capsids (Chong, 1981).

### **3. Replication of cytomegaloviruses**

Like for all herpesviruses the replication cycle of HCMV and MCMV is strictly regulated. CMV entry into host cell starts with adsorption of the virion on the cell surface (Fig. 2). This is mediated by interaction of viral glycoproteins to their corresponding surface receptors and leads to fusion of virus- and host membranes and delivery of the nucleocapsid to the cytoplasm of the host cells (Spear, 2003, 2004). HCMV is estimated to carry 20 viral integral membrane proteins (Mokarski, 2006). Five glycoproteins, gB, gH, gL, gM and gN are broadly conserved among the herpesvirus family. For most human herpesviruses cell surface proteoglycans like heparan-sulfate have been shown to play a role for initial contact with the cell, e.g. in alpha- (HSV-1, VZV), beta- (HCMV, HHV-6A, HHV-6B, HHV-7) and gammaherpesvirus (KSHV/HHV-8) subfamilies (Spear, 2003, 2004). Consistently, herpesviruses often exhibit a broad cell tropism for virus attachment- and entry steps. After virus entry nucleocapsids are transported to the nuclear pores, followed by release of the viral DNA to the nucleus and its circularization (Dohner, 2004; Smith, 2002; Welte, 2004). Viral gene expression is regulated in cascades. Three phases of gene expression are distinguished: immediate early (IE)-, early (E)- and late (L)- gene expression (Mocarski, 2001). The immediate early gene expression is initiated as soon as the viral genome enters the nucleus of the permissive cell. For the transcription of IE genes no de novo synthesis of viral proteins is needed. Parts of the transcripts have been suggested to originate from previous infections and to be transferred to the new host by viral tegument proteins (Bresnahan, 2000). IE proteins regulate the induction of early (E) genes expression (Mocarski, 1996). Early gene activation occurs mainly on the transcriptional level and expressed proteins are necessary for replication of the viral genome. For herpesvirus DNA replication two potential mechanisms are discussed. One model suggests analogous to bacteriophage lambda the replication of DNA as rolling circle (Boehmer, 1997, 2003). More recently, a recombination-dependent branching mechanism analogous to T-even bacteriophage replication was suggested (Wilkinson, 2003, 2004; Jackson, 2003). The start of DNA replication defines initiation of the late (L) phase. In this



## B. Introduction

---

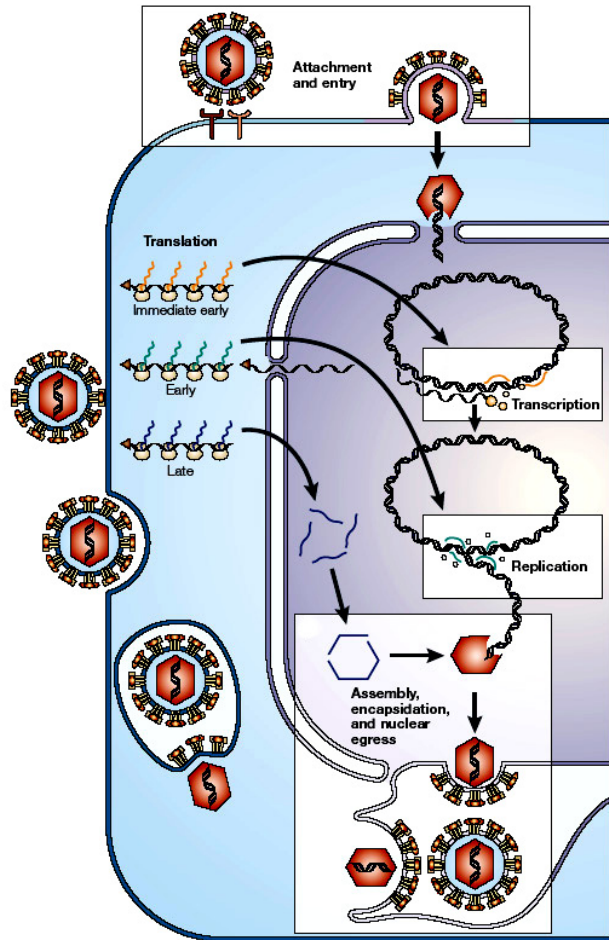
period of infection predominantly structural proteins are expressed, which are components of the virion or involved in virus assembly. DNA replication results in production of multi-genomic length concatemeric intermediates, which are cleaved down to genome length units during packaging into capsids (McVoy, 1994; Mocarski, 2001; Bogner, 2002; Schynts, 2003). It is suggested that nucleocapsids are actively transported in the nucleus and unify with a set of primary tegument proteins at the inner nuclear membrane (INM) (Forest, 2005; Klupp, 2006; Kotsakis, 2001; Wolfstein, 2006; Baldick, 1996).

Nucleocapsid export involves a complex process of nucleocapsid transitions through cellular membranes. This egress mechanism of the nucleocapsid out of the nucleus and acquisition of the viral envelope is discussed controversially. The single envelope theory assumes that the viral envelope corresponds to the outer nuclear membrane (ONM) and is already acquired at the stage of capsid egress from the nucleus (Wild, 2005; Leuzinger, 2005). The de- and re-envelopment model assumes that viral nucleocapsids acquire a first envelope by budding through the inner nuclear membrane (Fig. 2 and 4). Then nucleocapsids bud from the inner nuclear membrane (INM) into the space between INM and outer nuclear membrane (ONM). This process is termed primary envelopment. Next, viral particles fuse with the outer leaflet of the nuclear membrane or ER, thereby losing their primary envelope. Naked, premature virions are then released to the cytoplasm where a second tegumentation step and transport of the virions to the trans-Golgi-network takes place. Viral envelope proteins are assumed to be processed during transition through ER and the trans-Golgi-network (Enquist, 1998; Mettenleiter, 2002, 2004; Gershon, 1994). A secondary envelopment occurs at a not yet clearly defined compartment. It has been suggested that the second envelopment of the virions occurs after transit through the trans-Golgi-network by fusion with Golgi-derived vesicles that traverse through the cytoplasm to the plasma membrane of the cell, where the mature virions are released into the extracellular space by exocytosis (Gershon, 1994; Skepper, 2001; Mettenleiter, 2002, 2004, 2006).



## B. Introduction

**Figure 2. Herpesvirus replication.** Viral envelope glycoproteins mediate attachment and fusion with the cellular membrane. This leads to release of capsid encased viral DNA (red hexagons) into the cytoplasm and capsid transport to the nucleus. Next, viral DNA enters the nucleus by transfer through the nuclear pore-complex and circularises. Transcription of viral genes is regulated in a timed, cascaded fashion. Immediate early (IE) proteins (orange) exhibit mainly regulatory functions and are responsible for induction of 'early' (E) gene expression. E-proteins are necessary for viral replication (green). Late viral proteins (L, blue) are involved in late maturation events, e.g. capsid formation, DNA- packaging, and egress. Nucleocapsids bud through the nuclear envelope by enveloping- and de-enveloping events and traverse the cytoplasm to the trans-golgi-network, where virions mature. Mature virions reach the plasma membrane of the cell by exocytosis and are released to the extra-cellular space. Adapted from Coen, 2003.



Transport through the nuclear envelope of the cell poses a major logistic problem during herpesvirus morphogenesis.

### 4. The nuclear envelope

The nuclear envelope (NE) separates the cytoplasm from the nucleoplasm (see also reviews: D'Angelo, 2006; Gruenbaum, 2005; Foisner, 2001). It is composed of four domains: the outer nuclear membrane (ONM), the inner nuclear membrane (INM), the perinuclear space and the nuclear lamina (Fig. 3). The outer nuclear membrane is continuous with the rough endoplasmic reticulum (rER) and studded with ribosomes (D'Angelo, 2006). ONM and ER protein contents are similar in composition. Furthermore, the outer nuclear membrane provides attachment sites for structural elements of the cytoplasm. The perinuclear space is located between the outer- and the inner nuclear membrane and is continuous with the ER lumen, which enables molecules to

## B. Introduction

passively diffuse between the two compartments. The inner nuclear membrane harbors a unique set of membrane-associated- and integral proteins that link the nuclear membranes with nuclear lamina (NL) and chromatin (Ch) (Foisner, 2001; Chu, 1998). INM and outer nuclear membrane fuse at sites where nuclear pore complexes (NPC) span the nuclear envelope. NPCs are large protein assemblies with a estimated complex mass of around 125 MDa in *metazoa*. They are mediators of nucleo-cytoplasmic trafficking of soluble macromolecules (for review see: Tran, 2006).

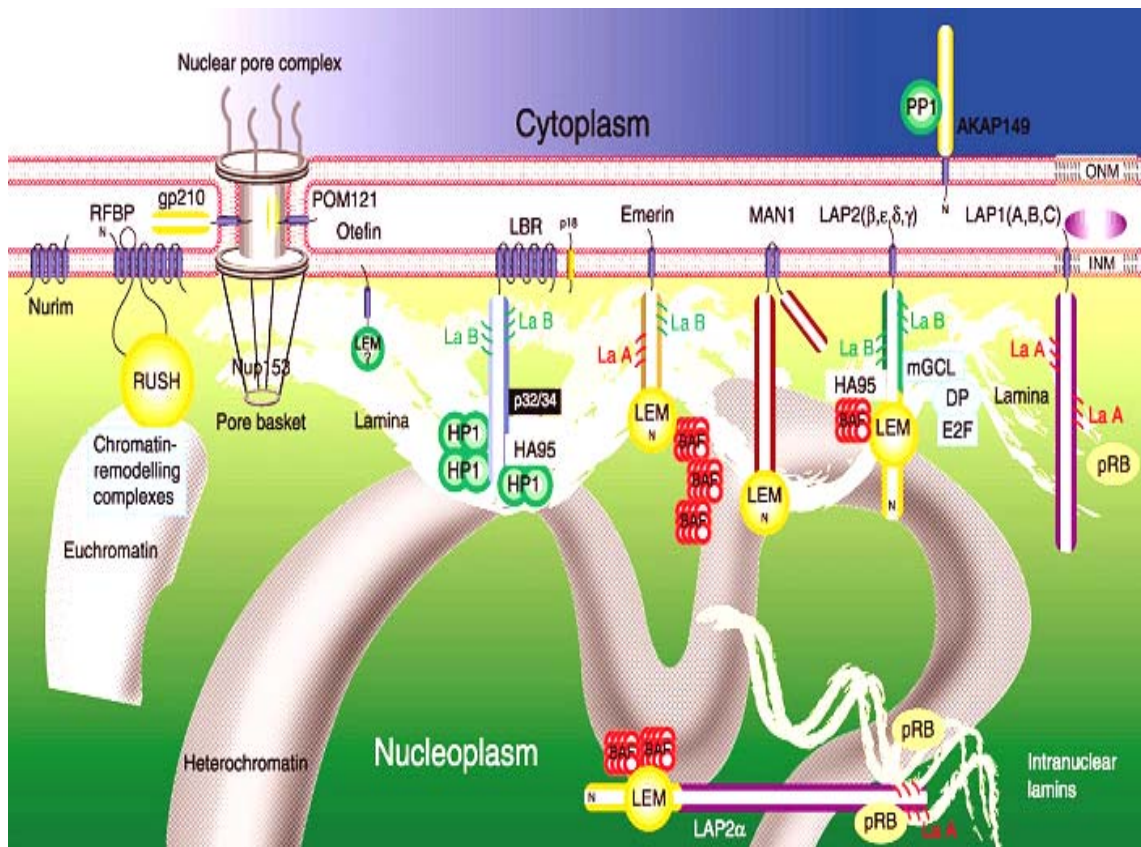


**Figure 3. Schematic diagram of the nuclear envelope showing nuclear membranes, nuclear pore complex, nuclear lamina and chromatin structures.** Integral INM proteins, associated proteins and their topology are depicted: Lamin B receptor (LBR/ p58) as complex, Emerin, MAN1 and lamina-associated polypeptides (LAPs), heterochromatin protein-1 (HP1), barrier-to-autointegration factor (BAF), A- and B-type lamins and HA95. Adapted from Foisner, 2001.

The nuclear lamina of higher eukaryotes underlines the INM and composes a dense meshwork of intermediate filaments made of lamin proteins and lamin associated proteins. The lamina, which has a depth of 20-80 nm provides a skeletal framework and attachment sites for chromatin and is therefore essential for nuclear integrity.

### 4.1 The lamin proteins

Lamins are type-V-intermediate filament proteins that consist of a globular amino-terminal 'head' domain, a long  $\alpha$ -helical coiled coil 'rod' domain and a globular carboxy-terminal 'tail' domain. The 'rod' domain mediates lamin dimerisation. Head-to-tail polymerization and assembly of higher order is mediated by head- and tail domains (Herrmann, 2003). Based on their biochemical properties and behavior during mitotic events nuclear lamins are grouped in A- and B-type lamins (Moir, 2000). A-type lamins (A, C, A $\Delta$ 10 and C2) are widely expressed in differentiated cells (D'Angelo, 2006). They arise from a single gene (LMNA) by alternative-spliced mRNA. Human lamins A and C are identical for their N-terminal 566 amino acids but possess different C-terminal endings (Muchir, 2004). Mature A-type lamins are obtained by initial C-terminal isoprenylation of prelamin A, which is then endoproteolytically cleaved by a metalloproteinase. Lamins C and C2 remain unmodified (Weber, 1989; Leung, 2001). The A-type lamins are presumably incorporated into the nuclear lamina at later time points of post mitotic nuclear assembly than B-type lamins. The B-type lamins are lamin-B1 and B2, which are encoded by the corresponding LMNB1- and LMNB2 genes. During development B-type lamins are expressed in all somatic cells (Muchir, 2004). Post-translational isoprenylation enables B-type lamins to attach to the INM during interphase and to remain attached to INM during mitotic disassembly of the NE (Gruenbaum, 2005). Although A-and B-type lamins are stable components of the nucleus it is unclear how they are organized. During telophase and early G1 phase lamins are mobile and have a half-life of about 30 min. Due to lamin polymerization in interphase lamins are almost immobile and have a prolonged half-life of 3 hours (Moir, 2000). The dynamic properties are regulated by lamin-binding proteins and post-translational modification (e.g. phosphorylation by cellular or viral kinases or de-phosphorylation). Several human diseases, like striated muscle diseases (e.g. Emery-Dreifuss muscular dystrophy), lipodystrophy syndromes, peripheral neuropathies (e.g. Charot-Marie-Tooth disorders) or premature aging syndromes (e.g. Hutchinson-Gilford progeria) can be linked to mutations in lamin A- and C-genes (Muchir, 2004; Sullivan, 1999; Wilkie, 2006).

### 4.2 Proteins and protein complexes interacting with lamins

Lamins bind *in vitro* to a number of INM proteins, including LBR (lamin B receptor-complex), emerin, MAN1, lamina-associated polypeptides-1 and -2 $\beta$  (LAP1, LAP2 $\beta$ ) and nesprin-1 $\alpha$  (Foisner, 2001; Zastrow, 2004) (Fig. 3). They also bind chromatin proteins (histone H2A or H2B dimers), soluble lamina-associated polypeptide-2 $\alpha$  (LAP2 $\alpha$ ), actin, barrier-to-autointegration factor (BAF), sterol-response-element-binding protein (SREBP), retinoblastoma protein (RB), Kruppel-like protein (MOK2) and presumably also to components of the RNA-polymerase-II-dependent transcription- and DNA-replication complexes (for review see Muchir, 2004; Schirmer, 2005; Gruenbaum, 2005). It is suggested that lamins and lamina associated proteins are functionally involved in chromatin organization, nuclear integrity, spacing of the NPCs and reassembly of nuclear components after mitotic events (D'Angelo, 2006). Moreover, multiprotein complexes that connect the nucleoskeleton and the cytoskeleton are proposed to be anchored by lamins via nesprins, UNC-83 and-84 or ZYG-12 (Zhen, 2002; Malone, 2003; Gruenbaum, 2005; Wilhelmsen, 2006). DNA replication and RNA polymerase II- dependent transcription is affected by alteration of nuclear lamin organization (Spann, 2002).

#### 4.2.1 The lamin B receptor-complex (LBR or p58)

One of the best characterized lamin- and chromatin-binding membrane proteins is the human lamin B receptor (LBR) or p58 (Fig. 3). LBR is widely expressed in cells of higher eukaryotes and the human gene has recently been characterized (Schuler, 1994). The LBR or p58 is a 615-amino acid protein, which comprises a nucleoplasmic N-terminal domain of about 210 amino acids and a hydrophobic carboxy-terminal domain with eight putative transmembrane segments that integrate LBR into the INM (Chu, 1998; Worman, 1990; Ye and Worman, 1994). The membrane spanning domain of LBR has a sterol-reductase activity and therefore may participate in steroid metabolism (Holmer, 1998; Schuler, 1994). The N-terminal part contains phosphorylation sites for Cdc2 kinase and protein kinase A as well as arginine-serine (RS) motives that

## B. Introduction

---

were proposed to mediate protein-protein interactions between components of the splicing machinery (Courvalin, 1992; Simos, 1992;). LBR *in vitro* and *in vivo* binds to B-type lamins. This interaction remains stable during mitosis, when the nuclear envelope is fragmented and the lamina is depolymerized (Meier, 1994; Margalit, 2005). *In vitro* LBR binds to double stranded (ds) DNA and to histone H3-H4 tetramers. Furthermore, LBR interacts with chromatin-associated protein HA95 and heterochromatin protein-1 (HP1), which is suggested to mediate gene silencing (review: Chu, 1998; Foisner, 2001; Gruenbaum, 2005). Like for lamins, mutations in LBR are linked to human diseases, e.g. Pelger-Huet anomaly (PHA) (for review: Gruenbaum, 2005; Muchir, 2004). During interphase LBR is arranged as a multimeric complex with nuclear A- and B-type lamins, with a LBR kinase of 150 kDa (p150) that phosphorylates LBR and LBR associated proteins (p32), with an integral membrane polypeptide p18 of unknown function and with p32 (Simos, 1994; Nikolakaki, 1996, Deb, 1996). The p32 protein localizes in the mitochondrial matrix as well as in the nucleus, it has an acidic iso-electric point and forms homo-trimers that build a channel-like structure (Jiang, 1999; Sunayama, 2004; Muta, 1997). p32 has been associated with apoptosis and regulation of RNA splicing (Sunayama, 2004) and with splicing factor 2 (SF2) (Krainer, 1991). It is also recruited by viral functions although its function is not clear. The p32-protein interacts with the human immunodeficiency virus type 1 (HIV-1) trans-activator *Rev* that is required for viral replication (Luo, 1994). It was also shown that p32 interacts with adenovirus core protein V (Matthews, 1998) and represses adenovirus major late transcription (Öhrmalm, 2006). It interacts with herpesvirus saimiri open reading frame 73 gene (Hall, 2002). Recently, it has been shown that human cytomegalovirus kinase UL97 binds p32. The complex is then transferred to the nuclear envelope, where it interacts with LBR and associated lamins (Marschall, 2005). Another LBR associated protein, the heterochromatin protein-1 (HP1) is also attacked by the viral machinery. HP1 binds LBR and interacts with histone 1 (H1) and cross-links the NE with the chromatin (Daujat, 2005). The human polyomavirus agnoprotein interacts with HP1 and is responsible for HP1 dissociation from the LBR and perturbation of the NE, which enables poliomavirus virions to egress from the nucleus (Okada, 2005).



## B. Introduction

---

### 4.2.2 LEM-domain proteins and BAF complexes

The LEM domain, a motif of about 40 residues, is a characteristic feature of inner nuclear membrane proteins Emerin, LAP2 proteins, MAN1 and LEM2 (Fig. 3). All LEM domain proteins interact with A- and/or B-type lamins *in vitro*. Moreover, these proteins have been shown to directly bind BAF (barrier to autointegration factor) (Lee, 2001, Shumaker, 2001; Lin, 2000; Furukawa, 1999; Segura-Totten, 2002, Chu, 1998; Mansharamani, 2004). LEM domain proteins are variable in length but, with the exceptions of MAN1 and LEM2, represent type II integral membrane proteins with a single membrane spanning domain close to the carboxy-terminus (Chu, 1998). MAN1 and LEM2 have two trans-membrane segments (Lin, 2000; Brachner, 2005). The trans-membrane region is flanked by a nucleoplasmic domain that is responsible for lamin binding and amino-terminal by the LEM domain, which is responsible for chromatin binding (Chu, 1998; Muchir, 2004). Chromatin binding occurs not directly by LEM domain but is mediated by BAF (Margalit, 2005; Tifft, 2006). BAF is a conserved 10 kDa protein that forms dimers and can be phosphorylated. These dimers bind LEM domain proteins and also to dsDNA, histone 3 (H3), histone 1.1, lamin A and transcriptional regulators (Bengtsson, 2006; Montes De Oca, 2005). LEM domain proteins can interact with other members of the protein family (e.g. MAN1 and emerin; Mansharamani, 2004). LEM domain proteins and the LBR complex are inter-connected by lamins and by HP1 and BAF with the chromatin. They form a network that is based on the integrity of lamin filaments and of the chromatin organization during interphase and mitosis (Gruenbaum, 2005). But lamins, BAF and a number of LEM domain proteins (e.g. LAP2 $\alpha$ ) are also present in the nucleus as soluble proteins and involved in cell-cycle regulation, replication and transcription (Furukawa, 2003; Vlcek, 2002; Haraguchi, 2001, Dechat, 2004). Moreover, these proteins presumably have a scaffolding function for multi-protein complexes (Gruenbaum, 2005). MAN1 has been shown directly to bind to receptor-regulated SMAD proteins (R-SMAD) and other members of the TGF $\beta$  superfamily and to be involved in signal transduction (Osada, 2003; Dijke, 2004; Worman, 2005). Again, like for lamins or the LBR complex, mutations in LEM domain proteins can be linked to severe

disease, e.g. X-linked Emery-Dreifuss muscular dystrophy, which is caused by mutations in emerin (Muchir, 2004; Holaska, 2006). Recently, it has been shown that emerin is necessary for HIV-1 infection. HIV-1 cDNA associated with emerin in vivo. Furthermore, the LEM-domain protein with associated BAF was essential for cDNA integration into chromatin (Jacque, 2006).

### **5. The egress of herpesvirus capsids from the nucleus**

The packaging of unit-length viral genomic DNA into pre-formed capsids takes place in the nucleus of the infected cell. Afterwards, the nucleocapsids have to leave the nucleus to access the cytosol where the mature virions are formed. The mechanism of this process, coined as nuclear egress, is to date intensively discussed (Mettenleiter, 2006; Klupp, 2006; Wild, 2005; Leuzinger, 2005). With more than 100 nm in diameter the size of a herpesvirus capsid exceeds the size tolerated by the nuclear pore complex (NPC), which mediates transport between nucleus and cytoplasm. One model suggests enlargement of the nuclear pores upon herpesvirus infection. Accordingly, capsids can use enlarged nuclear pores as a gateway for access to the cytoplasmic compartment (Wild, 2005; Leuzinger, 2005). Another, more accepted, model suggests that export of herpesvirus nucleocapsids requires a different strategy to penetrate the nuclear envelope: the budding of herpesvirus nucleocapsids through the nuclear envelope (Fig. 2, 4; Mettenleiter, 2002, 2004, 2006). In support for the second theory for HCMV or MCMV infected cells local nuclear membrane duplications and patches of wrapped viral capsids have been observed by ultra-structural analysis (Radsak, 1991; Rupp et al., manuscript in preparation). However, for capsids the inner nuclear membrane (INM) is not simply accessible, since it is stabilized by the nuclear lamina layer (NL). The nuclear lamina constitutes an orthogonal filamentous protein meshwork with a depth of 20-80 nm (Fig. 3). This lamina layer is only dissolved during mitosis due to lamin phosphorylation by specific cellular kinases (Gerace, 1980; Ottaviano, 1985; Otto, 2001; Peter, 1990; Dessey, 1988; Buendia, 2001).

Virus maturation events are controlled by multi-protein assemblies which require the interaction of a number of viral and cellular proteins. For MCMV-

## B. Introduction

infection it has been proposed that cellular protein kinase C is induced and recruited to the nuclear membrane. This is accompanied by phosphorylation of lamin B (Muranyi, 2002). Recently, the same has been confirmed for HSV-1 infection. It was suggested that modification of the nuclear lamina promotes the budding event of the herpesvirus nucleocapsids (Park, 2006). But also other viral encoded protein kinases like UL13 and Us3 from HSV-1 or the UL13 homologue BGLF4 from EBV have been linked to modulation of cellular activities and late virus maturation events (Kato, 2005, 2006; Kawaguchi, 2003; Klupp, 2001; Gershburg, 2006).

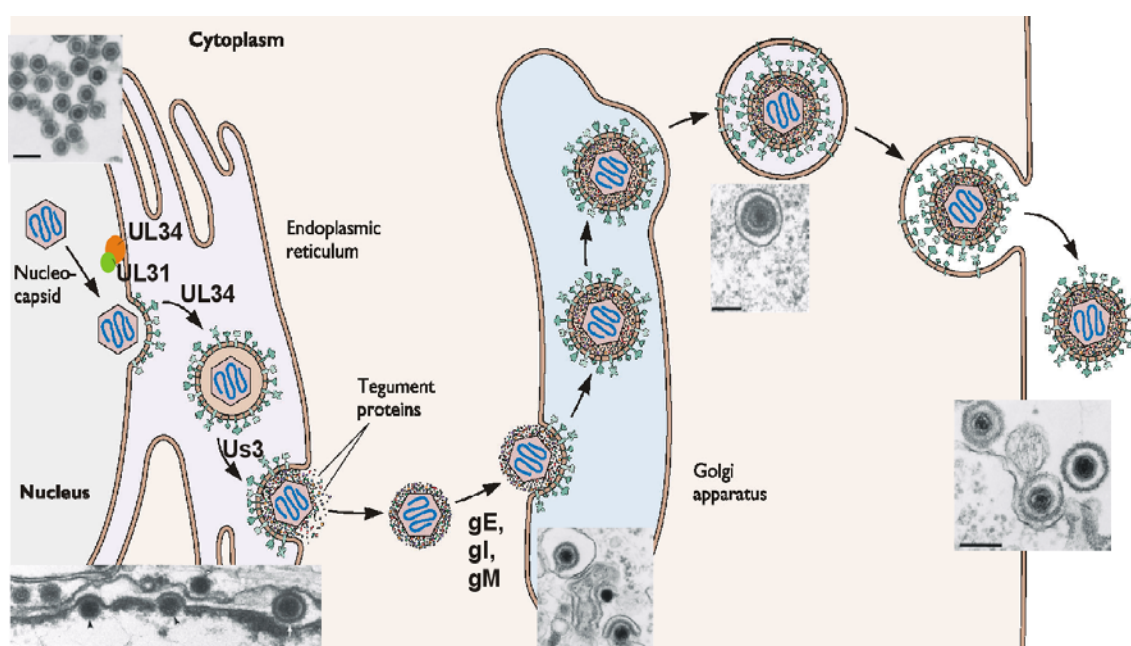


**Figure 4. Herpesvirus assembly and egress from the nucleus.** Demonstrated by a diagram is the de- and re-enveloping model of herpesvirus nuclear egress. Viral gene products involved in specific egress reactions are indicated. Reactions are illustrated by corresponding electron micrographs of cells infected by  $\alpha$ -herpesvirus pseudorabies virus (PrV). The nucleocapsid initially acquires an envelope by budding through the inner nuclear membrane. The enveloped nucleocapsid next fuses with the outer nuclear membrane and is released to the cytoplasm. In the cytoplasm the viral nucleocapsid acquires more tegument proteins and is transported to the trans-golgi-network. The final viral envelope is acquired upon budding of tegument associated capsid into a late compartment of the secretory pathway. Bar= 150 nm. Adapted from Flint (Principles of virology), first edition, 2000; and Mettenleiter, 2002, 2005, 2006.

The HCMV UL97 gene is homologous to protein kinases of other  $\alpha$ -,  $\beta$ - and  $\gamma$  – herpesviruses (Chee, 1989; Rawlinson, 1997; Wagner, 2000). The UL97 gene product function has been linked to nuclear egress inasmuch as a UL97 deletion mutation causes a 100-fold decrease in viral yield (Prichard, 1999;



## B. Introduction

Krosky, 2003; Azzeh, 2006; Prichard, 2005). Moreover, HCMV UL97 kinase is recruited by the cellular protein p32 to the nuclear envelope. This is thought to accumulate the p32-UL97 complex at the lamin B receptor complex for lamin phosphorylation (Marschall, 2005).

### 5.1 The nuclear egress complex (NEC)

Gene products involved in herpesvirus morphogenesis are often essential for viral growth. Studies in alpha-herpesviruses have shown that two conserved viral proteins, the prototypic UL31- and the UL34 gene products play a major role during primary envelopment (Klupp, 2000; Fuchs, 2002; Reynolds, 2001, 2002; Roller, 2000; Neubauer, 2002). In the gamma-herpesvirus EBV the BFRF1 and BFLF2 gene products (Farina, 2000, 2005; Gonnella, 2005; Lake, 2004) and in the beta-herpesvirus mouse cytomegalovirus (MCMV) the products of the M53- and M50 genes (Bubeck, 2004; Muranyi, 2002; Lötzerich, 2006) or HCMV gene products UL53 and UL50 (Dal Monte, 2002, Marshall, 2006) have this function. In MCMV both genes, the UL31 homologue M53/p38 and the UL34 homologue M50/p35 are located within the same HindIII fragment H of the 230 kbp MCMV genome (Fig. 5).

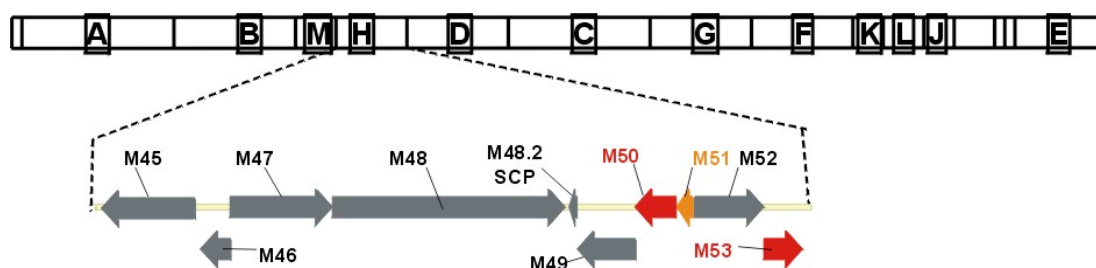


**Figure 5. Schematic diagram of the M50/p35 and M53/p38 localization within the MCMV genome.** (Top line) Hind III cleavage map of the 230-kb MCMV genome. (Second line) Position and transcriptional direction of M50/ p35 and M53/p38 within the HindIII fragment H.

The UL34 and related proteins are type II membrane proteins, which circulate in the contiguous membranes of ER and INM (UL34, M50, UL50, BFRF1) unless the nuclear protein UL31 or UL31 related proteins (M53, UL53, BFLF2) arrest

## B. Introduction

---

them in the INM. Apparently the complex formation by the two proteins, coined the nuclear egress complex (NEC), is pivotal for nuclear egress of herpesviral nucleocapsids (Ye, 2000; Roller, 2000; Klupp, 2000; Gonnella, 2005; Farina, 2005; Bubeck, 2004).

The NEC executes this task by interacting with mostly unknown cellular protein partners, which already reside in or are recruited to the INM. For instance, HSV-1 nuclear egress proteins UL31 and UL34 have been reported to bind lamins A and C *in vitro*. In addition, isolated expression of both proteins redistributed lamins A/C from the nuclear envelope to the nucleoplasmic compartment (Reynolds, 2003). Moreover, both HSV-1 NEC proteins are suggested to be involved in chromatin re-organization (Simpson-Holley, 2004). In MCMV infected cells M50/p35 recruits its viral interaction partner M53/p38 and cellular PKC to the INM (Muranyi, 2002). As described for MCMV and HSV-1 recruitment of the protein kinase C to the NE is accompanied by phosphorylation of lamins and alterations of the nuclear lamina (Muranyi, 2002; Park, 2006). These interactions are thought to displace the rigid nuclear lamina for nucleocapsid budding (Farina, 2005; Gonnella, 2005; Muranyi, 2002; Bubeck, 2004).

The MCMV-NEC (Fig. 6) interacts with further viral proteins. Nuclear M53/p38 binds to M94, which is a MCMV-primary tegument protein that is associated with virus capsids (Ruzsics, unpublished observation). In addition, M51, another tegument associated protein was identified as an interaction partner of M53/p38 by yeast two hybrid analysis (Fossum and Haas, unpublished data). Thus, M53/p38 might be an adaptor protein that links nucleocapsids and nuclear egress sites.

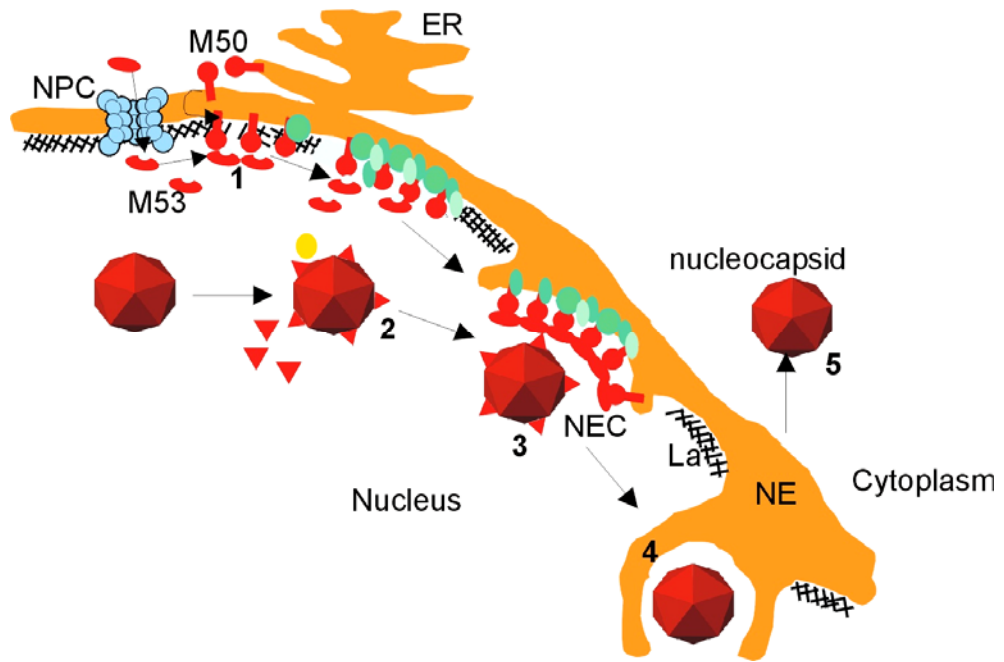


**Figure 6. Proposed working model for egress of MCMV capsids from the nucleus-the MCMV-nuclear egress complex (NEC).** (1) M50/p35 reaches the INM (inner nuclear membrane) of the nucleus by ER-diffusion and interacts with its viral NEC partner M53/p38. (2) The nucleocapsids acquire first tegument proteins. (3) The M50-M53 complex probably mediates nucleocapsid recruitment to the INM due to interaction of M53/p38 with capsid associated primary tegument. Viral MCMV-NEC proteins might also bind to several cellular proteins and presumably are involved in de-stabilization of the nuclear lamina or chromatin re-organization. (4) Nucleocapsids bud into the nuclear envelope (NE) and are released to the cytoplasm after de- and re-envelopment steps. ER (endoplasmic reticulum); NPC (nuclear pore complex); La (lamina).

**6. Aims and concepts**

The major aim of this work was to collect functional information about M53/p38 that can be associated with the MCMV nuclear egress machinery. At the starting point of this work it was known that cellular PKC is recruited to the nuclear envelope upon MCMV infection resulting in phosphorylation of cellular lamins and destabilization of the lamina. M50/p35 and M53/p38 were assumed to be involved in this process (Muranyi, 2002). M50/p35 binds M53/p38 and this binding is essential for productive MCMV infection (Bubeck, 2004). In absence of any detailed structural and functional information for the detailed analysis of M50/p35 a random Tn7-based mutagenesis procedure at single gene level was established and combined with the BAC-technology. This approach enabled a comprehensive gene analysis of the isolated viral gene and of the gene in the viral context and the binding site in M50/p35 for M53/p38 was identified (Bubeck, 2004). However, efficiency of the random mutagenesis was poor.

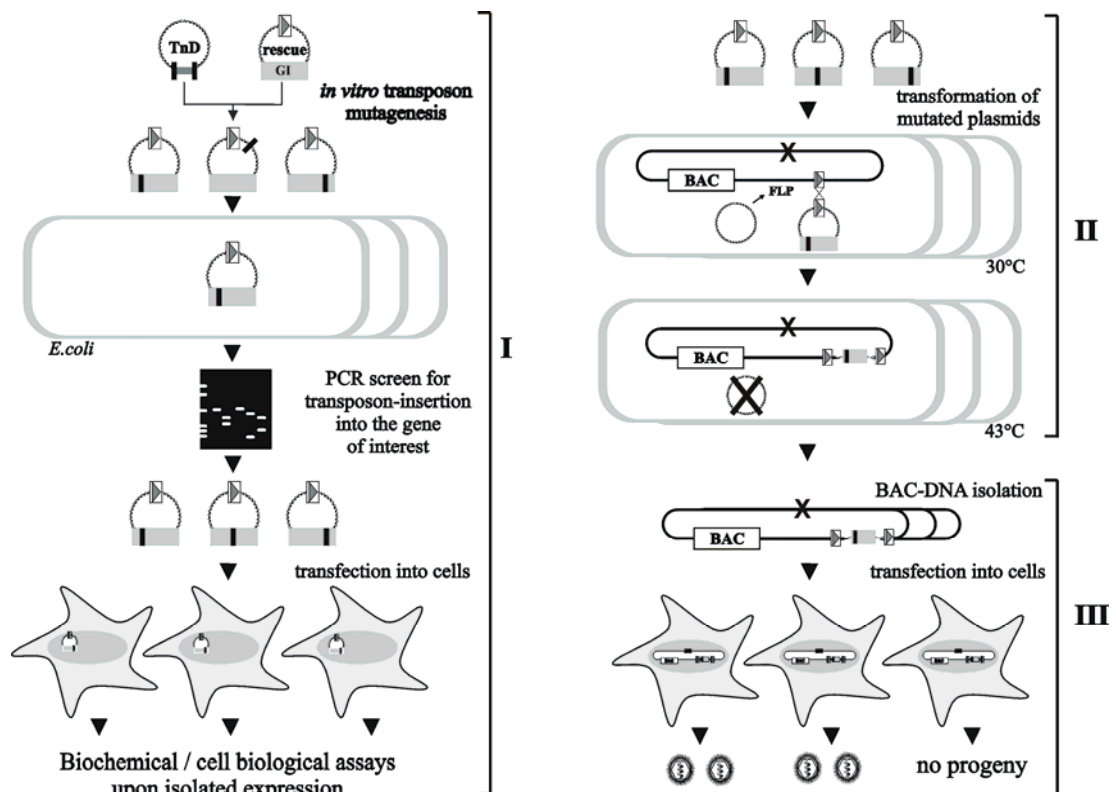


**Figure 7. Analysis of the essential MCMV gene M53.** (I) *In vitro* Tn7 based linker scanning mutagenesis of M53, DNA analysis of the transposon-inserted gene, transfection of mutated plasmids into eukaryotic cells and biochemical or cell biological assays upon isolated gene expression. (II) Re-insertion of mutated plasmids into the viral genome. (III) Virus reconstitution. Adapted from Bubeck, 2004.

## B. Introduction

---

Therefore, the first aim of this project was to establish an improved random Tn7 based linker scanning mutagenesis (Biery, 2000) for M53/p38. As the first mutational analysis of a herpesvirus UL31 family member, for the MCMV M53 gene a library of M53 insertion mutants was generated. A representative set of M53 mutants was re-inserted into the  $\Delta$ M53-MCMV-BAC for functional analysis in the genomic context (Fig. 7).

The interaction motives of UL34- and UL31-homologues are conserved among herpesviruses and prototypic UL31- and the UL34 gene products play a major role during primary envelopment (Klupp, 2000; Fuchs, 2002; Reynolds, 2001, 2002; Roller, 2000; Neubauer, 2002). Thus, a next aim of this project was to characterize the interaction of M53/p38 with M50/p35 and to localize the sequence required for M50/p35 binding.

A further aim of this work was to study the interaction of NEC proteins M50/p35 and M53/p38 with proteins of the cellular nuclear envelope. Since nuclear egress is intensively discussed but to date not well characterized, this may help to elucidate ongoing viral- and cellular processes. It has been described for different viruses that nuclear egress presumably is induced by interaction of viral proteins with cellular components of the NE (Marschall, 2005; Okada, 2005). Using pull-down assays after co-expression of the NEC proteins several cellular interaction partners of M50/35 and M53/p38 could be identified, which are mainly members of the LBR complex.

## C. Material and methods

### 1. Material

#### 1.1 Devices

Bacterial shaker (ISF-1-W)		Kühner, Adolf AG, Birsfelden, CH
Bio-photometer		Eppendorf, Hamburg, D
Centrifuges	Avanti™ J-20xp	Beckman Coulter GmbH, Krefeld, D
	L8-55M ultracentrifuge	Beckman Coulter GmbH, Krefeld, D
	Multifuge 3S-R	Heraeus Instruments, Gera, D
	Biofuge Stratos	Heraeus Instruments, Gera, D
	Centrifuge 5417 R	Eppendorf, Hamburg, D
Confocal microscopes	Leica DM IRB	Leica, Bensheim, D
	Zeiss Axiovert 200M	Zeiss, Jena, D
Fluorescence microscope (1x71)		Olympus, Hamburg, D
Developing-machine	Optimax TR	MS Laborgeräte, Wiesloch, D
Gel drying system (model 583)		Bio-Rad, Munich, D
Gel air dryer		Bio-Rad, Munich, D
Gene Pulser™		Bio-Rad, Munich, D
Gradient former model 150		Gibco BRL, Gaithers-burg, MD, USA
Incubator (B5050E)		Heraeus Instruments, Gera, D
Incubator (BB16CU)		Heraeus Instruments, Gera, D
Light-microscope (Axiovert 25)		Zeiss Carl AG, Goettingen, D
Mini-Protean 3 Cell		Bio-Rad, Munich, D
PCR systems	T Gradient	Biometra, Goettingen, D
	GeneAmp® PCR system	Applied Biosystems, 9700 New Jersey, USA
PerfectBlue™ Vertical electrophoresis system		Peqlab, Erlangen, D
Photo documentation apparatus (Eagle Eye)		Bio-Rad, Munich, D
Roler mixer SRT		Stuart, Staffordshire, UK
Semi-dry-transfer cell (Trans-blot-SD)		Bio-Rad, Munich, D
Sonifier 450		Branson, Danbury, GB
Sonifier-bath SONOREX SUPER RK 103H		Bandelin, Berlin, D
Thermo shaker 5436		Eppendorf, Hamburg, D

## C. Material and methods

---

Vortex-mixer	Bender/Hobein AG, Zurich, CH
Water bath F10	Julabo, Seelbach, D

### 1.2 Consumables

Cell culture dishes 60x 15mm (20 cm <sup>2</sup> )	Becton Dickinson, Heidelberg, D
100x 20mm (55 cm <sup>2</sup> )	Becton Dickinson, Heidelberg, D
150x 20mm (145 cm <sup>2</sup> )	Sarstedt, Nümbrecht, D
Cell culture plates (6-, 12-, 24-, 48-, 96 well)	Becton Dickinson, Heidelberg, D
Cell scratcher (25-, 39 cm)	Costar, Bodenheim, D
Chemiluminescence film (Hyperfilm <sup>TM</sup> ECL)	Amersham Biosciences, Freiburg, D
Cuvettes Condensor cuvettes (2 mm)	Bio-Rad, Munich, D
Unique cuvettes	Brand, Wertheim, D
Dishes (ø 9 cm for agar plates)	Grainer, Frickenhausen, D
Eppendorf reaction tubes (1.5 ml & 2 ml)	Eppendorf, Hamburg, D
Falcon reaction tubes (15 ml & 50 ml)	Becton Dickinson, Heidelberg, D
Hybond-P membrane	Amersham Biosciences, Freiburg, D
Spin cup columns and tubes (Handee <sup>TM</sup> )	Pierce, Rockford, USA
Ultracentrifugation tubes (25x89 mm)	Beckman Coulter GmbH Krefeld, D
Whatman paper (Blotting paper)	Macherey & Nagel, Düren, D
X-ray films (Biomax MR film)	Kodak, New Haven, CT, USA

### 1.3 Reagents

β-Mercaptoethanol	Sigma, Deisenhofen, D
1 kb-DNA ladder	New England Biolabs, Frankfurt/Main, D
Acetic acid	Merck, Darmstadt, D
Agarose	Invitrogen, Karlsruhe, D
Agar	Becton Dickinson, Heidelberg, D
Ammonium persulfate (APS)	Sigma, Deisenhofen, D
Ampicillin	Sigma, Deisenhofen, D
AmpliTaq DNA Polymerase	Applied Biosystems, New Jersey, USA

### C. Material and methods

---

Bacto tryptone	Difco Lab., Detroit, USA
Bromphenolblue	Serva, Heidelberg, D
Carboxy-methyl cellulose	Sigma, Deisenhofen, D
Chloramphenicol	Sigma, Deisenhofen, D
D-desthio biotin solution (10x)	IBA, Göttingen, D
Di-methyl sulfoxide (DMSO)	Merck, Darmstadt, D
Di-thio threitol (DTT)	Roth, Karlsruhe, D
Dulbecco's modified Eagle medium (DMEM)	Gibco, NY, USA
ECL plus Western Blot detection system	Amersham Biosciences, Freiburg, D
Ethylene diamine-tetra acetic acid (EDTA)	Fluka, New-Ulm, D
"Expand High Fidelity PCR System" Polymerase	Roche Diagnostics, Mannheim, D
Fetal calf serum (FCS)	Invitrogen, Karlsruhe, D
Glycerin	Carl Roth GmbH & Co, Karlsruhe, D
Glycine	Carl Roth GmbH & Co, Karlsruhe, D
HA-matrix (3F10, immobilized)	Roche Diagnostics, Mannheim, D
HA-peptide (YPYDVPDYA)	Roche Diagnostics, Mannheim, D
Hydrochloric acid (HCl)	Merck, Darmstadt, D
Isopropanol	Merck, Darmstadt, D
Kanamycin	Sigma, Deisenhofen, D
L-Glutamine	Invitrogen, Karlsruhe, D
Methanol	Carl Roth GmbH & Co, Karlsruhe, D
M-Per-mammalian protein lysis buffer	Pierce, Rockford, USA
Newborn calf serum (NCS)	Invitrogen, Karlsruhe, D
Nonidet P-40 (NP40)	ICN-Biomedicals Inc. Ohio, USA
N, N, N', N'-Tetra-methyl-ethylene-diamine (TEMED)	Sigma, Deisenhofen, D
Optiprep	Sigma, Deisenhofen, D
Para-formaldehyde (PFA)	Merck, Darmstadt, D
Penicillin	Gibco/BRL, Life Lab., Paisley, Scotland
Penicillin-Streptomycin	Invitrogen, Karlsruhe, D
Phenol/Chloroform (Roti-Phenol/C/I)	Carl Roth GmbH & Co, Karlsruhe, D
Phenol-red	Serva, Heidelberg, D
Phenyl-methyl-sulfon fluoride (PMSF)	Sigma, Deisenhofen, D
Phosphono acetic acid (PAA)	Sigma, Deisenhofen, D
Potassium chloride	Merck, Darmstadt, D
Potassium hydrogen phosphate	Merck, Darmstadt, D
Pro-mix <sup>TM</sup> (L-[ <sup>35</sup> S] in vitro cell labeling mix)	Amersham, Freiburg, D
Protease inhibitor cocktail (PIC)	Roche Diagnostics, Mannheim, D



## C. Material and methods

---

Protein A sepharose (CL-4B)	Pharmacia/LKB, Uppsala, S
Protein G sepharose (Fast Flow)	Pharmacia/LKB, Uppsala, S
Restriction enzymes and buffers	Biolabs, Frankfurt/Main, D
RNase A	Roche Diagnostics, Mannheim, D
Rotiphorese gel 30	Carl Roth GmbH & Co, Karlsruhe, D
RPMI 1640	Invitrogen, Karlsruhe, D
RPMI –Met/Cys	Invitrogen, Karlsruhe, D
Shrimp alkaline phosphatase (SAP)	Roche Diagnostics, Mannheim, D
Skim milk powder	Merck, Darmstadt, D
Sodium dodecyl sulfate (SDS)	Carl Roth GmbH & Co, Karlsruhe, D
Sodium acetate	Merck, Darmstadt, D
Sodium chloride	Merck, Darmstadt, D
Sodium di-hydrogen phosphate	Merck, Darmstadt, D
Sodium hydrogen carbonate	Merck, Darmstadt, D
Sodium hydroxide	Merck, Darmstadt, D
Strep Tactin regeneration buffer	IBA, Göttingen, D
Strep Tactin sepharose	IBA, Göttingen, D
(D+) Sucrose	Carl Roth GmbH & Co, Karlsruhe, D
Superfect	Quiagen, Hilden, D
T4-DNA ligase	New England Biolabs, Frankfurt/Main, D
Teleostier gelatine	Sigma, Deisenhofen, D
Tris	Carl Roth GmbH & Co, Karlsruhe, D
Triton-X-100	Carl Roth GmbH & Co, Karlsruhe, D
Trypsin/EDTA	Gibco/BRL, Life Lab., Paisley, Scotland
Tween 20	Merck, Darmstadt, D
Yeast extract	Becton Dickinson, Heidelberg, D
Zeocin	Invitrogen, Karlsruhe, D

### 1.4 Commercial kits

ECL <sup>PLUS</sup> Western Blot Detection System	Amersham Biosciences, Freiburg, D
Flag <sup>®</sup> M purification kit	Sigma, Saint Louis, USA
GFX Micro Plasmid Prep Kit	Amersham Biosciences, Freiburg, D

## C. Material and methods

---

GFX PCR DNA and Gel Band Purification Kit	Amersham Biosciences, Freiburg, D
Immobilon <sup>TM</sup> Western Chemiluminescent HRP Substrate	Millipore, Billerica, MA, USA
MBS-mammalian transfection kit	Stratagene, Cedar Creek, USA
M-Per-mammalian protein extraction kit	Pierce, Rockford, USA
NucleoBond PC100	Macherey-Nagel, Düren, D
Plasmid-Midi-Kit	Quiagen, Hilden, D
QIAquick PCR Purification Kit	Quiagen, Hilden, D
SilverQuest <sup>TM</sup> Silver Staining Kit	Invitrogen, Karlsruhe, D

### 1.5 Oligonucleotide-peptides

The used oligonucleotide peptides for cloning and sequencing were produced by Metabion, Martinsried, Munich, D and have a purity of at least 95%. Used primers are listed in the attachment.

### 1.6 Plasmids

#### 1.6.1 Commercially available and published plasmids

Litmus28:	NEB, Frankfurt a.M., D
pACYC177:	NEB, Frankfurt a.M., D
pCP20:	Cherepanov, 1995
pCR3:	Invitrogen, Karlsruhe, D
pEGFPN1:	Clontech, Mountain View, CA, USA
pGPS-4:	NEB, Frankfurt a.M., D
pOriR6K-zeo-ie:	Bubeck, 2004
pOriR6K-zeo-ie-M50:	Bubeck, 2004
pSMfr3:	Wagner, 1999
pSMfr3- $\Delta$ M50:	Bubeck, 2004
pST76K:	Posfai, 1997

## C. Material and methods

---

### 1.6.2 Plasmids constructed over the project

#### 1.6.2.1 M53/p38 expression plasmids

pCR3-M53: The M53 ORF was amplified from the Hind III fragment of the wtMCMV-BAC thereby using AB6-02 and AB7-02 primers and cloned into pCR3 using KpnI and BamHI resulting in pCR3-M53 (Bubeck, 2004).

pLit28-M53: For the linker scanning mutagenesis procedure the M53 ORF was cloned from pCR3-M53 (Bubeck, 2004) into Litmus28 (NEB, Frankfurt a.M., D) using KpnI and XbaI generating pLit28-M53.

pM53-EGFPN1, pM53-s106-EGFPN1, pM53-s137-EGFPN1 and pM53-s168-EGFPN1: The M53-green fluorescent protein (GFP) fusion proteins were generated as follows. The wt- and mutant M53 ORF were amplified by PCR using primers AB6-SpAs and AB7-02. The PCR products were inserted into BamHI and SpeI digested Litmus28 (NEB, Frankfurt a.M., D). Then the sub-cloned wt and mutant M53 fragments were isolated by SpeI and PmeI digestion and inserted into NheI and SmaI treated pEGFPN1 (Clontech, Mountain View, CA, USA).

#### 1.6.2.2 pOriR6k-zeo-ie derived plasmids

pM53- $\Delta$ 16-106: The NLS sequence was removed from the pM53- $\Delta$ 16-106NLS by AgeI digestion and re-ligation generated the pM53- $\Delta$ 16-106 construct carrying only the 16-106 deletion.

pM53- $\Delta$ 16-106NLS: To generate the N-terminal M53 deletion mutants lacking aa16 to 106, the pOriR6K-zeo-ie-M53 was amplified by inverse touch down PCR (Padgett, 1996) using 5'-SapI-delN and 3'-NdeI-SapI primers which carried an NLS coding sequence derived from the SV40 large T antigen. The PCR product was treated with SapI and re-ligated generating the pM53- $\Delta$ 16-106NLS construct in which the deleted sequence was replaced with the SV40 NLS.

### C. Material and methods

pM53- $\Delta$ 16-136NLS: The N-terminal M53 deletion mutant lacking aa16 to 136 was generated by insertion of the NLS21 and NLS22 annealed synthetic oligonucleotides into the *Age*I and *Bsp*HI treated pM53- $\Delta$ 16-106NLS resulting in pM53- $\Delta$ 16-136NLS.

pOriR6K-zeo-ie-FlagM53: The pOriR6K-zeo-ie-FlagM53 used for pull down analysis of cellular interaction partners of the M53-M50 complex, was constructed as follows. Synthetic oligonucleotides Flag1 and Flag2 were annealed and inserted into *Kpn*I and *Ear*I digested pOriR6K-zeo-ie-M53 resulting in pOriR6K-zeo-ie-FlagM53.

pOriR6K-zeo-ie-HAM50: The pOriR6K-zeo-ie-HAM50, used for pull down analysis of cellular interaction partners of the M53-M50 complex, was kindly provided by A. Bubeck, LMU, unpublished.

pOriR6K-zeo-ie-M53:

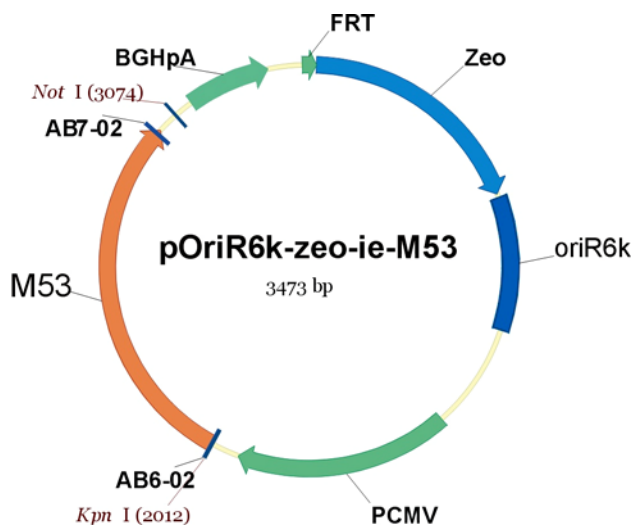


**Figure 8. Schematic representation of M53 inserted into the expression vector pOriR6k-zeo-ie.** Indicated the M53 ORF (orange), in blue the bacterial regulation elements (zeocin resistance gene and oriR6K) and in green elements for eukaryotic expression and insertion into the BAC genome (PCMV, BGHpA and FRT).

The M53 ORF was cloned into pOriR6K-zeo-ie rescue vector (Bubeck, 2004) from pCR3-M53 (Bubeck, 2004) using *Kpn*I and *Not*I resulting in pOriR6K-zeo-ie-M53 (Fig. 8) which was used due to its FRT-site as wt M53 rescue and expression vector in this study.

## C. Material and methods

pOriR6K-zeo-ie-STM50: The pOriR6K-zeo-ie-STM50, used for pull down analysis, was constructed as follows. Synthetic oligonucleotides ieST1 and ieST2 were annealed and inserted into pOriR6K-zeo-ie by Apal and XhoI resulting in pOriR6K-zeo-ie-ST. The M50 ORF was amplified by AB6-02 and M50Strep primers and cloned into pOriR6K-zeo-ie-ST by KpnI and XhoI.

M53-point mutants (Alanine-screening; L112A, H116A, F119A, P123A, D124A, L125A, E126A, K128A, Y129A, L130A, M133A, I137A, YL129,130A, KYL128-130A,  $\Delta$ 108-136A): Point mutations were introduced into the M53 ORF by mutated overlapping primers (see supplementary table for primer list) as follows. The M53 ORF was amplified by PCR using AB6-02 and reverse mutagenesis primers as well as AB7-02 and forward mutagenesis primers, thereby generating 5'- and 3'-M53 fragments, appropriately. The 5'-fragments were digested with KpnI/SapI, and 3'-fragments with SapI/MluI and then inserted into the KpnI and MluI treated pOriR6K-zeo-ie-M53 in a one step reaction.

### 1.6.2.3 Plasmid with temperature sensitive origin of replication ( $T_s$ )

pST76K-S4: The pST76K-S4 vector was generated by inserting a Tn7-based mini-transposon carrying the KpnI/SacI fragment of pGPS-4 (NEB, Frankfurt a.M., D) into pST76K (Posfai, 1997) thereby creating a new transposon donor vector with a temperature sensitive origin of replication.

### 1.6.2.4 MCMV-BACs

The  $\Delta$ M53-and  $\Delta$ M50-BACs were generated on the basis of pSM3fr-16FRT17, which served as wt MCMV-BAC in this study (Bubic, 2004). The  $\Delta$ M50-BAC was generated as described previously (Bubeck, 2004). For generation of the  $\Delta$ M53-BAC first a linear recombination fragment carrying a kanamycin resistance marker was generated by PCR on pACYC177 template (NEB) by using 5'-M53del and 3'-M53del primers (see supplementary table for primer list). Next, the M53-ORF (nucleotide positions 78461 to 79459 of MCMV strain Smith, according to Rawlinson (Rawlinson, 1996)) was deleted from pSM3fr-

### C. Material and methods

16FRT17 by ET recombination in *E. coli* using this linear recombination fragment as described previously (Wagner, 2004). All mutant MCMV BACs were generated by Flp mediated insertion of pOriR6K-zeo-ie derived expression plasmids into pSMfr3- $\Delta$ M50 or pSMfr3- $\Delta$ M53 (Bubeck, 2004; Lötzerich, 2006, table 1).

BAC-backbone	Inserted plasmid	Resulting mutant BAC
pSMfr- $\Delta$ M53	pOriR6K-zeo-ie-M53	pM53E
pSMfr- $\Delta$ M53	pM53- $\Delta$ 16-106NLS	pM53- $\Delta$ 16-106NLSE
pSMfr- $\Delta$ M53	pM53- $\Delta$ 16-106	pM53- $\Delta$ 16-106E
pSMfr- $\Delta$ M53	pM53- $\Delta$ 16-136NLS	pM53- $\Delta$ 16-136NLSE
pSMfr- $\Delta$ M53	pM53-L112A	pM53-L112AE
pSMfr- $\Delta$ M53	pM53-H116A	pM53-H116AE
pSMfr- $\Delta$ M53	pM53-F119A	pM53-F119AE
pSMfr- $\Delta$ M53	pM53-P123A	pM53-P123AE
pSMfr- $\Delta$ M53	pM53-D124A	pM53-D124AE
pSMfr- $\Delta$ M53	pM53-L125A	pM53-L125AE
pSMfr- $\Delta$ M53	pM53-E126A	pM53-E126AE
pSMfr- $\Delta$ M53	pM53-K128A	pM53-K128AE
pSMfr- $\Delta$ M53	pM53-Y129A	pM53-Y129AE
pSMfr- $\Delta$ M53	pM53-L130A	pM53-L130AE
pSMfr- $\Delta$ M53	pM53-M133A	pM53-M133AE
pSMfr- $\Delta$ M53	pM53-I137A	pM53-I137AE
pSMfr- $\Delta$ M53	pM53-YL129,130A	pM53-YL129,130AE
pSMfr- $\Delta$ M53	pM53-KYL128-130A	pM53-KYL128-130AE
pSMfr- $\Delta$ M53	pM53- $\Delta$ 108-136A	pM53- $\Delta$ 108-136AE
pSMfr- $\Delta$ M53	pOriR6K-zeo-ie-M53s106	pM53-s106E
pSMfr- $\Delta$ M53	pOriR6K-zeo-ie-M53s137	pM53-s137E
pSMfr- $\Delta$ M53	pOriR6K-zeo-ie-M53s168	pM53-s168E
pSMfr- $\Delta$ M53	pOriR6K-zeo-ie-M53s185	pM53-s185E
pSMfr- $\Delta$ M53	pOriR6K-zeo-ie-M53s233	pM53-s233E
pSMfr- $\Delta$ M53	pOriR6K-zeo-ie-M53s290	pM53-s290E
pSMfr- $\Delta$ M53	pOriR6K-zeo-ie-M53s309	pM53-s309E
pSMfr- $\Delta$ M53	pOriR6K-zeo-ie-M53s313	pM53-s313E
pSMfr- $\Delta$ M53	pOriR6K-zeo-ie-M53iX (in total 46 insertion mutants; see results 4., Fig. 21)	pM53-iXE
pSMfr- $\Delta$ M50	pOriR6K-zeo-ie-STM50	pSTM50E

**Table 1. BACs constructed during this study.**

## C. Material and methods

---

### 1.7 Bacterial strains

DH10B (Invitrogen, Karlsruhe, D): F<sup>-</sup> mcrA Δ(mrr-hsdRMS-mcrBC) φ80lacZΔM15 ΔlacX74 recA1 araD139 Δ(ara, leu)7697 galU galKλ<sup>-</sup> rpsL nupG

Pir1 (Invitrogen, Karlsruhe, D): F<sup>-</sup> Δlac169 rpoS (Am) robA1 creC510 hsdR514 endA recA1 uidA (ΔMluI)::pir-116

### 1.8 Cells

293	Adenovirus transformed human kidney-carcinoma cells (ATCC CRL 1573)
M2-10B4	Stroma-cell-line from bone marrow of BALB/c-mouse (ATCC CRL 1972)
NIH3T3	Contact inhibited murine fibroblasts of NIH Swiss-mouse (ATCC CRL 1658)
MEF	Murine embryonal fibroblasts of BALB/c-mouse (Serrano, 1997)

#### 1.8.1 Cell culture reagents

All cell culture reagents were received from Invitrogen (Gibco).

##### 1.8.1.1 Basal media

DMEM (+ 4500 mg/L-glucose; L-glutamine; L-pyruvate)  
RPMI 1640 (+ L-glutamine)  
RPMI 1640 (+ L-glutamine, - L-cystine; - L-methionine)

##### 1.8.1.2 Supplements and sera

D-PBS (-CaCl<sub>2</sub>; -MgCl<sub>2</sub>)  
L-glutamine (200 mM; 100x)  
NEAS (non essential amino acids; 100x)  
Penicillin-streptomycin-sulfate (100 IU/ml and 0.1 mg/ml)  
Sodium bicarbonate (7.5%)  
Trypsine/EDTA (0.5 g/l Trypsine; 0.2 g/l EDTA; 0.85 g/l NaCl)  
Foetal bovine sera (FCS)  
Newborn calf sera (NCS)

## 1.9 Viruses

The MCMV wild type (wt) and mutant viruses used in this study were derived from the bacterial artificial chromosomes (BACs) pSM3fr (Wagner, 1999), pSMfr3- $\Delta$ M50 (Bubeck, 2004) and pSMfr3- $\Delta$ M53 (Lötzerich, 2006) and constructed BACs, summarized in table 1. For virus reconstitution, BAC-DNA was transfected into MEF (see 2.4.2).

## 1.10 Antibodies

### 1.10.1 Primary antibodies

#### 1.10.1.1 Rabbit polyclonal antisera

Anti M50/p35	Muranyi, 2002
Anti Histone 3	Santa Cruz, California, USA
Anti Histone 4	Santa Cruz, California, USA

#### 1.10.1.2 Rabbit monoclonal antibodies

Anti Lamin B receptor (LBR)	Biomol, Hamurg, D
Anti Histone H3	Biomol, Hamburg, D
Anti Histone H4	Biomol, Hamburg, D

#### 1.10.1.3 Mouse monoclonal antibodies

CROMA 101 - pp89 (IE)	provided by S. Jonjic, University of Rijeka, Rijeka, Croatia
Anti HP1 $\alpha$	Biomol, Hamburg, D
Anti Histone H1	Santa Cruz, California, USA
Anti Histone H1.0	Abcam, Cambridge, UK

#### 1.10.1.4 Rat polyclonal antisera

Anti M53/p38	Eurogentec, Seraing, Belgium
Anti M86	Eurogentec, Seraing, Belgium



## C. Material and methods

---

### 1.10.1.5 Goat polyclonal antisera

Anti p32	Santa Cruz, California, USA
Anti Lamin B1	Santa Cruz, California, USA
Anti Lamin A/C	Santa Cruz, California, USA
Anti HP1 $\alpha$	Santa Cruz, California, USA
Anti MAN1	Santa Cruz, California, USA
Anti Emerin	Santa Cruz, California, USA
Anti LAP2	Santa Cruz, California, USA

### 1.10.2 Secondary antibodies

All secondary antibodies used in this study were pre-adsorbed to ensure minimal cross-reaction with serum proteins of other species.

#### 1.10.2.1 FITC-conjugates

Donkey anti-rabbit IgG	Dianova, Hamburg, D
Donkey anti-mouse IgG	Dianova, Hamburg, D
Donkey anti-rat IgG	Dianova, Hamburg, D
Donkey anti-goat IgG	Dianova, Hamburg, D

#### 1.10.2.2 Texas-Red-conjugates

Donkey anti-rabbit IgG	Dianova, Hamburg, D
Donkey anti-mouse IgG	Dianova, Hamburg, D
Donkey anti-rat IgG	Dianova, Hamburg, D
Donkey anti-goat IgG	Dianova, Hamburg, D

#### 1.10.2.3 Alexa-488-conjugates

Goat anti-mouse IgG	Mo Bi Tec, Goettingen, D
Goat anti-rabbit IgG	Mo Bi Tec, Goettingen, D
Goat anti-rat IgG	Mo Bi Tec, Goettingen, D

#### 1.10.2.4 Alexa-633-conjugates

Goat anti-mouse IgG	Mo Bi Tec, Goettingen, D
Goat anti-rabbit IgG	Mo Bi Tec, Goettingen, D
Goat anti-rat IgG	Mo Bi Tec, Goettingen, D

## C. Material and methods

---

### 1.10.2.5 Peroxidase (Pox)-conjugates

Donkey anti-rabbit IgG	Dianova, Hamburg, D
Goat anti-mouse IgG	Dianova, Hamburg, D
Goat ant-rat IgG	Dianova, Hamburg, D
Donkey anti-goat IgG	Dianova, Hamburg, D

## 2. Methods

### 2.1 Isolation and purification of nucleic acids

#### 2.1.1 Small scale isolation of plasmid DNA

LB medium  
10 g Bacto tryptone  
5 g yeast extract  
10 g NaCl  
add ddH<sub>2</sub>O to 1l  
sterilize at 121<sup>0</sup>C for 2.5 h

LB agar  
7.5 g agar in 500 ml LB medium  
sterilize at 121<sup>0</sup>C for 2.5 h

Antibiotics  
Zeocin: 30 µg/ml  
Kanamycin: 50 µg/ml  
Chloramphenicol: 25 µg/ml  
Ampicillin: 100 µg/ml

LB-zeo medium  
10 g Bacto tryptone  
5 g yeast extract  
10 g NaCl  
add ddH<sub>2</sub>O to 1l  
sterilize at 121<sup>0</sup>C  
for 2.5 h

LB-zeo agar  
7.5 g agar in 500 ml LB-  
zeo medium  
sterilize at 121<sup>0</sup>C  
for 2.5 h

### C. Material and methods

---

Solution I (resuspension buffer; Amersham)	100 mM Tris/HCl, pH 7.5 10 mM EDTA, 400 µg/ml RNase I
Solution II (lysis buffer; Amersham)	0.2 M NaOH 1% (w/v) SDS
Solution III (neutralization buffer; Amersham)	2.5 M KOAc 2.5 M HOAc

Additional requirements: Wash buffer (Amersham) and ddH<sub>2</sub>O.

Bacteria were cultivated at 37°C (or at 30°C for T<sub>s</sub> plasmids, see 1.6.2.3) on LB- or LB-zeo agar plates over night (ON) using appropriate antibiotics for selection of the plasmids of interest. Isolated colonies were picked and 3 ml LB- or LB-zeo medium (if zeocin was recommended for selection) supplemented with appropriate antibiotics were inoculated. The cultures were incubated over night (ON) at 37°C (or at 30°C for propagation of T<sub>s</sub> plasmids) in a bacteria shaker agitating at 180 rpm.

For small scale isolation of plasmids the GFX-Micro Plasmid Kit (Amersham) was used. 2 ml of bacterial suspension was pelleted in an Eppendorf reaction tube and the pellet was resuspended in 300 µl of solution I. For alkaline lysis 300 µl of solution II was added. Addition of 600 µl solution III then led to precipitation of SDS, chromosomal DNA and protein content. After centrifugation at 14.000 rpm for 5 min in an Eppendorf centrifuge 5415C the supernatant was transferred to glasfiber-matrix columns of the GFX Micro Plasmid Prep Kit (Amersham). Next the columns were centrifuged at 14.000 rpm for 1 min and after addition of 400 µl wash buffer (Amersham) this centrifugation step was repeated. To elute the plasmid-DNA which is bound to the columns 50-100 µl of ddH<sub>2</sub>O was added to the columns, incubated at room temperature (RT) for 1 min followed by centrifugation at 14.000 rpm for 2 min. 5 µl of the DNA preparation were analyzed by restriction pattern analysis.

## C. Material and methods

---

### 2.1.2 Large scale isolation of plasmid DNA

P1-resuspension buffer (Qiagen)	50 mM Tris/HCl, pH 8.0 10 mM EDTA 100 µg/ml RNase A
P2-lysis buffer (Qiagen)	1% (w/v) SDS 200 mM NaOH
P3-neutralisation buffer (Qiagen)	3 M KOAc pH 5.5 with acetic acid
QBT-equilibration buffer (Qiagen)	750 mM NaCl 50 mM MOPS 15% (v/v) EtOH 0.15% (w/v) Triton-X-100 pH 7.0
QC-wash buffer (Qiagen)	1 M NaCl 50 mM MOPS 15% (v/v) EtOH pH 7.0
QF-elution buffer (Qiagen)	50 mM Tris/HCl, pH 8.5 1.25 M NaCl 15% (v/v) EtOH
Ion-exchange columns (Qiagen)	Qiagen-tip 500

Additional requirements: Isopropanol, 70% EtOH and ddH<sub>2</sub>O.

250 ml LB- or LB-zeo medium (if zeocin was recommended for selection) were supplemented with appropriate antibiotics (see 2.1.1), inoculated with 5 ml of over night bacterial culture of one bacterial clone and incubated at 37<sup>0</sup>C (or at 30<sup>0</sup>C for propagation of T<sub>s</sub> plasmids) over night on a bacteria shaker at 180 rpm.

For isolation of up to 500 µg of plasmid-DNA the Qiagen Plasmid Midi Kit was used. Bacteria were pelleted (15 min; 6000 rpm; 4<sup>0</sup>C; GS-3 rotor, Sorvall) and resuspended in 10 ml buffer P1. Afterwards 10 ml of buffer P2 was added and lysed for 5 min at room temperature (RT). After addition of 10 ml neutralizing buffer P3 and incubation for 20 min on ice, SDS, proteins and chromosomal DNA was removed by centrifugation (30 min; 13.000 rpm; 4<sup>0</sup>C; SS-34 rotor,

## C. Material and methods

Sorvall). An Ion exchange column Qiagen-tip 500 was equilibrated with 10 ml buffer QBT and applied with the filtered cleared supernatant from the previous centrifugation step, thereby allowing the supernatant to enter the resin by gravity flow. The columns were next washed twice with buffer QC and plasmid-DNA was eluted with 15 ml buffer QF. Eluted DNA was afterwards precipitated with 10.5 ml isopropanol and centrifuged for 30 min at 4<sup>0</sup>C and 12.000 rpm in a SS-34 rotor. The DNA-pellet was washed with 70% ethanol, air-dried and dissolved in up to 500 µl ddH<sub>2</sub>O.

### 2.1.3 Small scale isolation of BAC-DNA

P1-resuspension buffer (Qiagen)	50 mM Tris/HCl, pH 8.0 10 mM EDTA 100 µg/ml RNase A
P2-lysis buffer (Qiagen)	200 mM NaOH 1% (w/v) SDS
P3-neutralisation buffer (Qiagen)	3 M KAc pH 5.5 with acetic acid

Additional requirements: Phenol/chloroform/isoamyl alcohol (25:24:1), Isopropanol, 70% EtOH and TE-buffer (supplemented with 10 µg/ml RNase A).

The CMV BAC-DNA has a size of over 230 kbp. In order to avoid damage of the BAC-DNA during preparation the probes should neither being harshly shaken nor vortexed. It was also recommended to use cut pipette-tips. 10 ml LB-media supplemented with appropriate antibiotics (see 2.1.1) were inoculated with one bacterial colony and incubated over night at 37<sup>0</sup>C. The bacterial suspension was transferred to a 15 ml Falcon reaction tube and centrifuged in a Heraeus-centrifuge (5 min; 3500 rpm). For bacterial resuspension and -lysis and for neutralization of the lysate buffers P1-P3 from the Qiagen Plasmid Midi Kit were used.

The bacterial pellet was resuspended in 300 µl P1 (Qiagen) and transferred to a 2 ml Eppendorf reaction tube. For alkaline lysis 300 µl P2 (Qiagen). After an incubation for 5 min at RT SDS, chromosomal DNA and protein contents were precipitated due to addition of 300 µl P3 (Qiagen) and an incubation on ice for

## C. Material and methods

10 min. After centrifugation in an Eppendorf centrifuge 5415C (14.000 rpm; 10 min; RT) the supernatant was carefully transferred to a new 2 ml Eppendorf reaction tube. DNA was extracted by addition of approximately 1 ml phenol/chloroform/isoamyl alcohol (25:24:1), which accumulates DNA in the upper watery phase after an additional 5 min centrifugation step at 14.000 rpm. Next, the watery phase was transferred to a new 2 ml Eppendorf reaction tube and DNA was precipitated by addition of 1 ml isopropanol followed by centrifugation (14.000 rpm; 20 min; 4°C). After a washing step with 1 ml of 70% ethanol the DNA pellet was air dried and resuspended in 100 µl TE-buffer (supplemented with 10 µg/ml RNase A). For the following restriction pattern analysis normally 45 µl of the isolated BAC-DNA was used.

### 2.1.4 Large scale isolation of BAC-DNA

S1-resuspension buffer (Macherey and Nagel)	50 mM Tris/HCl, pH 8.0 10 mM EDTA 100 µg/ml RNase A
S2-lysis buffer (Macherey and Nagel)	200 mM NaOH 1% (w/v) SDS
S3-neutralization buffer (Macherey and Nagel)	2.8 M KAc pH 5.1
N2-equilibration buffer (Macherey and Nagel)	100 mM Tris 900 mM KCl 15% (v/v) EtOH 0.15% (w/v) Triton-X-100 pH 6.3 with H <sub>3</sub> PO <sub>4</sub>
N3-wash buffer (Macherey and Nagel)	100 mM Tris 1.15 M KCl 15% (v/v) EtOH pH 6.3 with H <sub>3</sub> PO <sub>4</sub>
N5-elution buffer (Macherey and Nagel)	100 mM Tris 1 M KCl 15% (v/v) EtOH pH 8.5 with H <sub>3</sub> PO <sub>4</sub>

Additional requirements: Isopropanol, 70% EtOH and TE-buffer (10 mM Tris/HCl, 1 mM EDTA, pH 8.0).

## C. Material and methods

---

For large scale isolation of BAC-DNA the Nucleobond-AX 100 Kit from Macherey and Nagel was used. For pipetting of BAC-DNA it was recommended to use cut pipette tips to minimize shear forces that can damage the large BAC-DNA molecules. 200 ml LB-media supplemented with appropriate antibiotics (see 2.1.1) were inoculated with 5 ml bacterial pre-culture and incubated over night at 37<sup>0</sup>C in a bacteria shaker at 180 rpm. Bacteria were pelleted by centrifugation (6000 rpm; 15 min; GS-3 rotor). Next, the bacterial pellet was resuspended in 8 ml S1 buffer (Macherey and Nagel). For alkaline lysis 8 ml S2 buffer (Macherey and Nagel) was added to the bacterial suspension. After an incubation for 5 min at RT SDS, chromosomal DNA and protein contents were precipitated due to addition of 8 ml S3 buffer (Macherey and Nagel) and an incubation on ice for 10 min. Next, the bacterial lysate was cleared by filtration and applied to the equilibrated adsorption cartridge. Afterwards, a total volume of 12 ml of N3-washing buffer was applied to the cartridge in three steps and BAC-DNA was eluted twice by addition of 2x 2.5 ml buffer N5 that was pre-warmed to 50<sup>0</sup>C. DNA was precipitated with isopropanol, washed with 70% ethanol and finally the air dried BAC-DNA pellet was dissolved in 150 µl TE-buffer for 2 hours at 37<sup>0</sup>C or ON at 4<sup>0</sup>C and stored at 4<sup>0</sup>C.

### 2.1.5 Determination of DNA concentration and purity of the isolated DNA

In order to determine concentration and purity of the isolated DNA the optical density (OD) at 260 nm and at 280 nm was determined using an Eppendorf spectrophotometer. 1 OD<sub>260</sub> unit equals 50 µg/ml double-stranded DNA or 38 µg/ml single-stranded DNA or RNA. The measured OD<sub>260</sub> allowed the calculation of nucleic acid concentration of the sample. Absorption at 280 nm indicated the presence of protein contamination, because aromatic amino acids absorb strongly at 280 nm. The ratio between the two readings at OD<sub>260</sub> nm and OD<sub>280</sub> nm allowed an estimation about DNA sample purity. In the best case this ratio should range between 1.8 and 2.

## 2.2 Analysis and cloning of DNA

### 2.2.1 Restriction digest of DNA

Restriction endonucleases	New England Biolabs, Schwalbach, D
10x restriction buffer	New England Biolabs, Schwalbach, D

Restriction of DNA was performed with commercial restriction endonucleases in the recommended buffer systems. For restriction pattern analysis of plasmids, 5  $\mu$ l of a small scale plasmid preparation were used, which corresponds to approximately 0.5-1  $\mu$ g of DNA. Regularly the restriction was performed in a total volume of 40  $\mu$ l for 1-2 hours according to the instructions of the manufacturer thereby adding to 0.5-1  $\mu$ g of DNA 20 units of the restriction enzyme, 4  $\mu$ l of the recommended 10x buffer, 4  $\mu$ l of 10x BSA (if necessary) and ddH<sub>2</sub>O.

For analysis of BAC-DNA the restriction digest was performed in a total volume of 70  $\mu$ l, adding 7  $\mu$ l of the recommended 10x reaction buffer, 7  $\mu$ l of 10x BSA, 40 units of the respective restriction endonuclease and ddH<sub>2</sub>O to 45  $\mu$ l of a small scale BAC-DNA preparation. BAC-DNA digests were incubated 4 hours or over night according to the instructions of the manufacturer. For restriction pattern analysis of large scale DNA preparations of either plasmids or BACs 1.5  $\mu$ g of DNA were digested in a total volume of 40-70  $\mu$ l.

### 2.2.2 Dephosphorylation of DNA

To avoid re-circulation of cleaved, linearized vector DNA after restriction digest, the 5'-terminal phosphate groups from DNA fragments were dephosphorylated by alkaline phosphatase treatment (SAP, "shrimp alkaline phosphatase"; NEB). SAP (1 unit/pmol DNA) was directly added after the restriction digest and incubated for one hour at 37°C. Afterwards, SAP was heat-inactivated at 75°C for 20 min.



## C. Material and methods

### 2.2.3 Amplification of DNA by Polymerase Chain Reaction (PCR)

Oligonucleotides	Metabion, Martinsried, D
Template	10-100 ng matrix-DNA
Polymerase	AmpliTag DNA Polymerase (Applied Biosystems, New Jersey, USA)
10x reaction buffer containing 15 mM MgCl <sub>2</sub>	GeneAmp 10x PCR buffer (Applied Biosystems, New Jersey, USA)
Desoxynucleotides	PCR Nucleotide Mix (10 mM; Roche, Mannheim, D)

The Polymerase Chain Reaction is a tool for in vitro amplification of defined DNA sequences. The standard PCR reaction for a fast screening of generated random transposon insertion mutants was performed with DNA as a template at a concentration of 10 ng-100 ng in a total reaction volume of 50 µl and following conditions:

#### Reaction:

10 ng-100 ng	template-DNA
400 nM (each)	oligonucleotide-primer
10 µM (each)	dNTP-mix
0.1 vol.	10x GeneAmp PCR buffer containing 15 mM MgCl <sub>2</sub>
10 units	AmpliTag DNA Polymerase
0.1 vol.	DMSO (if needed)

#### Temperature-cycles:

- one cycle for 5 min at 94<sup>0</sup>C
- 25 repeating cycles with
  - 30 sec at 94<sup>0</sup>C
  - 45 sec at appropriate hybridization-temperature
  - 45 sec elongation-time at 72<sup>0</sup>C
- 7 min at 72<sup>0</sup>C

For cloning purposes the amplification of coding sequences longer than 1000 bp was performed by means of the Expand High Fidelity PCR system (Roche). The High Fidelity Polymerase of this kit possesses a prove-reading activity and

### C. Material and methods

is therefore more precise. Using a touch down program the PCR was performed in a total reaction volume of 100  $\mu$ l under following conditions:

#### Reaction:

10 ng-100 ng	template-DNA
400 nM (each)	oligonucleotide-primer
60 $\mu$ M (each)	dNTP-mix
0.1 vol.	10x Expand HF reaction buffer containing 15 mM MgCl <sub>2</sub>
3.5 units	Expand High Fidelity PCR system Polymerase
0.1 vol.	DMSO (if needed)

#### Temperature-cycles:

- one cycle for 5 min at 95<sup>o</sup>C
- 35 repeating cycles with
  - 30 sec at 94<sup>o</sup>C
  - 1 min at hybridization-temperatures dropping down per cycle from 62<sup>o</sup>C to 50<sup>o</sup>C
  - 1 min 30 sec elongation time at 68<sup>o</sup>C
- 6 min at 68<sup>o</sup>C

Polymerase Chain Reaction was performed using a thermo-cycler GeneAmp<sup>®</sup>PCR system 9700 (Applied Biosystems, New Jersey, USA). For calculation of the hybridizing-temperature ( $T_H$ ) of a primer the following formula was applied:

$$T_H (^{\circ}\text{C}) = 60 + [(G+C) \times 41 / N_{t_{\text{number}}}] - (600 / N_{t_{\text{number}}})$$

Here G+C corresponds to the number of cytosines and guanidins in the primer sequence and  $N_{t_{\text{number}}}$  to the length of the oligonucleotide primer.

10  $\mu$ l of the PCR reaction were tested for amplification on a 0.8% TAE/agarose gel. For purification of the amplified DNA the remaining 90  $\mu$ l of the PCR reaction were applied on a 1% TAE/agarose gel and the respective band was cut out and purified using the GFX<sup>™</sup> Gel Extraction and DNA Purification Kit (Amersham; see 2.2.4).

## C. Material and methods

---

### 2.2.3 Agarose gel electrophoresis

Agarose	Invitrogen, Karlsruhe, D
1x TAE (electrophoresis buffer)	40 mM Tris-acetate 1 mM EDTA
1x TBE (electrophoresis buffer BAC-DNA)	90 mM Tris 90 mM boric acid 1 mM EDTA, pH 8.3
Ethidiumbromide stock solution	10 mg/ml in TAE
5x DNA loading buffer	40% (w/v) sucrose 0.05% (w/v) brom-phenolblue 0.1 % (w/v) SDS 1 mM EDTA, pH 8.0
DNA length standard	1 kb "ladder", 1 µg/ml (Gibco/BRL, Eggenstein, D)

DNA fragments obtained by restriction enzyme digests or PCR reaction were separated and analyzed by agarose gel electrophoresis. Depending on the expected fragment size the digested plasmid DNA or PCR amplicon was separated in a 0.6-1% (w/v) TAE/agarose gel while digested BAC-DNA always was separated in a 0.8% TBE/agarose gel.

The agarose was dissolved due to heating in an appropriate volume 1x TAE- or TBE buffer and cooled down to 56°C. Afterwards 1 µg/ml ethidium bromide was added and the agarose was poured to a horizontal gel chamber. After setting of the agarose the gel was overlaid with 1x TAE- or TBE buffer and loaded with DNA-length-standard and probes that were supplemented with loading buffer. Separation was performed at constant voltage of 5 V/cm for ½ hour to one hour. For separation of BAC-DNA a constant voltage of 70 V for 14-16 hours was used. After electrophoresis DNA was visualized by UV-light using an Eagle-Eye imaging system.

## C. Material and methods

---

### 2.2.4 Isolation of DNA fragments from agarose-gels

Gel-extraction-system

GFX™ gel extraction- and DNA purification kit (Pharmacia/LKB, Uppsala, S)

If separated DNA fragments had to be used for further cloning steps, the respective DNA bands were cut from the gel and purified by means of the GFX™ gel extraction- and DNA purification kit (Pharmacia) following the instructions of the manufacturer. To prevent UV-light induced DNA damage, weak UV light was applied for DNA visualization while cutting. The content of eluted DNA was determined photometrically or estimated on a 1% TAE/agarose gel by means of the DNA length standard.

### 2.2.5 Annealing of synthetic oligonucleotides

For insertion of short DNA fragments into a vector, complementary oligonucleotides were synthesized (Metabion) and annealed to form a double stranded DNA fragment. Oligonucleotides were flanked by suitable overhangs as usually obtained after restriction enzyme cuts to allow the insertion into a respectively cut vector. Two complementary oligonucleotides were mixed to a concentration of about 40  $\mu$ M each, incubated at 75<sup>0</sup>C for 5 min and cooled down to RT for 30 min. 1  $\mu$ l of the annealed oligonucleotides, neat and diluted 1/50, were added to separate ligation reactions containing 100 ng of an adequately cut and purified vector fragment.

### 2.2.6 Ligation of DNA fragments

DNA-fragments were ligated by means of the T4-DNA ligase (NEB) with a molar ratio of 1:4 between the vector (100 ng) and the insert. Ligation was performed in a total volume of 10  $\mu$ l by mixing 400 units of T4-DNA ligase (2  $\mu$ l), 1  $\mu$ l of the respective 10x T4 ligase reaction buffer, DNA fragments and ddH<sub>2</sub>O. The reaction was incubated over night (ON) at 16<sup>0</sup>C for “blunt”-end DNA fragments or at RT for 1 hour for overlapping (“sticky”)-end DNA fragments.

## C. Material and methods

---

### 2.2.7 Transformation of recombinant DNA

#### 2.2.7.1 Preparation of electro-competent bacteria

Glycerol-solutions	15% glycerol (w/v) in H <sub>2</sub> O
	10% glycerol (w/v) in H <sub>2</sub> O

All preparation steps were performed on ice or at 4<sup>0</sup>C, using pre-cooled pipettes and solutions. For production of electro competent bacteria 400 ml LB-media (if necessary supplemented with antibiotics) were inoculated with 2 ml of an overnight bacteria culture and incubated at 37<sup>0</sup>C or at 30<sup>0</sup>C to an OD<sub>600</sub> of about 0.5 (after 2-4 hours of cultivation). Afterwards, the bacteria culture was put on ice and pelleted at 5000 rpm and 4<sup>0</sup>C for 10 min. To remove salt and medium components the bacteria pellet was washed twice by resuspension in 100 ml ddH<sub>2</sub>O followed by two steps of resuspension in 15% glycerol and subsequently four times pelleting at 5000 rpm and 4<sup>0</sup>C for 10 min. Afterwards the pellet was resuspended in 1.5 ml of 10% glycerol and 60 µl aliquots in Eppendorf reaction tubes were snap frozen in liquid nitrogen and stored at -80<sup>0</sup>C.

#### 2.2.7.2 Transformation of electrocompetent bacteria

SOC medium	20 g/l Bacto tryptone
	5 g/l yeast extract
	0.5 g/l NaCl
	2.5 mM KCl
	10 mM MgCl <sub>2</sub>
	20 mM glucose

The electroporation technique is based on the fact that by a short electric impulse (10 µs) of high field energy (~12.5 kV per cm) the permeability of the bacteria cell wall is increased which leads to an uptake of DNA molecules. To introduce plasmids into electrocompetent bacteria 2 µl of ligation mix were added to 60 µl of electrocompetent bacteria and transferred to a pre-cooled transformation cuvette (0,2 µm in diameter; BioRad). Next, the bacteria were pulsed with 2.5 kV, 200 Ω and 25 µF (Gene Pulser II; BioRad). Immediately after the pulse 1 ml of SOC medium was added and the bacteria were transferred to a 1.5 ml Eppendorf reaction tube for incubation at 37<sup>0</sup>C or 30<sup>0</sup>C.

## C. Material and methods

---

After one hour 50-200  $\mu$ l of bacteria culture were plated on pre-warmed agar plates supplemented with appropriate antibiotics and incubated at 37<sup>0</sup>C or 43<sup>0</sup>C over night.

### 2.2.8 Linker scanning mutagenesis of the M53 ORF

GPS<sup>TM</sup>-LS Linker-Scanning System NEB, Frankfurt  
a.M., D

For the mutagenesis procedure the M53 ORF was cloned from pCR3-M53 (Bubeck, 2004) into Litmus28 (NEB, Frankfurt a.M., D) using KpnI and XbaI generating pL-M53 which was used as target vector for the transposon mutagenesis. pST76K-S4, a new transposon donor vector with a temperature sensitive origin of replication, was generated by inserting the mini-transposon carrying the KpnI/SacI fragment of pGPS-4 (NEB) into pST76K (Posfai, 2004). pLit28-M53 was subjected to in vitro random transposon insertion mutagenesis using TnsABC\*-transposase (NEB) and pST76K-S4 (see 1.6.2.3) as donor according to the manufacturer instructions. The following setting was used:

Donor	1 $\mu$ l
Target	1 $\mu$ l
10x GPS Buffer	2 $\mu$ l
ddH <sub>2</sub> O	14 $\mu$ l
TnsABC* Transposase	1 $\mu$ l

After incubation of 10 min at 37<sup>0</sup>C which is needed for the assembly reaction 1 $\mu$ l of Start-B Solution was added (300mM MgAc). During an incubation time of one hour at 37<sup>0</sup>C the strand transfer reaction was performed. Afterwards the transposase was heat-inactivated at 75<sup>0</sup>C for 10 min, put on ice for 5 min and the reaction-mix was precipitated by addition of 2  $\mu$ l NaAc (3M NaAc, pH 5.2) and 100  $\mu$ l 100% EtOH and incubation for 15 min at -80<sup>0</sup>C. The resulting DNA-pellet was dissolved in 5-10  $\mu$ l ddH<sub>2</sub>O. *E. coli* DH10B cells (Invitrogen) were transformed by 2  $\mu$ l of the transposition mixture and insertion mutants were selected by chloramphenicol and ampicillin at 43<sup>0</sup>C to remove both the intact acceptor and donor plasmids. Plasmid DNA was prepared from this primary

### C. Material and methods

pool of insertion mutants and the 1084 bp KpnI/NsiI fragments containing the M53 ORF and the randomly inserted mini-transposons were isolated and re-cloned into KpnI/NsiI treated pOriR6K-zeo-ie rescue plasmid. Recombinants containing the M53 ORF with the mini-transposon insertions were selected by chloramphenicol and zeocin. Plasmid DNA was prepared from this secondary pool of insertion mutants and the mini-transposon was removed by PmeI digestion and re-ligation generating a pOriR6K-zeo-ie-M53mut insertion library, which was maintained in *E. coli* PIR1 (Invitrogen). Insertion sites were identified for selected clones by PCR screening and sequencing as described previously (Bubeck, 2004; Fig. 9).

The *in vitro* transposition reaction was also performed with a linearized KpnI/NotI-M53-fragment which was obtained by restriction of pOriR6K-zeo-ie-M53. Here instead of 60 min the strand transfer reaction was prolonged to 100 min. After heat-inactivation of the transposase the KpnI/NotI-M53-fragment was re-ligated for two hours at 16°C with the KpnI/NotI-digested pOriR6K-zeo-ie followed by precipitation.

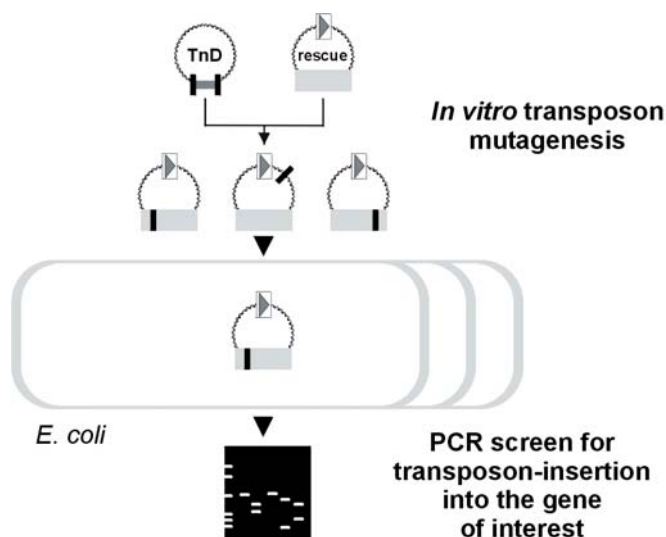


**Figure 9. General principle of a random mutagenesis of an essential viral gene.** In a first step the viral gene of interest (gray box) is sub-cloned into a rescue plasmid (rescue) containing one FRT site (open box with gray triangle). This plasmid is subjected to an *in vitro* Tn7-based random mutagenesis procedure, leading to a mutant library with 15 bp-insertions (black box) into the target plasmid. This mutant library is transformed into *E. coli* (open boxes) and single clones are screened by PCR for insertions into the gene of interest. Adapted from Bubeck, 2004.

## C. Material and methods

### 2.3 Cells and viruses

#### 2.3.1 Tissue culture

##### 2.3.1.1 Cultivation of cells

Cell line	Basic medium	Additives	Split/interval.
MEF	DMEM	10% FCS, 0,6% (w/v) Pen., 1,3% (w/v) Strep	1:3/3-4 days
M2-10B4	RPMI	10% FCS, 0,6% (w/v) Pen., 1,3% (w/v) Strep	1:6 /3-4 days
293	DMEM	10% FCS, 0,6% (w/v) Pen., 1,3% (w/v) Strep., 0,3 mg/ml Q	1:12/4 days
NIH-3T3	DMEM	5% NCS, 0,6% (w/v) Pen., 1,3% (w/v) Strep.	1:6/3-4 days

**Table 2. Cell lines used during this work.** List of Cell lines and culture media, prepared from the commercial available basic media and additives. In the last column the dilution of the cells for each split and the split interval is indicated.

All cell lines were cultivated on culture dishes in an incubator at 37<sup>0</sup>C, 5% CO<sub>2</sub> and 95% relative humidity. Cells were split every 3-6 days in a ratio between 1:2 to 1:12 (see table 2). In order to split confluent cells the medium was removed, cells were washed with 2-10 ml PBS and detached from the bottom of the culture dish by a treatment with few drops of trypsin/EDTA for 1-2 min at RT. Detached cells were resuspended in fresh medium thereby inactivating the trypsin. A pertinent amount was transferred to a new culture dish with fresh medium. NIH 3T3 murine fibroblast (ATCC CRL 1658), M2-10B4, a bone marrow stromal cell line (ATCC CRL 1972), human 293 cells (ATCC CRL 1573), and mouse embryonic fibroblasts (MEF) were propagated as described previously (Menard, 2003).

##### 2.3.1.2 Freezing and thawing of eukaryotic cells

Freezing medium

10% (v/v) DMSO  
40% (v/v) FCS  
in DMEM medium

For freezing cells were detached from the culture dish by trypsin treatment, centrifuged (Haereus) at 315x g for 5 min and resuspended at a concentration of 5x 10<sup>6</sup> to 1x 10<sup>7</sup> cells in freezing medium. This suspension was aliquoted to pre-cooled Cryotubes<sup>TM</sup> (Nunc), which were cautiously cooled down to -80<sup>0</sup>C and after 48-72 hours transferred for long terms storage to liquid nitrogen.



## C. Material and methods

---

Cells were thawed at 37<sup>0</sup>C in a water bath and as soon as possible supplemented with 10 ml of appropriate medium to dilute toxic DMSO. After centrifugation at 315x g for 5 min (Heraeus) cells were resuspended in fresh culture medium and transferred to culture dishes.

### 2.3.2 Working with MCMV

#### 2.3.2.1 Generation of recombinant MCMV-BACs

The  $\Delta$ M53-BAC was generated on the basis of pSM3fr-16FRT17 (Bubic, 2004). A linear recombination fragment carrying a kanamycin resistance marker was generated by PCR on pACYC177 template (NEB) by using 5'-M53del and 3'-M53del primers. The M53-ORF (nucleotide positions 78461 to 79459 of MCMV strain Smith, according to Rawlinson (Rawlinson, 1996)) was deleted from pSM3fr-16FRT17 by ET recombination in *E. coli* using this linear recombination fragment as described previously (Wagner, 2004). The wt and mutant rescue plasmids were inserted into the  $\Delta$ M53-BAC at the FRT site as described previously (Bubeck, 2004). Here mutagenesis was performed in the RecA-recombinase negative *E.coli*-strain DH10B by means of the pCP20 plasmid which carries the FLP-recombinase, an ampicillin resistance-cassette and a temperature-sensitive (T<sub>s</sub>) origin of replication (ori). This origin causes a low copy number per bacteria and replicates at 30<sup>0</sup>C. For FLP mediated recombination, bacteria were kept for 15 min under non-selective conditions. Afterwards, 150  $\mu$ l of bacteria were plated on Cam/Zeo plates and cultured at 43<sup>0</sup>C. At non permissive temperature of more than 37<sup>0</sup>C the pCP20 plasmid got lost (Fig. 10). On the following day single colonies were picked for small scale BAC-DNA preparation in order to test for single recombination events.

## C. Material and methods

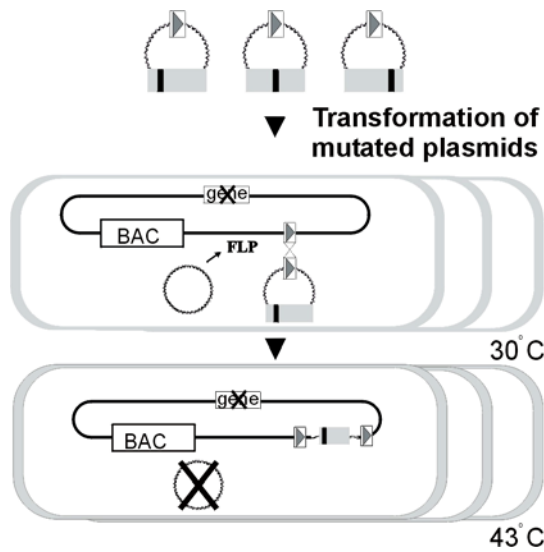


**Figure 10. Re-insertion of mutated plasmids into the viral genome.** To re-insert the gene mutants into the viral genome the respective MCMV-BAC and a FLP recombinase expressing plasmid (FLP) are maintained in *E.coli*. Subsequently, the rescue plasmids are transformed into *E.coli*. FLP recombinase mediates site-specific recombination between the FRT sites and unifies the BAC and the rescue plasmid. Selection with chloramphenicol and zeocin identifies BACs with the inserted rescue plasmid carrying the mutated gene of interest. Adapted from Bubeck, 2004.

### 2.3.2.2 Reconstitution of recombinant MCMV-BACs to virus

The wt and mutant MCMV-BACs were reconstituted to virus by transfection of semi-confluent MEF on 6 cm dishes with 1.5  $\mu$ g of purified BAC-DNA by means of Superfect<sup>®</sup> transfection reagent (Qiagen, see 2.4.2). Thereby BAC-DNA was added up to 150  $\mu$ l with media (without supplements) and mixed gently. After addition of 10  $\mu$ l Superfect<sup>®</sup> transfection reagent and mixing the solution was incubated at RT for 10-15 min. Afterwards the probes were added up to 1 ml with supplemented medium, transferred to PBS-washed cells and incubated in an incubator for 2.5-3.5 hours. After incubation the Superfect/DNA mixture was removed from the cells and replaced by fresh culture media. Always two independent BAC clones were transfected in two replicates. 24 hours after transfection cells were re-plated onto 10 cm dishes and then re-fed weekly. Cultures were inspected during six weeks after transfection (Fig. 11). As control pM53E DNA was transfected and a reconstitution experiment was considered valid when pM53E DNA derived virus plaques occurred during the second week post transfection.

The wild type (wt) MCMV Smith strain was recovered from pSM3fr-BAC (Wagner, 1999). All mutant viruses were derived from the pSM3fr-16FRT17-BAC carrying an FRT site between the genes m16 and m17. Growth properties of the 16FRT17 MCMV are identical to the (wt) MCMV both in vitro and in vivo

## C. Material and methods

(Bubic, 2004). Reconstituted viruses were propagated on M2-10B4 cells (Menard, 2003) and titrated on MEF by a plaque assay (Reddehase, 1985).

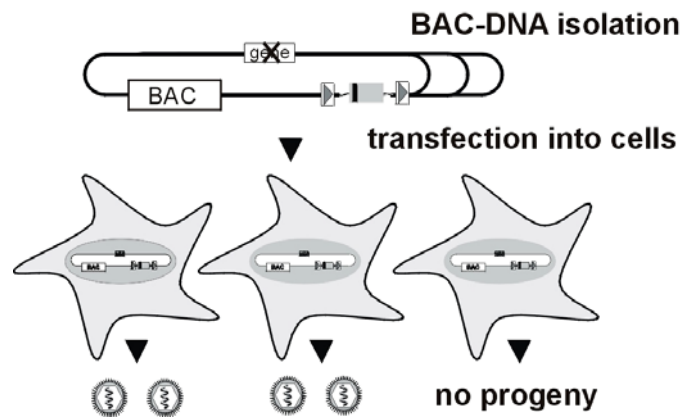


**Figure 11. Virus-reconstitution.** BAC-DNA was isolated and transfected into eukaryotic cells for virus-reconstitution and cells were screened for viral plaques. Adapted from Bubeck, 2004.

### 2.3.2.3 MCMV virus stock preparation

VSB (Virus Standard Buffer)

0.05 M Tris/HCl  
0.012 M KCl  
0.005 M EDTA  
pH 7.8 with HCl

For a high titer virus stock preparation M2-10B4-cells were cultured on 12-30 dishes (14 cm) and at a confluency of 80% each dish was infected with around 1 ml of reconstituted virus supernatant from lysed 10 cm culture dishes. Alternatively, at a confluency of 30% cells were infected with an MOI of 0.1. After 3-5 days, when cells showed up an overall cytopathic effect, the virus-cell suspension was harvested and transferred to sterile 250 ml centrifugation beaker. All following steps of virus stock preparation were performed on ice or in centrifuges cooled to 4°C. Next, the harvested virus-cell suspension was centrifuged at 5400x g (Beckmann; Avanti™ J-20xp; JLA 16-250) for 15 min to separate free virus particles which remained in the supernatant from cells and cell-associated virus particles in the pellet. For isolation of the cell-associated virions the pellet was resuspended in 5 ml of DMEM and homogenized in a glass homogenisator (douncer; 20 strokes). Afterwards, cell debris was removed by a second centrifugation step at 17.400x g (Beckmann; Avanti™ J-

## C. Material and methods

20xp; JA 25-50) for 10 min. To concentrate viral particles, supernatants from both steps were combined and centrifuged at 25.000x g (Beckmann; Avanti™ J-20xp; JLA 16-250) for three hours. Next, the pellet was resuspended in 4 ml of VSB medium and homogenized with a douncer (20 strokes). Afterwards virus homogenate was carefully loaded on a 10 ml sucrose cushion of 15% sucrose in VSB (SW28 ultracentrifugation tube). After an ultracentrifugation step of one hour at 30.000x g (Beckman, SW28) the pellet of purified viral particles was resuspended in 1-2 ml VSB medium and aliquoted to 60 µl aliquots which were snap frozen in liquid nitrogen and stored at -80°C.

### 2.3.2.4 Growth curves

The growth kinetics of different mutant viruses were compared to each other and wt MCMV in multi-step growth conditions. NIH3T3 fibroblasts were grown on 12 well plates (Nunc) one day before the start of the experiment to obtain cell numbers around  $3 \times 10^5$  per well for the day of infection. Cells were infected with a MOI of 0.1 in a volume of 1 ml. In order to allow virus adsorption infected cells were incubated for 1 hour at 37°C in an incubator. Afterwards the infectious supernatant was exchanged by 1 ml of supplemented medium. After infection supernatant was collected from cells every day over a period of 7 days, stored at -80°C and virus titer was determined by plaque assay. Samples were taken in duplicates for each day.

### 2.3.2.5 MCMV titer determination by plaque assay

Carboxymethyl cellulose containing medium (500 ml)	3.75 g carboxymethyl cellulose (Sigma) 388 ml ddH <sub>2</sub> O to be autoclaved 5 ml L-glutamine 5 ml penicillin/ streptomycin (0.6% (w/v) Pen.; 1.3% (w/v) Strep) 25 ml FCS 50 ml 10x MEM 2.5 ml NEAS 24.7 ml NaHCO <sub>3</sub> (7.5%)
--	--

## C. Material and methods

For determination of MCMV virus titers MEF were cultured on 48 well plates. At a confluency of 100% the medium of each well was replaced by 400  $\mu$ l of serial diluted virus suspension (normally  $10^{-2}$  to  $10^{-7}$  in supplemented DMEM). Titrations were done in duplicates. After one hour of incubation in a CO<sub>2</sub>-incubator to allow virus adsorption, infectious supernatant was removed and cells were overlaid with carboxymethylcellulose containing medium to avoid virus spread. After 4-5 days plaques were counted and virus titer was determined by means of the following equation:

$$\text{Virus titer (PFU/ml)} = \frac{\text{counted plaques} \times \text{dilution factor}}{\text{vol. of virus dilution (0.4 ml)}}$$

### 2.4 Analysis of proteins

#### 2.4.1 Transfection of eukaryotic cells using calciumphosphate-precipitation

CaCl <sub>2</sub>	0.25 M
2x HEBS	16 g/l NaCl 0.72 g/l KCl 0.25 g/l Na <sub>2</sub> HPO <sub>4</sub> x2H <sub>2</sub> O 10 g/l HEPES 2 g/l glucose pH 7.05 with NaOH, sterile filtered

For transient transfection of eukaryotic cells by calciumphosphate-precipitation cells should have a confluency of 50-70% (Sambrook, 2001). 7  $\mu$ g (for 6 cm dishes; 14  $\mu$ g-10 cm; 28  $\mu$ g-14 cm) of plasmid-DNA was transferred to a 15 ml Falcon reaction tube and supplemented with 250  $\mu$ l CaCl<sub>2</sub> solution (500  $\mu$ l for 14  $\mu$ g; 1000  $\mu$ l for 28  $\mu$ g). While mixing permanently 250  $\mu$ l of 2x HEBS buffer was dropped to the probe (500  $\mu$ l for 14  $\mu$ g; 1000  $\mu$ l for 28  $\mu$ g). After an incubation at RT for 15 min the mixture was supplemented with 3 ml (for 6 cm dishes; 6 ml-10 cm; 12 ml-14 cm) of pre-warmed medium and transferred to PBS washed cells. Cells were incubated with this mixture over night. For longer incubation times than 24 hours the medium had to be exchanged. This was the

## C. Material and methods

---

method of use for transient transfection of 293 cells. Expressed proteins were analyzed 24 hours after transient transfection.

### 2.4.2 Transfection of eukaryotic cells using Superfect<sup>®</sup> transfection reagent

For transient transfection of eukaryotic cells by Superfect<sup>®</sup> transfection reagent (Quiagen) semi-confluent NIH3T3- or MEF cells on a 6 cm dish were transfected with a total of 7 µg of plasmid-DNA. DNA, 150 µl serum free DMEM and 15 µl Superfect<sup>®</sup> transfection reagent were mixed and incubated at RT for 15 min. Afterwards, the mixture was supplemented with 1 ml of pre-warmed medium and transferred to PBS washed cells. After 2.5-3.5 hours the transfection mixture was exchanged to pre-warmed, supplemented medium. Expressed proteins were analyzed 24-48 hours after transient transfection.

### 2.4.3 Protein extraction from eukaryotic cells

All steps of protein extraction, preparation of nuclei and pull down assays were performed on ice. With exception of total lysis buffer all buffers were supplemented with 1x PIC (Roche) to stabilize proteins.

#### 2.4.3.1 Protein extraction from eukaryotic cells using total lysis buffer

Total lysis buffer	62.5 mM Tris, pH 6.8
	2% (v/v) SDS
	10% (v/v) glycerol
	6M Urea
	5% (v/v) β-mercapto-ethanol
	0.01% (w/v) bromo-phenolblue
	0.01% (w/v) phenolred

For protein extraction cells were scratched from a 6-10 cm dish by a cell scratcher 24 hours after transfection or infection, transferred to a 15 ml Falcon reaction tube and pelleted at 310x g (1200 rpm, Heraeus-centrifuge) for 5 min at RT. The cell pellet was next resuspended in 1 ml PBS, transferred to a 1.5 ml

## C. Material and methods

Eppendorf reaction tube, pelleted at 830x g (2800 rpm, 5417-R-centrifuge) for 5 min at RT and resuspended in up to 350 µl of total lysis buffer. Normally, 10-20 µl of total protein extract was analyzed by SDS-PAGE (see 2.4.8) and Western Blot (see 2.4.9). Alternatively, for analysis of infected cells, total lysis buffer was added directly to the cell culture dish and lysis was performed for 10 min on ice.

### 2.4.3.2 Protein extraction from eukaryotic cells using IP lysis buffer

IP lysis buffer	150 mM NaCl 20 mM Tris, pH 8.0 1% Triton-X-100
-----------------	--

PIC (Protease inhibitor cocktail ,100x)	Complete Mini (Roche, D)
---	--------------------------

For analysis of protein-protein interaction 1/20 of the 1 ml PBS-cell suspension was transferred to a new 1.5 ml Eppendorf reaction tube, pelleted at 830x g (2800 rpm, 5417-R-centrifuge) for 5 min at RT and resuspended in 50 µl of total lysis buffer to determine total protein load by SDS-PAGE and Western Blot. The rest of cell suspension was pelleted at 830x g (2800 rpm, 5417-R-centrifuge) for 5 min at RT and lysis was performed with 1 ml of IP lysis buffer for 30 min on ice. Next, cell debris was pelleted at 20.800x g (14.000 rpm, 5417-R-centrifuge) for 30 min at 4<sup>0</sup>C and supernatant was transferred to a new 1.5 ml Eppendorf reaction tube.

### 2.4.3.3 Protein extraction from eukaryotic cells using high salt lysis buffer

High salt lysis buffer	450 mM NaCl 20 mM Tris, pH 8.0 1% Triton-X-100
------------------------	--

DNase	Benzonase <sup>®</sup> Nuclease, 25 U/µl (Novagen, Madison, WI, USA)
-------	--

PIC (Protease inhibitor cocktail ,100x)	Complete Mini (Roche, D)
---	--------------------------

## C. Material and methods

---

For analysis of cellular interaction partners of M53/p38 and M50/p35 instead of the IP lysis buffer a high salt lysis buffer was used. Lysis was performed 90 min on ice in presence of 125 U Benzonase<sup>®</sup> Nuclease. In addition, total cell lysates were supplemented with 250 U Benzonase<sup>®</sup> Nuclease. Afterwards HA-or Flag-tag pull down was performed (see 2.4.6 and 2.4.7).

### 2.4.3.4 Preparation of nuclear extracts

Hypotonic buffer	10 mM HEPES, pH 7.9 10 mM KCl 1.5 mM MgCl <sub>2</sub>
Lysis buffer	M-Per <sup>®</sup> mammalian protein extraction reagent (Pierce, Rockford, USA)

For preparation of nuclear extracts 293 cells were scratched from a 10 cm dish by a cell scratcher 24 hours after transfection, transferred to a 15 ml Falcon reaction tube and pelleted at 310x g (1200 rpm, Heraeus-centrifuge) for 5 min at RT. Next, the cell pellet was resuspended in 1 ml PBS and transferred to a 1.5 ml Eppendorf reaction tube. 1/20 of the 1 ml PBS-cell suspension was transferred to a new 1.5 ml Eppendorf reaction tube, pelleted at 830x g (2800 rpm, 5417-R-centrifuge) for 5 min at RT and resuspended in 50 µl of total lysis buffer to determine total protein load by SDS-PAGE (see 2.4.8) and Western Blot (see 2.4.9). The rest of cell suspension was collected by centrifugation at 830x g (2800 rpm, 5417-R-centrifuge) for 5 min at RT and the cell pellet next was resuspended in 600 µl hypotonic buffer. After incubation on ice for 10 min, cells were lysed by three repeated sonication steps of five seconds. The nuclei were collected by centrifugation at 20.800x g (14.000 rpm, 5417-R-centrifuge) for 30 min at 4<sup>0</sup>C and treated with up to 400 µl M-Per<sup>®</sup> mammalian protein extraction reagent.



## C. Material and methods

### 2.4.4 Metabolic labeling of proteins and co-immunoprecipitation

Starvation medium	Bio Whittaker™ RPMI 1640 with L-glutamine, without L-cystine or L-methionine (Cambrex, Verviers, Belgium)
[ <sup>35</sup> S]-cystine and methionine Promix	L-[ <sup>35</sup> S]-in vitro cell labeling mix; 14.3 mCi/ml (Amersham, Freiburg; D)
Protein A-sepharose	CL-4B (Amersham, Uppsala; S); 50% suspension, 5x washed in washing-buffer B, stored in buffer D
Protein G-sepharose	4 fast flow (Amersham, Uppsala; S); 50% suspension, 5x washed in washing-buffer B, stored in buffer D
Buffer B	1 mM Tris, pH 8.0 150 mM NaCl 2 mM EDTA 0.1 % Triton-X-100
Buffer D	10 mM Tris, pH 8.0
PIC (Protease inhibitor cocktail ,100x)	Complete Mini (Roche, D)

Sub-confluent 293 cells on 6 cm dishes were co-transfected with pOriR6K-zeo-ie-M53 or pOriR6k-zeo-ie-M53mut with 3.5 µg of pOriR6K-zeo-ie-M50 or pOriR6K-zeo-ie vector (Bubeck, 2004) by Ca<sub>2</sub>PO<sub>4</sub> precipitation (see 2.4.1). Twenty-four hours after transfection cells were washed once with pre-warmed (37<sup>0</sup>C) PBS and starvation medium and incubated for 40 min in an incubator with 4 ml/dish of starvation medium. Newly synthesized proteins were labeled by adding of warm (37<sup>0</sup>C) labeling medium (starvation medium supplemented with 300 µCi/ml <sup>35</sup>S-methionine and cystine mixture; Promix, Amersham) for one hour. The cells were lysed on an ice-chilled metal plate by adding of 1ml/dish of IP lysis buffer (supplemented with 1x PIC; see 2.5.3.2), lysates were

## C. Material and methods

transferred to an Eppendorf reaction tube, centrifuged at 4<sup>0</sup>C for 15 min (12.000x g, Eppendorf centrifuge) and 900 µl of supernatant were transferred to a new Eppendorf reaction tube without disturbing the pellet. Next, pre-absorption was performed at 4<sup>0</sup>C for 60 min on a roll incubator by adding of 50 µl of protein A- or G-sepharose to the cleared lysate. After centrifugation at RT for 2 min (12.000x g) the co-immunoprecipitation was carried out as described previously (Bubeck, 2004). To 900 µl pre-absorbed lysate 5 µl of an M50/p35 specific polyclonal rabbit antiserum (Muranyi, 2002) was added and incubated at 4<sup>0</sup>C on a roll incubator for 60 min followed by addition of 50 µl Protein-A Sepharose (Amersham) and incubation at 4<sup>0</sup>C on a roll incubator for 45 min to precipitate the M50/p35 specific-complexes. M53/p38 was precipitated on 50 µl Protein-G Sepharose beads (Amersham) with 5 µl of a specific rat polyclonal antiserum raised against a synthetic peptide representing the 15 N-terminal amino acids of M53/p38 (Bubeck, 2004). Afterwards the mixture was centrifuged for 2 min at RT (12.000x g) and the beads with bound proteins were washed five times with IP lysis buffer (supplemented with 1 x PIC) to remove unspecific bound proteins followed by a final washing step with buffer D (supplemented with 1 x PIC) to reduce the salt content. Beads were taken up in 50 µl of 2x sample buffer and boiled at 95<sup>0</sup>C for five min to elute the proteins. After centrifugation for 2 min at RT (12.000x g) eluted proteins in the supernatant were analyzed by SDS-PAGE (see 2.4.8).

### 2.4.5 Strep-tag pull down assay

Buffer W (Washing buffer)	150 mM NaCl 100 mM Tris/HCl, pH 8.0 1 mM EDTA
Buffer E (Elution buffer)	150 mM NaCl 100 mM Tris/HCl, pH 8.0 1 mM EDTA 2.5 mM desthiobiotin (IBA, Göttingen, D)

### C. Material and methods

---

Strep-Tactin <sup>®</sup> Sepharose	50% suspension in 150 mM NaCl, 100 mM Tris/HCl, pH 8.0, 1 mM EDTA, Strep-Tactin, 5 mg/ml covalently coupled to Sepharose 4FF beads (IBA, Göttingen, D)
-------------------------------------	--

Sub-confluent 293 cells on 6 cm dishes were co-transfected with 3.5 µg of the construct pOriR6K-zeo-ie-STM50 expressing Strep II-tagged M50/p35 and 3.5 µg of plasmid pOriR6K-zeo-ie-M53 or pOriR6k-zeo-ie-M53mut by Ca<sub>2</sub>PO<sub>4</sub> precipitation (see 2.4.1). Twenty-four hours after transfection the cells were washed with PBS, scratched from the plates and re-suspended in PBS. 5% of the cell suspension was lysed directly in total lysis buffer (62.5mM Tris, pH 6.8; 2% SDS [v/v]; 10% glycerol [v/v]; 6M Urea; 5% β-mercaptoethanol [v/v]; 0.01% bromophenolblue [w/v]; 0.01% phenolred [w/v]) and the samples were separated by sodium dodecyl sulfate polyacrylamide gel electrophoresis (SDS-PAGE, see 2.4.8) and analyzed by Western Blot (see 2.4.9) to determine the total protein load. The rest of the cell suspension was collected by centrifugation and pellets were lysed in hypotonic buffer (10 mM HEPES, pH 7.9; 10 mM KCl; 1.5 mM MgCl<sub>2</sub>) by sonication.

The nuclei were collected by centrifugation at 20.800x g (14.000 rpm, 5417-R-centrifuge) for 30 min at 4<sup>0</sup>C, treated with up to 400 µl M-Per<sup>®</sup> mammalian protein extraction reagent (Pierce; see 2.5.3.4) and transferred to a Handee<sup>™</sup> Spin cup column (Pierce). Next, 100 µl Strep-Tactin Sepharose (IBA) was added to pull down Strep II-tagged M50/p35 complexes and incubated for 1 hour at 4<sup>0</sup>C on a roll incubator. The Strep II-tag is a short peptide (8 amino acids; WSHPQFEK), which binds with high selectivity to Strep-Tactin, an engineered streptavidin. After a centrifugation step at 20.800x g (14.000 rpm, 5417-R-centrifuge) for 2 min pulled down protein complexes were washed five times with 400 µl of buffer W and centrifuged at 20.800x g (14.000 rpm, 5417-R-centrifuge) for 1 min at 4<sup>0</sup>C. Protein complexes were eluted from the Handee<sup>™</sup> Spin cup column (Pierce) to a new 1.5 ml Eppendorf reaction tube by addition of 100 µl desthiobiotin supplemented buffer E to the Strep-Tactin Sepharose (IBA), incubation for 20 min and centrifugation for 2 min at 20.800x g at 4<sup>0</sup>C. 50

## C. Material and methods

---

$\mu$ l of eluted samples were separated by SDS-PAGE and analyzed by Western Blot (see 2.4.8 and 2.4.9).

### 2.4.6 HA-tag pull down assay

Anti-HA Affinity Matrix

50% suspension in PBS, clone 3F10, rat IgG<sub>1</sub>, 3.5 mg/ml, covalently coupled to agarose beads (Roche, Mannheim, D)

HA peptide

1 mg/ml, YPYDVPDYA, recognized by Anti-HA clones 3F10 and 12CA5 (Roche, Mannheim, D)

For analysis of cellular interaction partners of M50/p35 alone or in complex with M53/p38 sub-confluent 293 cells on 10 cm dishes were transfected with 7  $\mu$ g of the construct pOriR6K-zeo-ie-HAM50 expressing HA-tagged M50/p35 or co-transfected with 7  $\mu$ g of plasmid pOriR6K-zeo-ie-M53 by Ca<sub>2</sub>PO<sub>4</sub> precipitation (see 2.4.1). Twenty-four hours after transfection the cells were washed with PBS, scratched from the plates and re-suspended in PBS. 5% of the cell suspension was lysed directly in total lysis buffer and the samples were separated by SDS-PAGE (see 2.4.8) and analyzed by Western Blot (see 2.4.9) to determine the total protein load. The rest of the cell suspension was lysed in 1 ml high salt lysis buffer (see 2.4.3.3). Afterwards 100  $\mu$ l of Anti-HA Affinity Matrix (Roche) was added to 1 ml lysate and incubated for 90 min at 4<sup>0</sup>C on a roll incubator. Next, The HA matrix was pelleted at 20.800x g (14.000 rpm, 5417-R-centrifuge) for 2 min and supernatant was removed. The matrix was then washed five times with high salt lysis buffer and once with 10 mM Tris, pH 7.6. After a final centrifugation step at 20.800x g (14.000 rpm, 5417-R-centrifuge) for 2 min the low salt buffer was totally removed and proteins were eluted by addition of 100  $\mu$ l 2x SDS sample buffer. 50  $\mu$ l of eluted sample was separated by SDS-PAGE and analyzed by Western Blot. Alternatively, up to 100  $\mu$ l of eluted sample was analyzed by SDS-PAGE and silver staining. Furthermore, proteins were eluted also under non-denaturing conditions by

## C. Material and methods

---

addition of 100  $\mu$ l HA peptide (1 mg/ml) and analyzed by SDS-PAGE and Western Blot or silver staining (see 2.4.8-2.4.10).

### 2.4.7 Flag-tag pull down assay

Anti-Flag M2 Affinity Matrix	50% suspension in glycerol, clone M2, murine IgG <sub>1</sub> , covalently coupled to agarose beads (Sigma, Saint Louis, Missouri, USA)
Flag peptide	5 $\mu$ g/ $\mu$ l (3x peptide solution), MDYKDHDGDYKDHDIDYKDDDDK, recognized by Anti-Flag M2 monoclonal antibody (Sigma, Saint Louis, Missouri, USA)
Buffer W (Washing buffer)	150 mM NaCl 50 mM Tris/HCl, pH 7.4

For analysis of cellular interaction partners of M50/p35 alone or in complex with M53/p38 sub-confluent 293 cells on 10 cm dishes were transfected with 7  $\mu$ g of the construct pOriR6K-zeo-ie-FlagM53 expressing Flag-tagged M53/p38 or co-transfected with 7  $\mu$ g of plasmid pOriR6K-zeo-ie-M50 by Ca<sub>2</sub>PO<sub>4</sub> precipitation (see 2.4.1). Probes were treated and analyzed as described for the HA pull down assay (see 2.4.6) thereby using 60-100  $\mu$ l of Anti-Flag M2 affinity resin, buffer W (150 mM NaCl; 50 mM Tris/HCl, pH 7.4) for washing and 2x SDS sample buffer or alternatively 100  $\mu$ l of 200 ng/ $\mu$ l Flag peptide for protein elution.

### 2.4.8 SDS-PAGE

Acrylamid-solution (RotiphoreseGel 30)	29.2% (w/v) acrylamid 0.8% (w/v) N, N-methylen-bisacrylamid (Carl Roth GmbH & Co, Karlsruhe, D)
--	--

### C. Material and methods

---

APS solution	10% (w/v) APS (ammonium persulfate) in ddH <sub>2</sub> O
N, N, N', N',-tetra-methyl-ethylene-diamine (TEMED)	Sigma, Deisenhofen, D
SDS solution	20% (w/v) in ddH <sub>2</sub> O
4x Upper-Tris stacking gel buffer	0.5 M Tris 0.4% (v/v) SDS pH 6.8
4x Lower-Tris separating gel buffer	1.5 M Tris 0.4% (v/v) SDS pH 8.8
Electrophoresis buffer (Laemmli)	50 mM Tris 0.4 M glycine 0.1 % (w/v) SDS
2x SDS sample buffer	400 mM Tris, pH 8.8 2 M Sucrose 10 mM EDTA, pH 8.0 0,02% BPB 50 mM DTT (freshly added) 4% (v/v) SDS (freshly added)
4x SDS sample buffer	800 mM Tris/HCl, pH 8.8 2 M Sucrose 20 mM EDTA, pH 8.0 0.04% BPB 100 mM DTT (freshly added) 8% (v/v) SDS (freshly added)
Gel fixation buffer	40% (v/v) MetOH 10% (v/v) acetic acid in ddH <sub>2</sub> O
Molecular weight marker (for metabolic labeled proteins)	1 µl [ <sup>14</sup> C]-methylated proteins (14.3 kDa-200 kDa), 0.37-3.7 Mbq/mg (10-100 µCi/mg) protein, 1.85 kBq/ml (5 µCi/ml), Amersham, Freiburg, D

## C. Material and methods

---

SDS-PAGE standards	10 $\mu$ l of prestained SDS-PAGE standard; low range (BioRad, Munich, D) or PageRuler™ Prestained Protein Ladder (Fermentas, St.-Leon-Rot, D)
--------------------	--

For separation of metabolic labeled proteins denaturing 11.5-13.5% SDS gradient gels were poured by means of a gradient mixer from a ready to use, gas-stabilized, watery acrylamide stock solution with bisacrylamide. All gels were prepared by means of 4x Lower-Tris buffer (pH 8.8) in the separating gel and 4x Upper-Tris buffer (pH 6.8) in the stacking gel in presence of 0.4% SDS. After polymerization of the separation- and stacking gel the gel was fixed in the electrophoresis apparatus and overlaid with electrophoresis buffer. Protein probes were taken up in up to 50  $\mu$ l of 2x SB and boiled for five min at 95°C before gel-loading. Proteins were separated at constant 20 mA for 20-24 hours. Afterwards the gel was fixated (see 2.4.10) for 45 min and vacuum-dried at 80°C for 2 hours (BioRad gel drying system). Last, the gel was exposed against a X-ray film (Kodak, Biomax MR film, New Haven, CT, USA) at -80°C for 1-7 days.

For analysis of proteins by Western Blot normally 10  $\mu$ l of total cell lysates (1:100 of probe) or up to 50  $\mu$ l of samples after pull down assay were separated by 10-15% SDS-PAGE using a Minigel-system (BioRad, Richmond, USA). Percentage of the SDS-gel thereby was chosen according to the expected molecular weight of the analyzed protein and the desired resolution. Proteins were separated at constant 160 V for 60-75 min.

### 2.4.9 Western Blot

Blotting buffer	25 mM Tris 190 mM glycine 20% methanol
TBS-T	150 mM NaCl 10 mM Tris/HCl, pH 8.0 0.02% Tween 20 (freshly added)

## C. Material and methods

---

Detection-kits	ECL <sup>PLUS</sup> Western Blot Detection System (Amersham, Freiburg, D) and Immobilon <sup>TM</sup> Western Chemi-luminescent HRP Substrate (Millipore, Billerica, MA, USA)
----------------	---

### 2.4.9.1 Sandwich construction

After SDS-PAGE proteins from the gel were transferred to a Hybond-P-PVDF-membrane (Amersham, Freiburg, D) which was activated 5 min by methanol and equilibrated in blotting buffer. For this procedure the gel was placed on the activated membrane and both together were placed between three layers of Whatman paper above and below that were soaked in blotting buffer. Next, the sandwich was transferred to a “Semidry-Blotting”-apparatus (BioRad, Freiburg, D) and blotting was performed for 40 min at constant 18 V and RT.

### 2.4.9.2 Detection of blotted proteins

For immunodetection of proteins, first the blotted PVDF-membrane was incubated over night at 4<sup>0</sup>C with 5% (w/v) nonfat milk powder in TBS-T to block unspecific binding sites. Next, the membrane was incubated at RT for one hour with primary antibody that was diluted 1:300-1:2000 in TBS-T. Afterwards the membrane was washed in ~100 ml TBS-T for at least 90 min thereby exchanging the washing buffer every 20 min. The PVDF-membrane was then incubated for one hour at RT with horseradish peroxidase-conjugated secondary antibody which was usually diluted 1:7500 in TBS-T and afterwards washed again for at least 90 min with TBS-T thereby exchanging the washing buffer every 20 min. For detection of the proteins the peroxidase coupled to the secondary antibody was traced by chemiluminescent-detection by means of either the ECL<sup>PLUS</sup> Western Blot Detection System (Amersham, Freiburg, D) or the Immobilon<sup>TM</sup> Western Chemiluminescent HRP Substrate (Millipore, Billerica, MA, USA) thereby following the instructions of the manufacturers. Afterwards, for detection of the reaction the membrane was exposed to a



## C. Material and methods

---

chemiluminescence film (Hyperfilm<sup>TM</sup> ECL, Amersham, Freiburg, D) for one sec up to one hour.

### 2.4.10 Silver-staining

Fixative	40% (v/v) ethanol 10% (v/v) acetic acid made with ddH <sub>2</sub> O
PerfectBlue <sup>TM</sup> Vertical electrophoresis system	Peqlab, Erlangen, D
SilverQuest <sup>TM</sup> Silver Staining Kit	Invitrogen, Karlsruhe, D

For analysis of cellular interaction partners of M50/p35 alone or in complex with M53/p38 sub-confluent 293 cells on 10 cm dishes were transfected with 7 µg of the construct pOriR6K-zeo-ie-FlagM53 expressing Flag-tagged M53/p38 or co-transfected with 7 µg of plasmid pOriR6K-zeo-ie-M50 by Ca<sub>2</sub>PO<sub>4</sub> precipitation (see 2.4.1). In addition, cells were transfected with 7 µg of the construct pOriR6K-zeo-ie-HAM50 expressing HA-tagged M50/p35 or co-transfected with 7 µg of plasmid pOriR6K-zeo-ie-M53. Alternatively, 293 cells were co-transfected with both pOriR6K-zeo-ie-HAM50 and pOriR6K-zeo-ie-FlagM53. Cell lysis was performed as described above (see 2.4.3.3), thereby using high salt lysis buffer. HA-tag pull down and Flag-tag pull down were performed as described above (see 2.4.6 and 2.4.7) and proteins were eluted by addition either of 2x SDS-sample buffer to the matrix or by the respective peptide. Up to 60 µl of eluted protein samples were separated by SDS-PAGE (see 2.4.8) with a PerfectBlue<sup>TM</sup>Vertical electrophoresis system (Peqlab, Erlangen, D) on a 8-16% gradient gel at constant 30 mA for 4 hours. Afterwards the gel was fixated in 100 ml fixative over night and silver staining was performed according to the instructions of the manufacturer. Last, the gel was air dried for 80 min by means of a air gel dryer (BioRad, Munich, D).

## C. Material and methods

---

### 2.4.11 Confocal laser scanning microscopy

PBS	137 mM NaCl 2.7 mM KCl 4.3 mM Na <sub>2</sub> HPO <sub>4</sub> 1.4 mM KH <sub>2</sub> PO <sub>4</sub> pH 7.5
Fixative	3% (w/v) para-formaldehyde in PBS (freshly prepared or thawed)
Quench-solution	50 mM NH <sub>4</sub> Cl 20 mM glycine in PBS
Permeabilization buffer	0.2% (v/v) Triton-X-100 in PBS
Blocking buffer	0.2% (v/v) teleostier-gelatine in PBS (Sigma, Deisenhofen)
Embedding media	Histogel, (Linaris, Bettingen a. Main, D)

In order to visualize the intracellular localization of wt- and mutant M53/p38, M50/p35 and cellular interaction partners of the viral proteins, double-immunofluorescence-stainings were performed and localization was determined by means of a confocal laser scanning microscope. If not indicated all steps of the procedure were performed at RT.

NIH 3T3 cells were grown on 12 well plates on glass cover slips and transfected (see 2.4.2) or infected at a confluency of 60-80%. After 24 hours cells were washed twice with 2 ml/well PBS and fixated for 20 min with 1 ml/well of 3% para-formaldehyde/PBS (Muranyi, 2002). After two additional washings with 2 ml/well PBS cells were quenched for 20 min by addition of 1 ml/well NH<sub>4</sub>Cl/glycine-solution and again washed twice 2 ml/well with PBS. Afterwards cells were permeabilized by incubation with 1 ml/well of 0.2% Triton-X-100/PBS for 10 min, washed three times with 2 ml/well PBS and stabilized by incubation in 1 ml/well of 0.2% teleostier-gelatine/PBS for 10 min. Next, cells were incubated for 45 min with primary antibodies which were diluted 1:2000 in PBS,

### C. Material and methods

---

washed four times with 2 ml/well PBS and stabilized again for 10 min by incubation in 1 ml/well of 0.2% teleostier-gelatine/PBS. Afterwards an incubation for 45 min in the dark with FITC- or Texas Red-conjugated secondary antibody followed, which was diluted 1:75 in PBS for FITC- and 1:150 in PBS for Texas Red- conjugated antibody. Last, cells were washed two times with 2 ml/well PBS, embedded with "Histogel" (Linaris) on a cover slip and analyzed at the confocal microscope (Leica).

Wt and mutant M53/p38 was visualized with the specific polyclonal rat antiserum as primary antibody (Eurogentec) and fluorescein-conjugated goat anti-rat IgG (Dianova) as secondary antibody. M50/p35 was visualized with polyclonal rabbit antiserum as primary antibody (Muranyi, 2002) and Texas-red-conjugated donkey anti-rabbit IgG (Dianova) as secondary antibody.

## D. Results

### **1. M53/p38 is expressed with late kinetics and is essential for MCMV replication**

#### **1.1 Optimization of M53/p38 detection by Western-blot analysis**

The optimal virus load for the detection of M53/p38 in infection experiments was determined on NIH 3T3 cells infected with wt MCMV at different multiplicity of infection (MOI) of 0.1, 0.2, 0.5 and 1.0. 24 hours post infection total cell lysates were prepared and proteins were separated by SDS-PAGE. Cell lysates from uninfected NIH 3T3 cells or transfected with pOriR6K-ie-zeo-M53 were analyzed as negative- or positive controls, respectively. Furthermore, a lysate from wt MCMV infected NIH 3T3 cells served as positive control. M53/p38 signals were visualized by Western-blot using rat antiserum specific to the N-terminal 15 amino acids (aa) of the M53/p38 ORF at a dilution of 1:2000 (Bubeck, 2004). The M53/p38 specific signal at 38 kDa was detectable in analyzed infected and transfected probes but was missing in uninfected NIH 3T3 cells. The strongest M53/p38 signal was detectable for the lysate from NIH 3T3 cells infected at an MOI of 0.5 (Fig. 12, lane 6). As a second the same probes were analyzed by SDS-PAGE and Western-blot and probed at a dilution of 1:2000 with rabbit antiserum specific for the late MCMV protein M50/p35 which has a predicted molecular weight of 35 kDa and interacts with M53/p38. In accordance with the results for M53/p38 the strongest M50/p35 signal was detectable for the lysate from NIH 3T3 cells infected at an MOI of 0.5 (Fig. 12, lane 6). Therefore, for all further infection experiments an MOI of 0.5 was used.

## D. Results

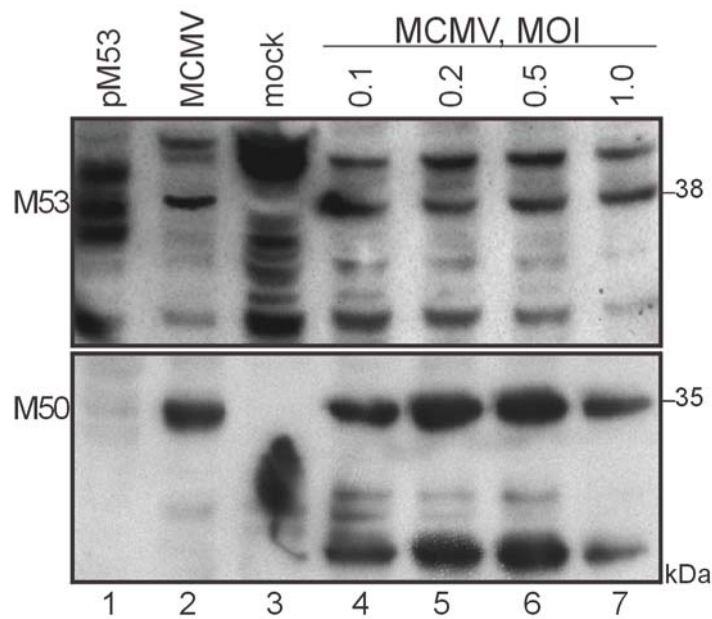


**Figure 12. Determination of proper MOI for infection experiments.** NIH 3T3 fibroblasts were infected at different MOI with wt MCMV and cell lysates were prepared 24 hours after infection (lanes 4-7). As controls NIH 3T3 cells were mock transfected (lane 3) or transfected with pOriR6k-ie-M53 (M53) and cell lysate was prepared 24 hours post transfection (lane 1). Additionally, already tested wt MCMV lysate was probed as expression control (lane 2). Proteins were separated by SDS-PAGE and M53/p38 and M50/p35 signals were visualized by Western blot using specific antisera.

### 1.2 Determination of the expression kinetics of M53/p38

M50/p35 follows early-late expression kinetics upon MCMV infection (Bubeck, 2004). Therefore, we wanted to know, if the same is true for M53/p38. The expression kinetics of M53/p38 was determined on NIH 3T3 cells infected with wt MCMV at an MOI of 0.5. Cell lysates were prepared at different times after infection and proteins were separated by SDS-PAGE. M53/p38 signals were visualized by Western-blot using rat antiserum specific to the N-terminal 15 amino acids (aa) of the M53/p38 ORF (Bubeck, 2004). The M53/p38 specific 38 kDa band became detectable at 18 hours post-infection (Fig. 13A, lane 4). M53/p38 gradually accumulated at later time points (Fig. 13A, lane 5-6) with a maximum of 36 hours after infection.

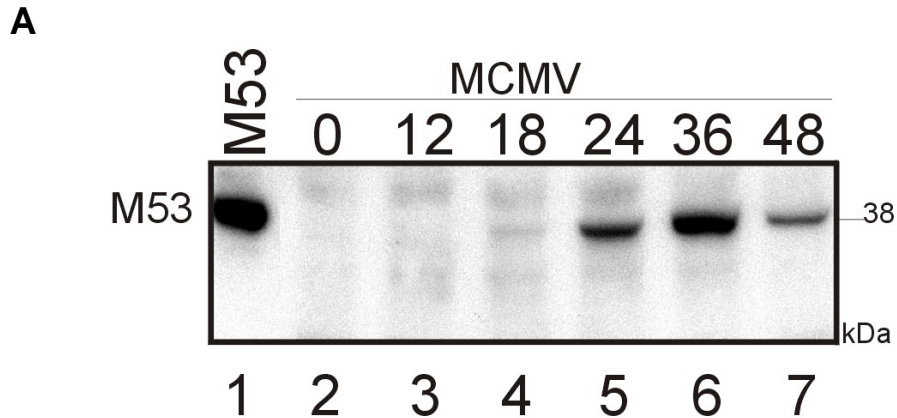


**Figure 13A. Expression kinetics of M53/p38.** NIH 3T3 fibroblasts were infected with wt MCMV and cell lysates were prepared at indicated time points (hours) after infection (lanes 2-7). As a control NIH 3T3 cells were transfected with pOriR6k-ie-M53 (M53) and cell lysate was prepared 24 hours post transfection (lane 1). Proteins were separated by SDS-PAGE and the M53/p38 signal was visualized by Western blot using specific rat antiserum.

To confirm that M53/p38 is a true late protein, the DNA replication was blocked in infected cells by addition of 300  $\mu$ g/ml phosphono-acetic acid (PAA; Sigma) to prevent the expression of late MCMV genes (Gold, 2002). M53/p38 was clearly detectable 24 hours after infection in the untreated cells (Fig. 13B, lane 3) whereas PAA treatment abolished expression of the protein (Fig. 13B, lane 6). In the controls the expression of the major capsid protein (M86), another late gene product, was blocked by PAA treatment while the expression of the immediate-early gene product pp89 was not affected. Therefore, M53/p38 expression follows late kinetics.

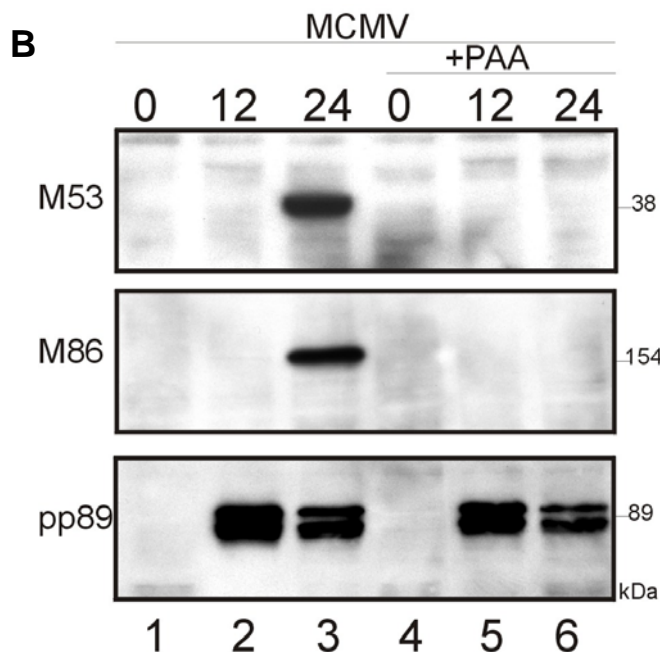


**Figure 13B. Expression kinetics of M53/p38.** NIH 3T3 fibroblasts were infected with wt MCMV in the absence or in presence of phosphono-acetic acid (PAA), (lanes 1-3 and 4-6, respectively). Cell lysates were prepared from infected cells at indicated time points (hours) after infection. Proteins were separated by SDS-PAGE and signals for M53/p38, M86 and pp89 were visualized by Western blots using specific antisera.

## D. Results

### 1.3 M50/p35 and M53/p38 co-locate to the nuclear membrane

M53/p38 is diffusely distributed in the nucleus of transfected 293 endothelial cells expressing only M53/p38, whereas isolated M50/p35 is found in nuclear and ER membranes (Muranyi, 2002). After co-expression of both proteins, M53/p38 is redistributed to the nuclear envelope. Since human 293 cells can not be productively infected by MCMV a different cell system had to be used to study the sub-cellular localization of M53/p38 and M50/p35 after transfection or infection. To this end, NIH 3T3 fibroblasts were transfected either with wt M53/p38 or wt M50/p35. Sub-cellular localization of wt M53/p38 or wt M50/p35 was analyzed by confocal microscopy after indirect immunofluorescence staining with specific antisera (Fig. 14A). Used antisera and secondary antibodies showed no cross-reactivity to cellular proteins in mock transfected NIH 3T3 fibroblasts (Fig. 14A, first horizontal row). After isolated expression of wt M53/p38 (Fig. 14A, M53) the typical diffuse nuclear staining pattern was detectable. There was no cross-reactivity of the anti-M50 sera to M53/p38 (Fig. 14A, second horizontal row).

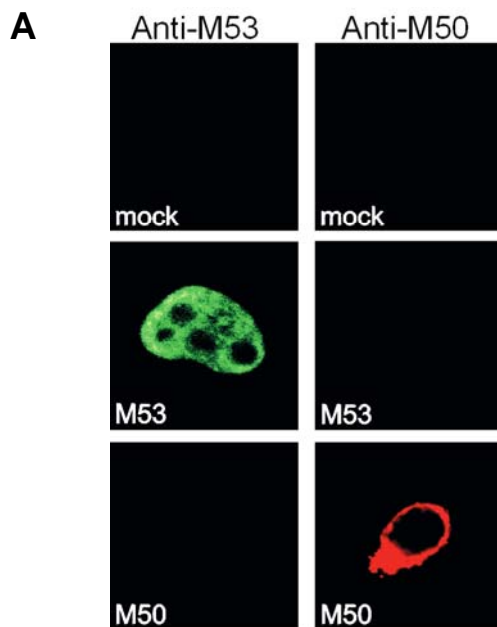


**Figure 14A. Sub-cellular localization of M53/p38 and M50/p35.** NIH 3T3 cells were mock transfected, transfected with either wt M53 or with wt M50/p35. Single transfected cells were stained with rat specific antiserum against M53/p38 and co-stained with rabbit specific antiserum against M50/p35. For detection of M53 a fluorescein-conjugated secondary antibody was used (green). For detection of M50 a Texas red coupled secondary antibody was used (red). No cross-reactivity of the sera could be detected.

Isolated expressed M50/p35 was found in nuclear and ER membranes as described for 293 cells. The specific anti-M53 sera did not cross-react with wt M50/p35 (Fig. 14A, third horizontal row). Next, sub-cellular localization of wt M53/p38 or wt M50/p35 after co-expression of both proteins and infection of

## D. Results

NIH 3T3 cells were analyzed by confocal microscopy after indirect immunofluorescence staining. The phenomenon described for transfection of 293 cells was also detectable after transfection and infection of NIH3T3 fibroblasts with MCMV (Fig. 14B). Co-expression of M50/p35 and M53/p38 changed the distribution of M53/p38 to the nuclear envelope. Additionally to these findings, 24 hours after infection or transfection of NIH3T3 cells M50/p35 localized consistently in peri-nuclear structures (Fig. 14B, second vertical row). Furthermore, performing indirect immunofluorescence staining 24 hours after infection of cells with MCMV, in contrast to transfected cells, M53/p38 is also detectable in these structures co-localized with M50/p35 (Fig. 14B, second horizontal row). In infected cells the morphology of the NEC positive peri-nuclear structures was not characteristic for an ER staining.

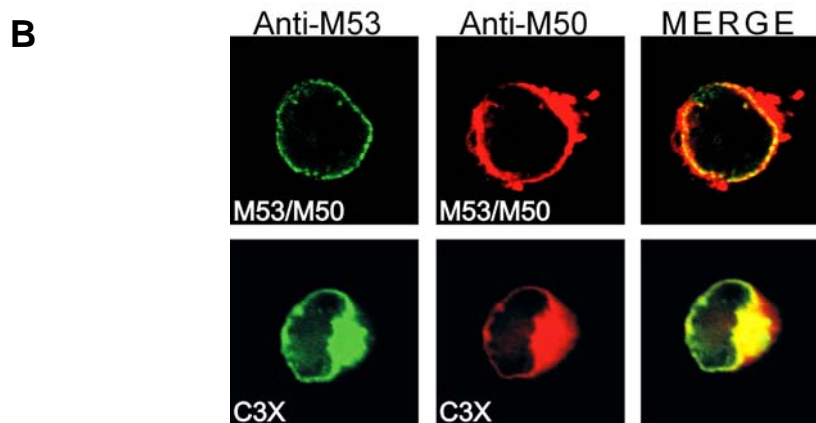


**Figure 14B. Subcellular localization of M53/p38 and M50/p35.** NIH 3T3 cells were either co-transfected with M53/p38 and M50/p35 or infected with wt MCMV (C3X) at an MOI of 0.5. Transfected or infected cells were stained with rat specific antiserum against M53/p38 and co-stained with rabbit specific antiserum against M50/p35. For detection of M53 a fluorescein-conjugated secondary antibody was used (green). For detection of M50 a Texas red coupled secondary antibody was used (red).

### 1.4 M50/p35 directly binds to M53/p38

M50/p35 directly binds to M53/p38 and the binding region of M50/p35 is essential for MCMV growth (Bubeck, 2004). We predicted that the binding region of M53/p38 to M50/p35 should also represent an essential function.



## D. Results

In order to set up a system to test binding of M53/p38 to M50/p35, 293 cells were either mock transfected, transfected with pM53 or pM50, expressing wtM53 or wtM50, respectively, or co-transfected with pM53 and pM50. Cell lysates were prepared and co-immunoprecipitation was performed. Half of the lysates were precipitated with specific rabbit anti-M50/p35 sera and protein A-sepharose (Amersham; Fig. 15, lanes 1-4). The other half was precipitated with specific rat anti-M53/p38 sera and protein G-sepharose (Amersham; Fig. 15; lanes 5-8). Using anti-M50/p35 sera M50/p35 was precipitated indicated by a specific band at 35 kDa (Fig. 15, lane 3). M53/p38 could be clearly co-precipitated indicated by a specific band at 38 kDa (Fig. 15, lane 4).

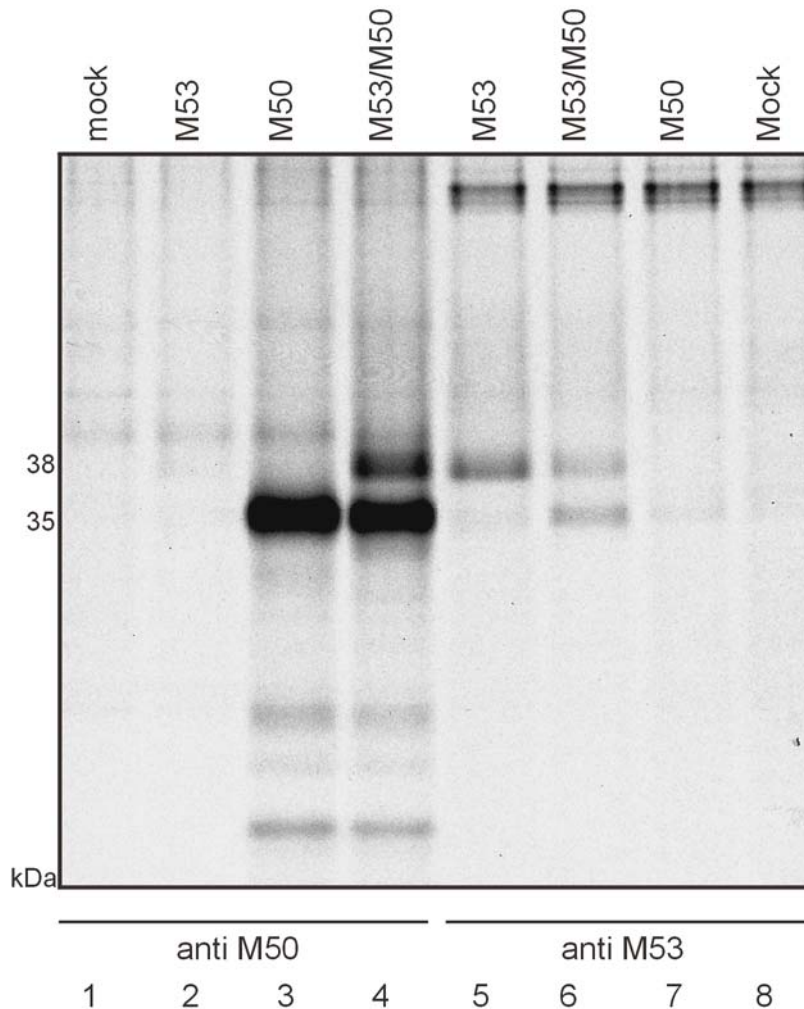


**Figure 15. Co-immunoprecipitation of M53/p38 and M50/p35.** Plasmids expressing M53/p38 (lane 2,5) or M50/p35 (lane 3,7) were transfected into 293 cells. In parallel wt M53 was co-transfected with wt M50/p35 (lanes 4 and 6). Cells were radioactively labeled and probes were either precipitated with protein-A sepharose using anti-M50/p35 specific rabbit serum (lanes 1-4) or with anti-M53/p38 specific rat serum on protein-G sepharose (lanes 5-8). Samples were analyzed by SDS-PAGE followed by autoradiography.

## D. Results

For lysates of mock- or pM53 transfected cells no specific bands could be detected (Fig. 15, lanes 1, 2). Using anti-M53/p38 sera from rat M53/p38 was weakly precipitated (Fig. 15, lane 5). M50/p35 also weakly co-precipitated together with M53/p38 (Fig. 15, lane 6). No specific bands were detectable for controls “mock” and “M50” (Fig. 15, lanes 7, 8). Using anti-M53/p38 sera and protein G-sepharose the intensity of the specific signals was weaker compared to signal intensity after anti-M50/p35 immunoprecipitation. Thus, in all further co-immunoprecipitation experiments the specific anti-M50/p35 together with protein A-sepharose were used to detect the M50/p35-M53/p38 complex.

As an alternative method to radioactive co-immunoprecipitation a non-radioactive pull down assay was tested. pM50ST expressing Strep-II tagged M50/p35 was co-expressed with wt and mutant M53/p38 constructs.

To test specificity of this assay, 293 cells were either mock transfected, transfected with pM50, expressing wt M50/p35 or transfected with pM50ST, expressing M50ST. Furthermore, pM50ST or pM50 were co-transfected with pM53, expressing wt M53/p38. As controls for protein load- and expression total cell lysates were separated by SDS-PAGE and subjected to Western-blot analysis using M53/p38- or M50/p35 specific antiserum (Fig.16, T, upper- and middle panel). The specific M53-band at 38 kDa became detectable only for the co-transfected probes (Fig. 16, upper panel, T, lanes 3, 5). The specific M50-band at 35 kDa became detectable in the transfected- and co-transfected probes but was missing in the mock control (Fig. 16, middle panel, T, lanes 2, 3, 4, 5). Using the Strep-II tag pull down assay only proteins bound to M50 should be recovered by Strep-Tactin sepharose beads from lysates of 293 cells. Next, bound proteins were eluted from the beads by desthiobiotin, separated by SDS-PAGE and subjected to Western-blot analysis using M53/p38 specific antiserum. As predicted, the specific 38 kDa band of M53/p38 was only detectable in the lysate of 293 cells co-transfected with pM50ST and pM53 (Fig. 16, B, lane 3) but not in the cell lysate of 293 cells co-transfected with pM50 and pM53 (Fig. 16, B, lane 5). Furthermore, no unspecific signals were detectable in mock control or probes M50ST and M50 (Fig. 16, B, lanes 1, 2, 4), indicating high specificity of this assay. This convinced us that the tagged M50/p35 protein had kept the properties of wt M50/p35 with regard to M53/p38 binding.

## D. Results

Therefore, for further experiments this pull down assay was used to confirm the results obtained by co-localization- and immunoprecipitation experiments.

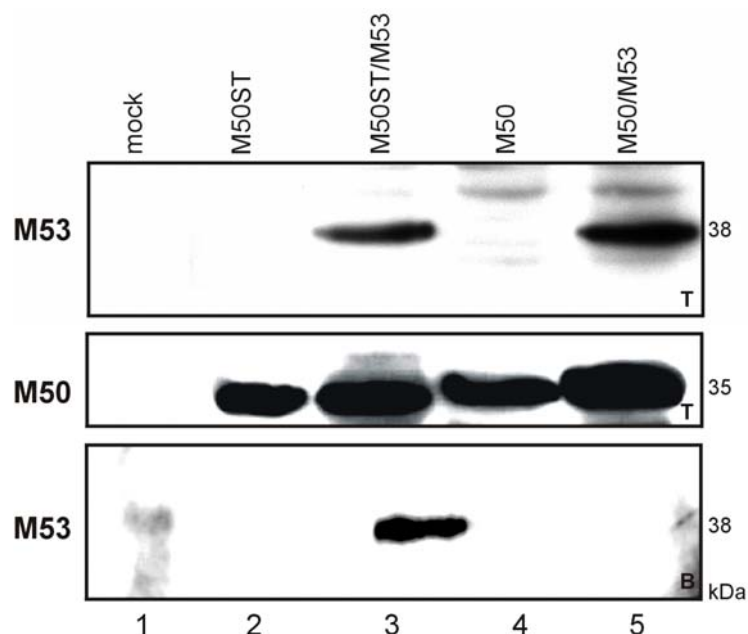


**Figure 16. Pull down assay of M53/p38 with Strep tagged M50/p35.** Wt M50/p35 or M50ST were transfected into 293 cells. In parallel wt M53 was co-transfected either with M50ST or wt M50/p35 into 293 cells. Total cell lysates were analyzed to test the protein expression by Western blot using specific antiserum against M53/p38 (upper panel, M53, total protein-T) or against M50/p35 (middle panel, M50, total protein-T). Proteins complexed with M50ST were precipitated by Strep-Tactin Sepharose. Desthiobiotin eluates were analyzed by SDS-PAGE and blotted on membranes. Wt M53/p38 protein was detected by Western blot with M53/p38 specific antiserum (lower panel, M53, bound protein-B).

### 1.5 The M53 ORF is essential for viral growth and infectivity can be reconstituted by ectopic re-insertion of the wild-type M53 gene into the M53 deletion genome

#### 1.5.1 Deletion of endogenous M53/p38 leads to loss of functionality of MCMV-infection

M53/p38 can be co-precipitated with M50/p35, indicating functional interaction between both gene products (Bubeck, 2004). Inactivation of genes homologous to M50 and M53 in  $\alpha$ -herpesviruses severely affects viral growth in cell culture (Reynolds 2001, Fuchs 2002). Deletion of UL31 or UL34 from HSV-1 genome severely reduces the viral growth but the genes are not strictly essential (Liang, 2004). In contrast, the M50 gene is essential for virus reconstitution in MCMV

## D. Results

---

and involved in the egress of the MCMV capsid from the nucleus (Bubeck, 2004). To test essentiality of M53/p38 for MCMV replication, the M53 ORF was deleted from the MCMV-BAC using ET recombination in *E. coli*. The construct was tested for infectivity by transfection into MEFs and NIH3T3 cells. No infectious virus could be reconstituted by transfection of m16/17FRT- $\Delta$ M53 BAC, thus the M53 ORF is essential for virus reconstitution from genomic BACs.

### 1.5.2 Ectopic expression of M53 reverts the null-phenotype of the $\Delta$ M53-MCMV-BAC

The null-phenotype of m16/17FRT- $\Delta$ M53-BAC was reverted in order to ensure that the inability to gain infectious virus after transfection of m16/17FRT- $\Delta$ M53-BAC was solely due to the deletion of the M53 gene. By using the rescue plasmid pOriR6K-*ie-zeo* carrying an FRT site (Bubeck, 2004) the M53 ORF was re-inserted into the m16/17FRT- $\Delta$ M53-BAC at its FRT site in Flp expressing *E. coli*. The Flp recombinase directs the site specific recombination between the FRT sites located on the rescue plasmid and the BAC (for construction principles see material and methods: 1.6.2.4, 2.3.2.1 and (Bubeck, 2004)).

The rescue inserted the M53 ORF into the deletion BAC at the position between genes m16 and m17 resulting in pM53E-BAC. The predicted genome sequence of pM53E-BAC was confirmed by restriction pattern analysis (Fig. 17A) and sequencing at the position of the predicted genetic changes. Transfection of MEF cells with pM53E-BAC DNA resulted in viral progeny (M53E-MCMV). However, the growth of M53E-MCMV was slightly attenuated compared to the BAC derived wt virus. Under multi-step growth conditions the ectopic expression of the M53 gene in M53E-MCMV resulted in moderately (0.7 log) lower end-titers five days post-infection compared to the parental BAC-derived MCMV (Fig. 17B).

## D. Results

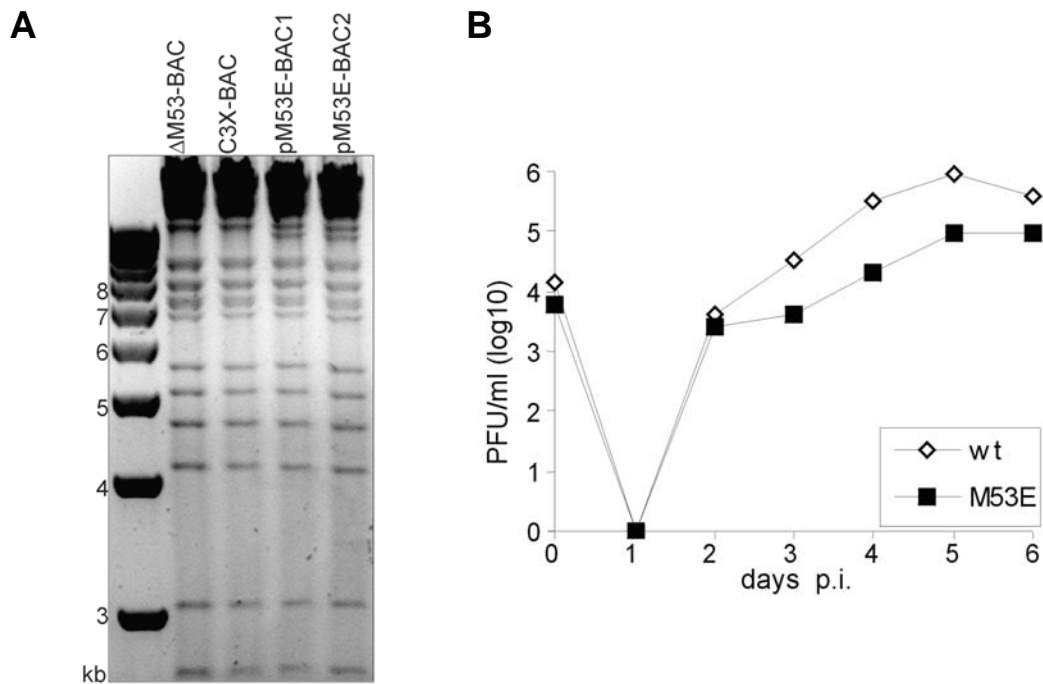


**Figure 17. Ectopic rescue of the M53 deletion mutant. (A) Restriction analysis of  $\Delta$ M53-BAC, C3x-BAC and pM53E-BAC.** Respective BAC-DNA was analyzed by NotI-restriction and DNA was separated on a BAC-TBE-agarose gel. Single insertion of pM53 into the  $\Delta$ M53-BAC is accompanied by an additional band at around 11 kb. Multiple insertions can be determined by an additional band at 3.5 kb. **(B) Growth kinetics of the viruses derived from pSMfr3 (wt) or pM53E (M53E) were determined on NIH 3T3 cells.** Sub-confluent cultures were infected with the respective viruses. Supernatants of the infected cells were harvested on the indicated days and the infectious progeny was quantified by plaque assay.

Attenuation of M53E-MCMV compared to the wt MCMV was observed in four independent experiments and may be due to the altered expression kinetics of ectopic M53/p38 from a late gene to a gene controlled by the immediate early (ie) promoter of HCMV and expressed throughout the replication cycle. Clearly, the M53 gene is essential for MCMV growth and the M53 null phenotype can be reverted by ectopic expression of the M53 ORF. These findings could be confirmed by a trans-complementation assay. A trans-complemented M53 deletion virus was unable to produce viral progeny under non-complementing conditions (Lötzerich, 2006).

## D. Results

### **2. Construction of an insertion mutant library of the M53 ORF and analysis of the mutants in the context of the MCMV genome**

In the comprehensive mutant library for the M50 gene the efficiency of the in vitro transposon mediated mutagenesis was only 10% (Bubeck, 2004). We wanted to improve the efficiency of the in vitro transposition reaction in order to generate a comprehensive library of M53 insertion mutants.

Donor: 20 ng Target: 80 ng	pGPS4/ Litmus 28	pST76k-S4/ Litmus 28	pST76k-S4/ Litmus 28-M53	pST76k-S4/ pOriR6kie-M53
Selection marker	Amp/ Cm	Amp/ Cm	Amp/ Cm	Zeo/ Cm
Bacteria host strain	DH10B	DH10B	DH10B	Pir
Permissive temperature	37 <sup>0</sup> C	43 <sup>0</sup> C	43 <sup>0</sup> C	43 <sup>0</sup> C
Transposition/ reaction	3550	6750	7920	1500

**Table 3. Transposon donor- and acceptor combinations used in this study.**

Different strategies for Tn7-based transposon mediated mutagenesis were tested (table 3). Since pGPS4 (NEB) and our rescue vector pOriR6K-ie-zeo-M53 carry the same origins of replication this transposon donor-acceptor combination could not be used for mutagenesis. Therefore, the M53 ORF was first sub-cloned into the Litmus 28 vector which served as acceptor for Tn7-based transposon mediated mutagenesis. In addition we constructed a new transposon donor plasmid pST76K-S4, which based on pGPS4 (NEB) and carries the Tn7 derived mini-transposon and a conditional origin of replication to allow donor plasmid elimination after the transposition reaction at non-permissive temperature (Posfai, 1997). Furthermore, the origins of replication of pST76K-S4 and pOriR6K-ie-zeo-M53 are different, which enabled to use this

## D. Results

---

transposon donor-acceptor combination. Using the new transposon donor plasmid pST76k-S4 for in vitro transposition in combination with Litmus 28 (NEB) the number of colony forming transpositions in one reaction was improved 90% compared to pGPS4 and Litmus 28, which were used for the transposon mediated mutagenesis of M50/p35 (Bubeck, 2004). Furthermore, using pST76k-S4 in combination with Litmus 28-M53 (pLitM53) the efficiency of transposition was even higher. In contrast by using the rescue plasmid pOriR6K-ie-zeo-M53 as transposon acceptor plasmid in combination with pST76k-S4, the efficiency of transpositions dropped by 80% compared to Litmus 28-M53 as acceptor.

Restriction analysis of pOriR6K-ie-zeo-M53 after in vitro transposition revealed, that the Tn7 derived mini-transposon was inserted randomly into the rescue vector but preferentially inserted into the vector backbone and not into the M53-ORF (Fig. 18A and B). Using pLitM53 and pST76k-S4 for in vitro transposition could increase the number of inserted Tn7 derived mini-transposon into the M53-ORF to 30% (Fig. 18C). A transposition into linearized M53 was not useful due to site specific preference of inserted transposon. Therefore, as the most effective transposon donor-acceptor combination, for transposon mediated mutagenesis of M53/p38 the transposon donor vector pST76k-S4 and the acceptor pLitM53 were used. Next, after in vitro transposition acceptor plasmids carrying the mini-transposon were selected and purified as a pool (for principle see Fig. 18E).



## D. Results

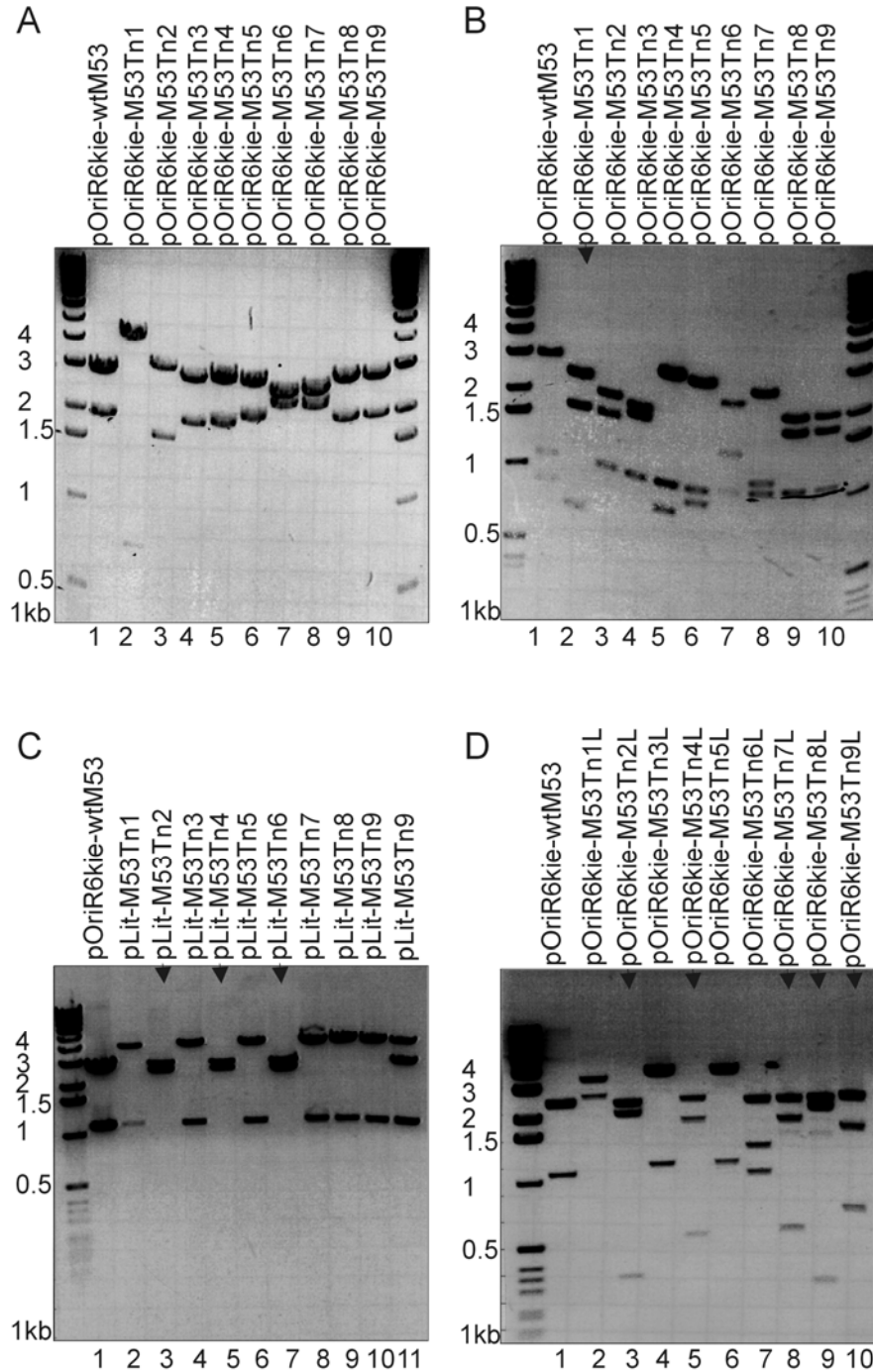


**Figure 18A-D. Construction of an insertion mutant library of the M53 ORF.** (A-D) Restriction analysis of M53-mutant libraries. (A) Different DNA preparations of poriR6k-ie-zeoM53 after transposition with pST76k-S4 were analyzed by NotI-restriction. As control wt M53 in poriR6k-ie-zeo was analyzed. The transposon inserted at various sites of the construct. (B) KpnI/NotI restriction of these DNA preparations revealed that the transposon preferentially inserted into the vector but not into the M53-ORF (black arrowheads for M53 insertion). (C) Different DNA preparations of pLit-M53 after transposition with pST76k-S4 were analyzed by KpnI/XbaI-restriction, As control wt M53 cloned to pLit was analyzed (black arrowheads for M53 insertion). (D) After transposon mutagenesis in pLit-M53 the library was purified as a pool and sub-cloned into pOriR6k-ie-zeo. Different DNA preparations of poriR6k-ie-zeoM53TnL were analyzed by KpnI/NotI-restriction (black arrowheads for M53 insertion).



## D. Results

E

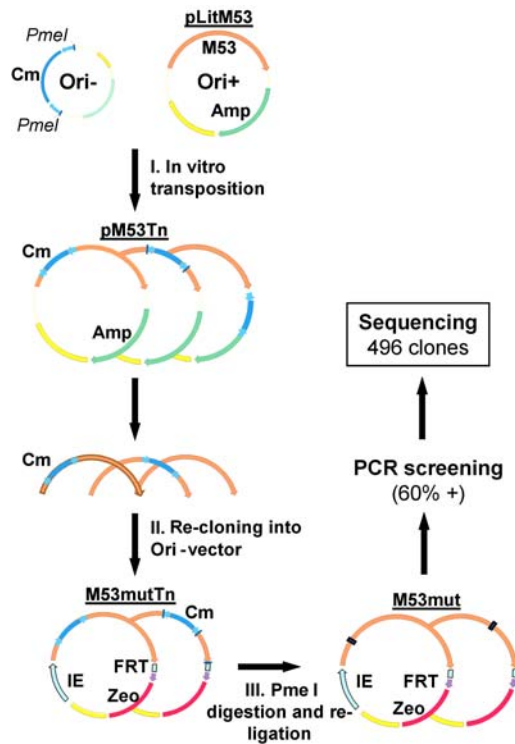


**Figure 18E. Principle of random transposon insertion mutagenesis.** In a first step in vitro transposition reaction was performed with pLit-M53 and pST76k-S4. Next, acceptor plasmids pM53Tn carrying the mini-transposon were selected and purified as a pool. In a third step M53-ORF which is increased in size due to transposon insertion was cloned by KpnI/NsiI to pOriR6k-ie-zeo resulting in M53mutTn. Removal of the Tn7-based transposon by PmeI restriction and religation resulted in 5 aa insertions in the M53-ORF. From a library of 28,000 pOriR6K-ie-zeo-M53 mutants 986 independent clones were screened by PCR and 498 plasmids with an insertion in the M53 ORF were sequenced.

Selection for M53 ORF with inserted transposon and increased in size due to the inserted transposon, was achieved by isolation of the ORF and insertion into the rescue plasmid pOriR6K-ie-zeo (Fig. 18D). PmeI digestion then removed the mini-transposon and subsequent re-ligation resulted in insertion of 5 aa or of a stop codon into the coding sequence. This provided a library of 28,000 pOriR6K-ie-zeo-M53 mutants. From this library 986 independent random clones were screened by PCR and 498 plasmids with an insertion in the M53 ORF were sequenced. Depending on the primary insertion site in the codons, both read through- and truncation mutants were found, some at the very same amino acid position (Fig. 19).

## D. Results

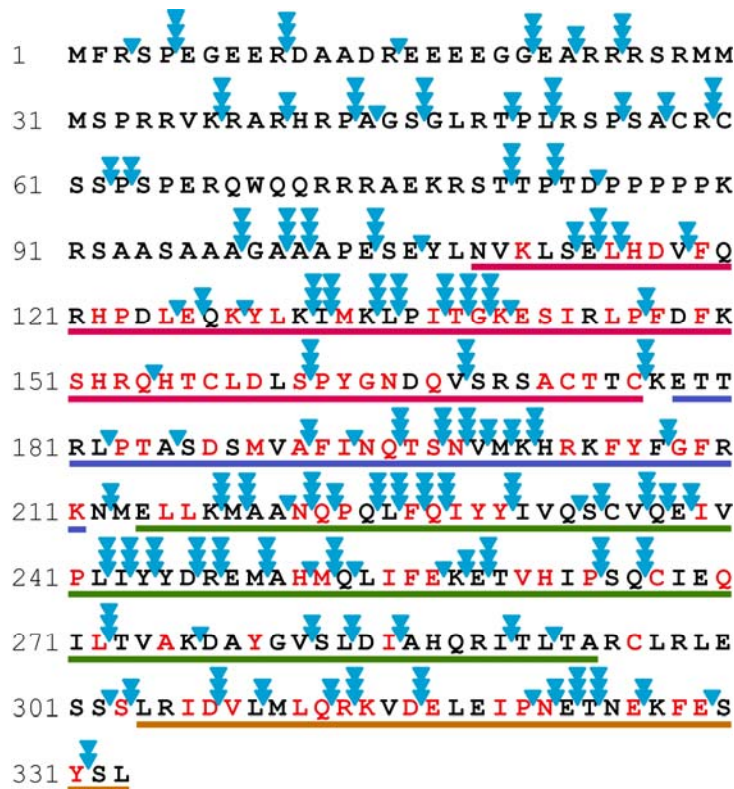


**Figure 19. Analysis of 498 M53 insertion mutants.** Displayed is the amino acid sequence of M53/p38. Arrowheads indicate transposon insertion sites. Three arrowheads indicate more than three insertions at the same position of the M53-ORF; Two arrowheads represent two insertions leading to the introduction of 5 aa into the M53 ORF. One arrowhead indicates transposon insertion at one site of the M53-ORF. Underlined parts of the M53 amino acid sequence indicate the conserved regions described in Fig.20. Red letters indicate aa which are strictly conserved in  $\beta$ -herpesvirus.

From this set a total of 46 in frame insertion mutants representing a distribution of about one insertion per 10-15 aa and 8 stop mutants were selected for the complementation assays and were re-inserted one by one into the m16/17FRT- $\Delta$ M53-BAC (Re-insertion principle see figure 10).

## D. Results

### 3. Alignment of the aa-sequence of a total of 36 members of the UL31 family indicates conserved and not-conserved regions

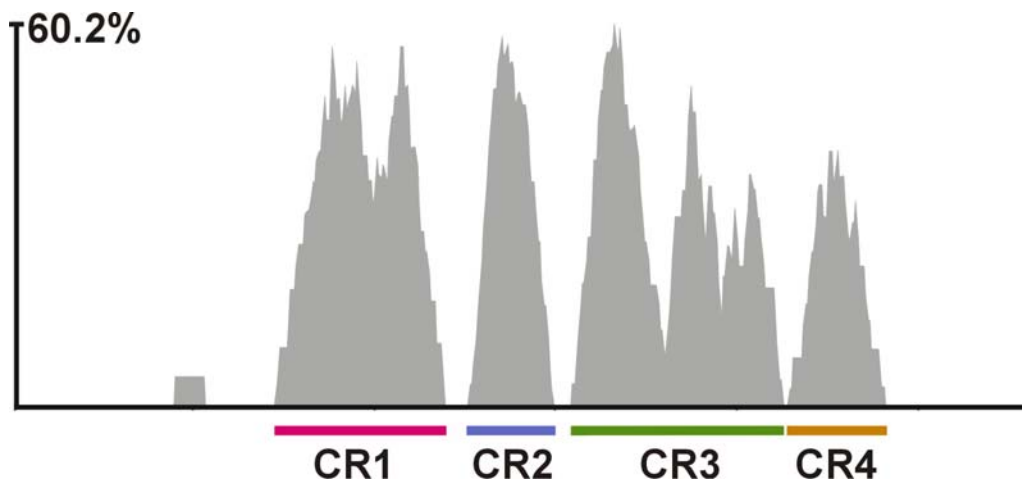


**Figure 20. Analysis of M53 insertion mutants by ectopic cis-complementation of  $\Delta$ M53-BAC.** Sequence comparison of the M53/p38 homologues. The amino acid sequence of M53/p38 was aligned to all 36 UL31 family members by use of the Vector NTI Align X program (Invitrogen) via the BLOSUM 62 similarity matrix. The depicted similarity plot was calculated using a 5-aa window size and with scores for identity and strong and weak similarities of 1.0, 0.5 and 0.2, respectively. The x-axis represents the number of the amino acids of the consensus sequence. Conserved regions one to four (CR1-4) are indicated below the diagram.

Using the AlignX program (Invitrogen) the aa-sequence of a total of 36 members of the UL31 family ([www.sanger.ac.uk/Software/Pfam](http://www.sanger.ac.uk/Software/Pfam), accession number PF02718; (Bateman, 2004)) were aligned (Fig. 20). The average similarity between beta-herpesvirus UL31 members is 47.5% and 25.1% within the whole family. However, the homology is not equally distributed along the sequences. A variable N-terminal and a conserved region including the central and C-terminal 2/3 of the proteins were identified with a similarity of 84.6% among the beta-herpesviruses and 44% for the whole family. Furthermore, when the entire UL31 family was aligned, the similarity plot indicated four peaks along the conserved region, which may reflect strictly conserved domains and were assigned as conserved regions one to four (CR1-CR4). We assumed that, according to the sequence conservation, lethal mutations should accumulate in the conserved central and C-terminal regions (corresponding to aa 115-333 of M53/p38) rather than in the N-terminal variable region (corresponding to aa 1-114 of M53/p38). We expected to find the binding site(s) for M50/p35 within one of the four conserved regions.

## D. Results

### 4. Ability of the selected M53-mutant set to rescue the M53 null phenotype: Confirmation of the in silico predicted sequence homology

1 MFRSPEGEERDAADREEEEGGEARRRSRMM  
31 MSPRRV<sup>▼</sup>KRARHRP<sup>▼</sup>AGSGLRT<sup>▼</sup>PLRSPS<sup>▼</sup>ACRC  
61 SSPSPERQWQQRRAEKRSTTPTDPPPPK  
91 RSAASAA<sup>▼</sup>AGAAPE<sup>▼</sup>SE<sup>▼</sup>YLNVKLSEL<sup>▼</sup>HDFVQ  
121 RHPDLEQ<sup>▼</sup>KYLK<sup>▼</sup>IMKLPIT<sup>▼</sup>GKESIRLP<sup>▼</sup>FDFK  
151 SHR<sup>▼</sup>QHTCLDLS<sup>▼</sup>PYGNDQ<sup>▼</sup>V<sup>▼</sup>SRSACTTCKETT  
181 RL<sup>▼</sup>PTA<sup>▼</sup>SDSMVA<sup>▼</sup>FINQ<sup>▼</sup>TSN<sup>▼</sup>VMK<sup>▼</sup>HRKFY<sup>▼</sup>FGR  
211 KN<sup>▼</sup>MEL<sup>▼</sup>LK<sup>▼</sup>MAANQPQLF<sup>▼</sup>Q<sup>▼</sup>IYYIVQ<sup>▼</sup>SCVQ<sup>▼</sup>EIV  
241 PLI<sup>▼</sup>YYDREMA<sup>▼</sup>HMQLIFEKETVHIPSQ<sup>▼</sup>CIEQ  
271 IL<sup>▼</sup>TVAKDAYGV<sup>▼</sup>SLDIAHQRI<sup>▼</sup>T<sup>▼</sup>L<sup>▼</sup>TARCLRLE  
301 SSSL<sup>▼</sup>RL<sup>▼</sup>ID<sup>▼</sup>V<sup>▼</sup>LM<sup>▼</sup>LQ<sup>▼</sup>R<sup>▼</sup>KVDELEIPNETNEKFES  
331 YSL

**Figure 21. M53 mutants and their ability to rescue virus growth of the  $\Delta$ M53 genome.** Displayed is the amino acid sequence of M53/p38. Arrowheads indicate transposon insertion sites. Open arrowheads indicate insertions leading to a stop codon; filled arrowheads represent insertions leading to the introduction of 5 aa into the M53 ORF. Light green arrowheads indicate mutants that rescued the  $\Delta$ M53 phenotype. Black arrowheads indicate those mutants that were not able to rescue the  $\Delta$ M53 phenotype. Underlined parts of the M53 amino acid sequence indicate the conserved regions described in Fig.20.

First, the ability of the selected mutant set to rescue the M53 null phenotype was tested. To this end, M53 mutants were re-inserted into the  $\Delta$ M53-MCMV-BAC, which was then transfected into MEF (reconstitution principle see figure 11). The results of the virus reconstitution screen are summarized in figure 21. All in frame insertions within the N-terminal part of the M53 ORF (aa 1-114) gave rise to viral progeny. In contrast, 32 out of 37 insertion mutants in the central- and C-terminal domains had a lethal phenotype. The clusters of lethal mutants are interspersed by single viable insertion mutants. The 14 viable

## D. Results

insertion mutants showed viral plaques comparable to the MCMV-M53E virus. A set of 8 truncation mutants was chosen to test the essentiality of the four conserved sequence clusters. All truncation mutants turned out to be non-functional. Altogether, loss-of-function-mutants accumulated in the conserved central- and C-terminal part of M53/p38. The less conserved N-terminal domain tolerated a number of insertions suggesting that this domain has a less stringent function.

### **5. The N-terminal 1/3 of M53/p38 contains a nuclear localization signal**

Within the non-conserved N-terminal region of M53/p38 two overlapping bipartite nuclear localization sequences (NLS) are predicted at aa 24-41. In order to test this, the N-terminal domain of the wt M53 protein from aa 16-106 was deleted thereby creating mutant M53- $\Delta$ 16-106. The very N-terminal 15 aa were kept as target sequence for the M53/p38 peptide specific antibody (Bubeck, 2004). After insertion into m16/17FRT- $\Delta$ M53-BAC the M53- $\Delta$ 16-106 was not able to rescue the null phenotype of the genome (Fig. 22). After transfection of NIH 3T3 cells with pOriR6K-ie-zeo expressing the M53- $\Delta$ 16-106 cytoplasmic staining was observed instead of the diffuse nuclear staining typical for wt M53/p38 (Fig. 22). To prove that the loss of function of the M53- $\Delta$ 16-106 mutant was due to protein miss-location we inserted the 9aa NLS from the SV40 large T antigen into M53- $\Delta$ 16-106 to create M53- $\Delta$ 16-106NLS. The heterologous NLS restored the correct nuclear localization of the protein (Fig. 22). The existence of an NLS within the N-terminal part of M53/p38, was tested by a fusion between aa 1-106 of M53/p38 and the EGFP ORF. NIH 3T3 cells expressing EGFP showed fluorescent protein in both cytoplasm and nucleus whereas the M53/1-106-EGFP fusion construct was restricted to the nucleus.

## D. Results

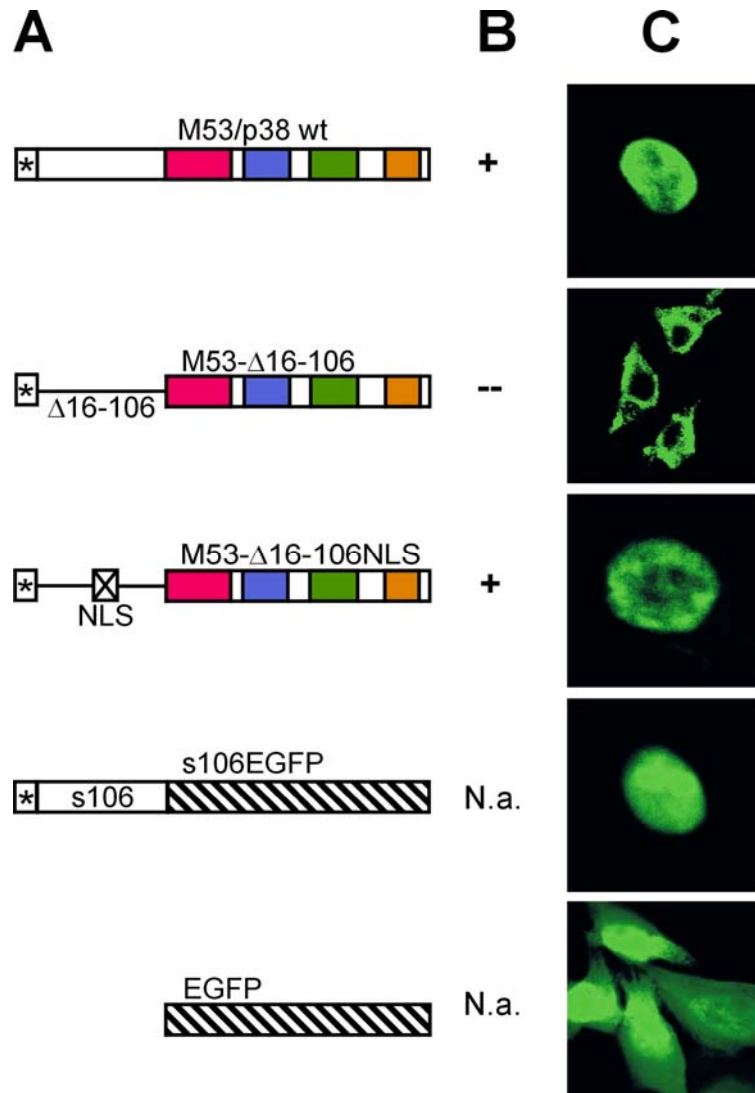


**Figure 22. Functional analysis of N-terminal deletion mutants of M53.** (A) Schematic representation of the different deletion constructs. The epitope for the anti-M53/p38 serum is indicated by a star at the very N-terminus of the diagrams. The variable sequences are represented by open boxes. The conserved regions are shown as shaded boxes. The deleted sequences are indicated by a line. The inserted SV40-NLS is indicated by a crossed box. The EGFP sequence is shown as a diagonally hatched box. (B) Wt M53 and mutants M53- $\Delta$ 16-106 and M53- $\Delta$ 16-106NLS were reinserted into  $\Delta$ M53-BAC. BAC DNA was isolated and transfected into MEF cells and screened for plaque formation and the rescue result is indicated (+, -, N.a.-not applicable). (C) Sub-cellular localization of expressed proteins with N-terminal deletions. NIH 3T3 fibroblasts were transfected with the indicated constructs. The localization of the expressed proteins were visualized by indirect immunofluorescence for the wt M53, M53- $\Delta$ 16-106 and M53- $\Delta$ 16-106NLS. Endogenous fluorescence was recorded for EGFP and mutant s106EGFP.

Finally, also the mutant M53- $\Delta$ 16-106NLS, lacking aa 16 to aa 106 but carrying the SV40 NLS, but not M53- $\Delta$ 16-106 rescued the null phenotype of m16/17FRT- $\Delta$ M53-BAC. Thus, nuclear targeting of the protein is the only essential function of the N-terminal part of M53/p38.

## **6. The M50/p35 binding site of M53/p38**

### **6.1 Using M53-stop and N-terminal deletion mutants the M50/p35 binding site of M53/p38 can be located to CR1 of M53/p38**

We predicted that binding of M53/p38 to M50/p35 should represent an essential function. Therefore, the pool of lethal M53 mutants should contain mutants which have lost the ability to bind to M50/p35. For a first rough mapping of the binding region the selected set of M53/p38 truncation mutants was analyzed. To this end, NIH 3T3 fibroblasts were transfected either with wt M53/p38 or M53/p38 mutants in the presence or absence of M50/p35 co-expression. Sub-cellular localization of wt and mutated M53/p38 was analyzed by confocal microscopy after indirect immunofluorescence staining with specific antisera (Fig. 23A). After isolated expression all truncation mutants as well as the wt M53/p38 (M53) showed the typical diffuse nuclear staining pattern (Fig. 23A, first vertical row).

After co-transfection with M50/p35 the diffuse nuclear staining and no co-localization with M50/p35 was observed only for the stop mutant s106 lacking all four conserved regions (Fig. 23A, second horizontal row). All other stop mutants, s137, lacking CR 2-4 and the C-terminal part of CR1 and s168, lacking CR 2-4 (Fig. 23A, third and fourth horizontal rows), co-localized with M50/p35 at the nuclear rim. In addition, M53 $\Delta$ 16-106, lacking the NLS, lost the ability to be transported to the nucleus (see Fig. 22) and therefore did not co-localize with M50/p35, whereas functional M53 $\Delta$ 16-106NLS did (Fig. 23B).



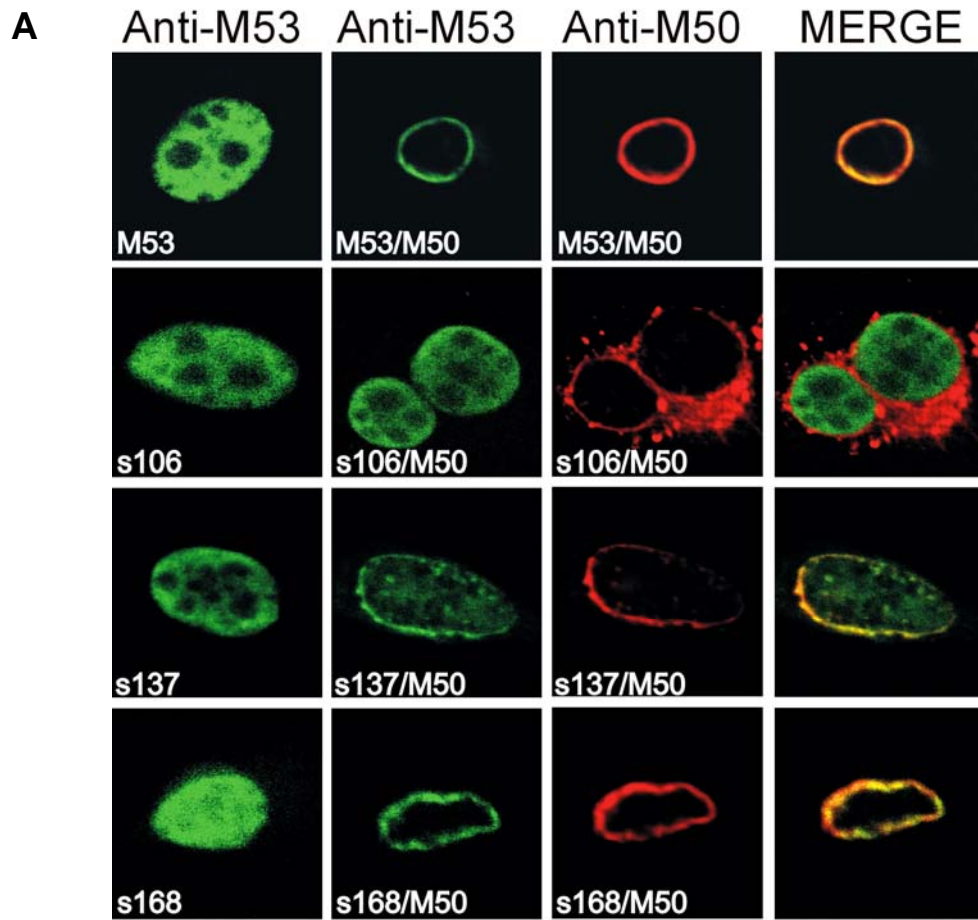


**Figure 23A. Analysis of the interaction of M53 stop mutants with M50/p35.** Localization of M53 stop mutants. NIH 3T3 cells were transfected with M53 stop mutants s106, s137 or s168 alone (first vertical row) or together with wt M50/p35 (second to fourth vertical rows). Single transfected cells were stained with rat specific antiserum against M53/p38. For detection a fluorescein-conjugated secondary antibody was used (green). Co-transfected cells were treated as described above and co-stained with an M50/p35-specific rabbit serum, which was detected by Texas red coupled secondary antibody (red). As control wt M53/p38 was used (first horizontal row).



D. Results

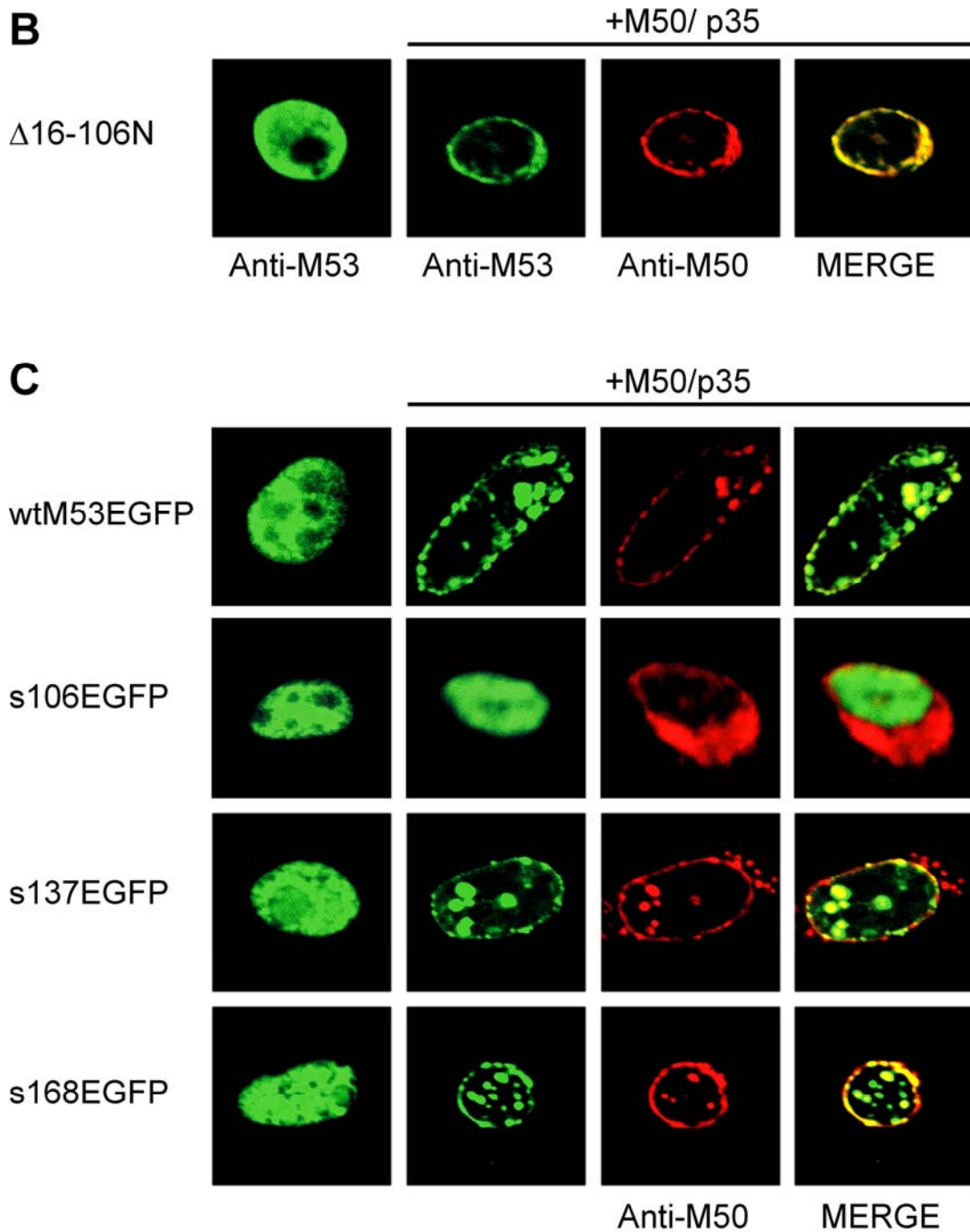


**Figure 23B and C. Analysis of the interaction of M53 stop- and N-terminal deletion mutants with M50/p35.** (B) Localization of M53 N-terminal deletion mutant M53 $\Delta 16-106NLS$ . NIH 3T3 cells were transfected with M53 $\Delta 16-106NLS$  alone (first vertical row) or together with wt M50/p35 (second to fourth vertical rows). Single transfected cells were stained with rat specific antiserum against M53/p38. For detection a fluorescein-conjugated secondary antibody was used (green). Co-transfected cells were treated as described above and co-stained with an M50/p35-specific rabbit serum, which was detected by Texas red coupled secondary antibody (red). (C) Localization of M53-stop mutants fused to EGFP. NIH3T3 cells were transfected with wt M53 or mutant M53 fused to EGFP (first vertical row) or co-transfected with wt M50/p35 (second to fourth vertical row). Co-transfected cells were stained with rabbit specific antiserum, which was detected by Texas red coupled secondary antibody (red).

## D. Results

---

Furthermore, NIH 3T3 cells expressing wtM53-EGFP fusion construct or fusion constructs of M53 truncation mutants and EGFP in presence of M50/p35 co-expression were analyzed. Sub-cellular localization of wt and mutated M53/p38 was investigated by confocal microscopy after indirect immunofluorescence staining with specific antisera. In isolated expression wtM53- and mutant EGFP fusion constructs were diffusely distributed in the nucleus, as described for wtM53 (Fig. 23C, first vertical row). After co-expression with M50/p35 the wtM53-or s137- and s168-EGFP fusion constructs co-localized together with M50/p35 to the nuclear envelope but showed a more punctuated staining than wtM53/p38 (Fig. 23C, first, third and fourth horizontal rows). Fusion construct s106-EGFP was present in the nucleus but lost the ability to co-localize with M50/p35 (Fig. 23C, second horizontal row).

These co-localization experiments indicated a critical role of M53/p38 aa 1-137 for interaction with M50/p35. To confirm the results obtained by sub-cellular localization of the M53 truncation mutants, we performed co-immunoprecipitation experiments with the stop mutants. 293 cells were co-transfected with expression plasmids containing mutant M53 constructs and pM50 expressing wt M50/p35. Controls were transfected with plasmids expressing wt M50, wt M53 or M53 truncation mutants alone. Cell lysates were precipitated by specific antisera. The wt M53/p38 was co-precipitated in the presence of M50/p35 when M50 specific antiserum was used (Fig. 24A, lane 3). The M53s106 stop mutant was unable to bind to M50/p35 (lane 5). All other stop mutants M53s137, M53s168, and M53s185 bound M50/p35 as shown by the specific bands corresponding to the expected molar masses after co-precipitation with anti-M50/p35 (lanes 7, 9 and 11).

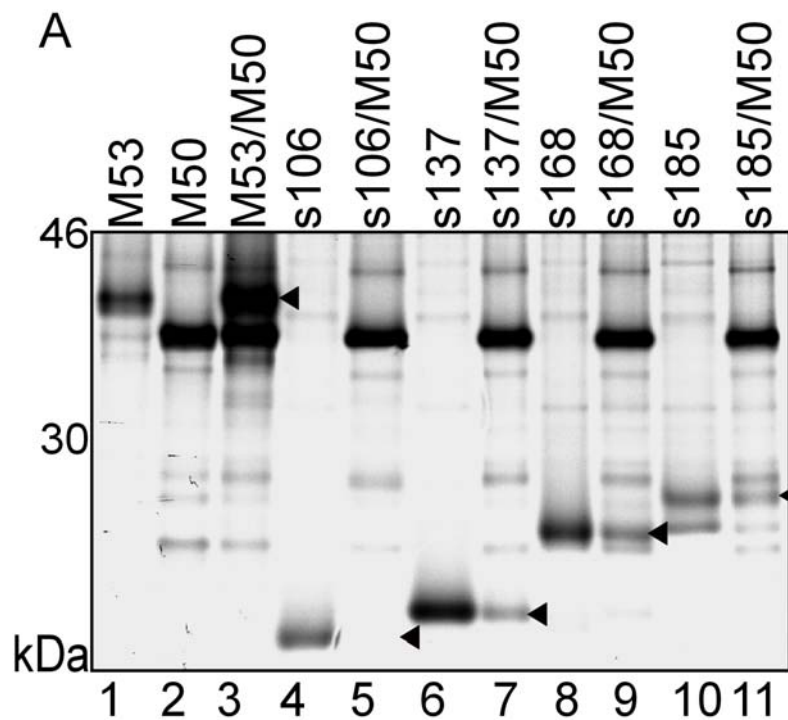


**Figure 24A. Co-immunoprecipitation of M53 stop mutants and M50/p35.** Plasmids expressing wt M53/p38 (lane 1), wt M50/p35 (lane 2) and M53 stop mutants (lanes 4, 6, 8, 10) were transfected into 293 cells. In parallel wt M53/p38 and M53 stop mutants were co-transfected with wt M50/p35 (lanes 3, 5, 7, 9, 11). Cells were radioactively labeled and single transfected probes were precipitated with anti-M53/p38 specific rat serum on Protein-G Sepharose. Protein complexes with wt M50 were precipitated with Protein-A Sepharose using anti-M50/p35 specific rabbit serum (lanes 3, 5, 7, 9, 11; black arrowheads). Samples were analyzed by SDS-PAGE followed by autoradiography.

Furthermore, also the M53 $\Delta$ 16-106NLS mutant, containing 9 aa of the SV40 NLS and lacking the N-terminal part of the protein till aa 106, but not M53 $\Delta$ 16-106, lacking the same N-terminal aa but also the SV40 NLS, co-precipitated with M50/p35 (Fig. 24B).

The binding pattern was further tested in pull down assays after co-transfection of pM50ST expressing Strep-II tagged M50/p35 with wt and mutant M53 constructs. From the lysates of co-transfected 293 cells proteins bound to M50ST were recovered by Strep-Tactin Sepharose beads. The M50ST complexes were eluted from the beads by desthiobiotin and separated by SDS-PAGE and subjected to Western-blot analysis using M53/p38 specific antiserum. The data were in full agreement with the results obtained by co-immunoprecipitation with wt M50/p35 (Fig. 24C).

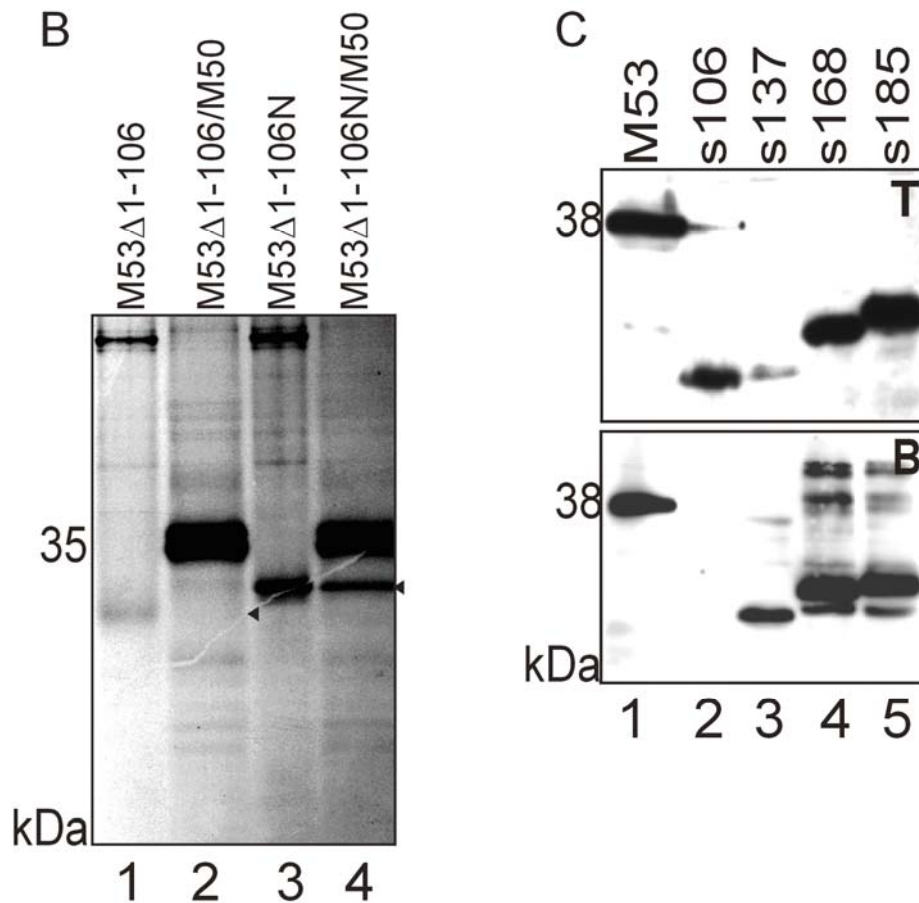


**Figure 24B and C. (B) Co-immunoprecipitation of M53 N-terminal deletion mutants and M50/p35.** Plasmids expressing M53 $\Delta$ 1-106 (lane 1) or M53 $\Delta$ 1-106N (lane 3) were transfected into 293 cells. In parallel both M53 mutants were co-transfected with wt M50/p35 (lanes 2 and 4). Cells were radioactively labeled and single transfected probes were precipitated with anti-M53/p38 specific rat serum on Protein-G Sepharose. Protein complexes with wt M50 were precipitated with Protein-A Sepharose using anti-M50/p35 specific rabbit serum. Samples were analyzed by SDS-PAGE followed by autoradiography. **(C) Pull down assay of M53 stop mutants with Strep tagged M50/p35.** Wt M53/p38 and M53 stop mutants were co-transfected with M50ST into 293 cells. Total cell lysates were analyzed to test the protein expression by Western blot using specific antiserum against M53/p38 (upper panel, total protein-T). Proteins complexed with M50ST were precipitated by Strep-Tactin Sepharose. Desthiobiotin eluates were analyzed by SDS-PAGE and blotted on membranes. Wt M53/p38 and mutant proteins were detected by Western blot with M53/p38 specific antiserum (lower panel, bound protein-B).

These data, together with the functionality of M53 $\Delta$ 16-106NLS mutant in virus context suggested that a short sequence of M53/p38 CR1 is required for M50/p35 binding.

## 6.2 Using M53 insertion mutants the M50/p35 binding can be located to the beginning of CR1 and the most important residues are probably represented by aa 115 to 131 of the M53/p38 protein

To describe the contribution of specific residues involved in M50/p35-M53/p38 interaction we analyzed M53/p38 mutants with insertions in the region between aa 106 and aa 138 by confocal microscopy and by the M50ST mediated protein pull down assay. NIH 3T3 cells were transfected with different M53/p38 insertion mutants alone or together with pM50. As expected, all analyzed M53 insertion mutants showed a diffuse nuclear staining after isolated expression (Fig. 25A, first vertical row). After co-transfection with pM50 only mutant M53i128 was not able to co-localize with M50/p35 at the nuclear rim (Fig. 25A, third horizontal row). All other insertion mutants tested, i.e. i104, i115, i131 and i138 tolerated the 5 aa insertion in as much as they were recruited to the NE by M50/p35 co-expression.

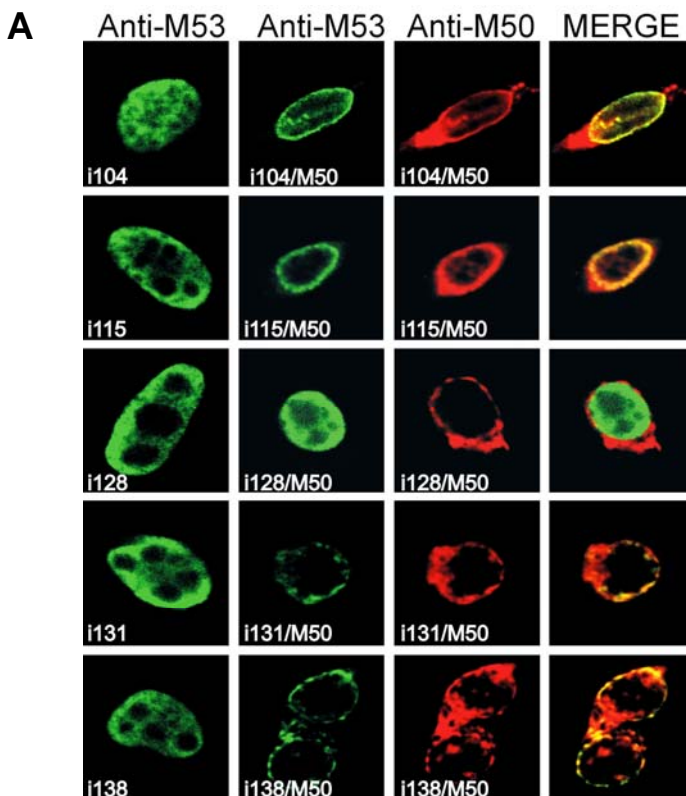


**Figure 25A. Analysis of the interaction of M53 insertion mutants with M50/p35.** Localization of M53 insertion mutants. NIH 3T3 cells were transfected with M53 insertion mutants i104, i115, i128, i131 or i138 alone (first vertical row) or together with wt M50 (second to fourth vertical rows). Single transfected cells were stained with rat specific antiserum against M53/p38. For detection a fluorescein-conjugated secondary antibody was used (green). Co-transfected cells were treated as described above and co-stained with an M50/p35 specific rabbit serum, which was detected by Texas red coupled secondary antibody (red).

## D. Results

In addition, 293 cells were co-transfected with pM50ST and the same set of M53/p38 insertion mutants which was used in the co-localization experiments. In parallel, the total cell lysates were analyzed to determine the expression of the M53/p38 mutants by Western-blot. Furthermore, for Strep II-tag pull down experiments instead of standard cell lysates nuclear extracts were processed to enrich the nuclear M53/p38. Among the mutants tested, only the insertion mutant M53i128 was not pulled down by M50ST (Fig. 25B, lane 3), which is in line with the results of the co-localization studies shown above.

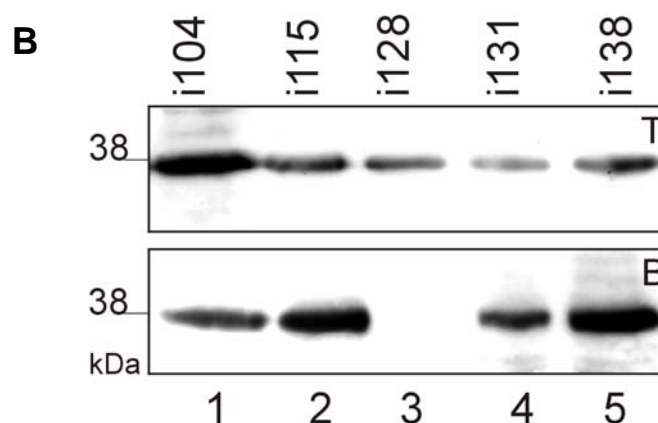


**Figure 25B. Pull down analysis of M53 insertion mutants with Strep tagged M50/p35.** 293 cells were co-transfected with M53 insertion mutants and M50ST. Total cell lysates were analyzed by SDS-PAGE and Western blot using specific M53/p38 antiserum (upper panel, T). Proteins complexed with M50ST were precipitated with Strep-Tactin Sepharose and desthiobiotin eluted proteins were separated by SDS-PAGE. Signals for M53/p38 insertion mutants were visualized by Western blot using specific antiserum against M53/p38 (lower panel, B).

Taken together, co-localization- and protein-protein interaction assays using several C-terminal truncation and insertion mutants indicated that the region of M53/p38 which is necessary for M50/p35 binding is located at the start of CR1 and the most important residues are probably represented by aa 115 to 131 of the M53/p38 protein.



---

## **7. Characterization of the M50/p35 binding site of M53/p38**

### **7.1 Distinct M53-point mutants lost to some extent the ability to localize to M50/p35**

Insertions of five amino acids helped to identify a binding motif but the contribution of the inserted amino acids that differ between the different insertion mutants is difficult to evaluate. In order to define the relative role of individual amino acids with respect to M50/p35 binding the 12 amino acids which are conserved in beta-herpesviruses within the N-terminal half of CR1 (aa 112-137) were one by one replaced by alanine. After transfection of NIH 3T3 cells with the M53/p38 point mutants alone or co-transfection with M50/p35, respectively, the sub-cellular localization of the M53/p38 mutants was analyzed. All M53/p38 point mutants showed a diffuse nuclear staining when expressed alone (Fig. 26, first vertical row). After co-expression with M50/p35, the intra-nuclear distribution of M53 point mutants fell into three classes of phenotypes:

- i. Mutants that redistributed to the nuclear rim and recruited M50/p35 similar to wt M53/p38 (M53P123A, M53D124A, and M53E126A).
- ii. Mutants that had apparently lost the ability to redistribute to the nuclear rim in presence of M50/p35 (M53Y129A (Fig. 26), M53L130A and M53I133A).
- iii. Mutants with intermediate phenotypes. Several mutants fell into this class and their phenotypic appearance was variable. One subset showed abundant diffuse intra-nuclear staining in addition to co-localization with M50/p35 at the nuclear rim (M53L112A (Fig. 26), M53H116A, M53F119A, M53I137A). The second type of mutants co-localized with M50/p35 at least to some extent.

## D. Results

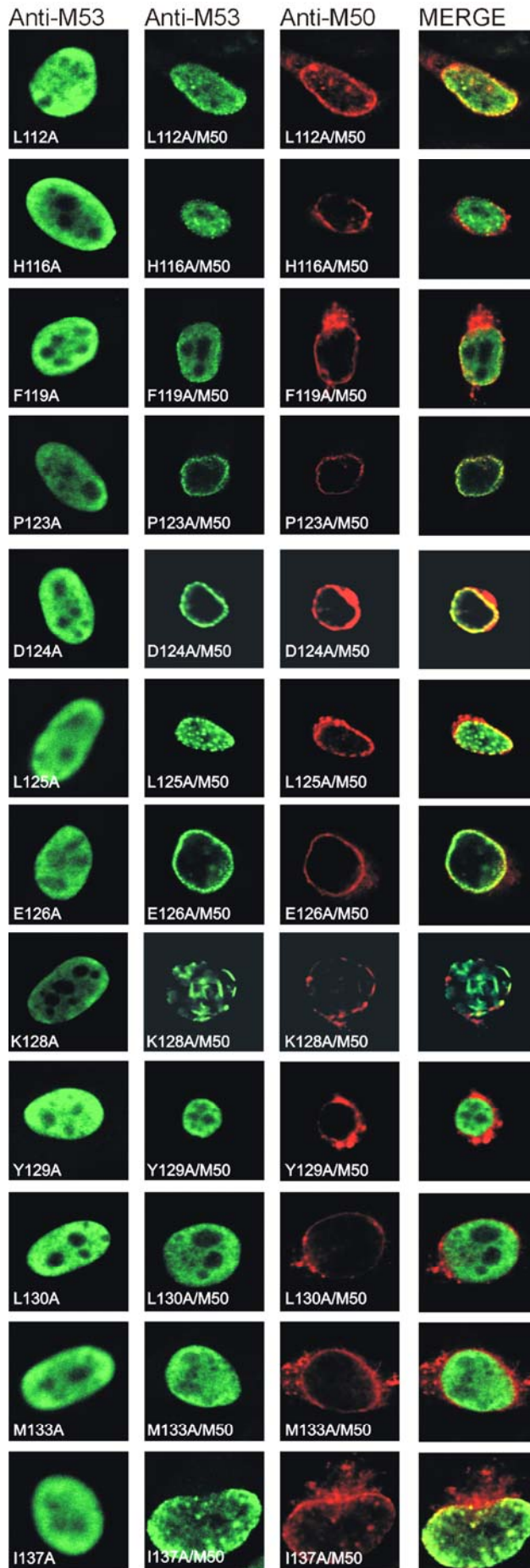


**Figure 26. Functional analysis of M53 point mutants.** Sub-cellular localization of M53 point mutants. NIH 3T3 cells were transfected alone with M53 point mutants L112A, L125A, K128A and Y129A (first vertical row) or co-transfected with wt M50/p35 (second to fourth vertical rows). Single transfected cells were stained with rat specific antiserum against M53/p38. For detection a fluorescein-conjugated secondary antibody was used (green). Co-transfected cells were treated as described above and co-stained with an M50/p35 specific rabbit serum, which was detected by Texas red coupled secondary antibody (red).



## D. Results

The remarkable phenotype, however, was a new distribution of M53/p38 mutants upon co-expression of M50/p35 resulting in the formation of discrete intra-nuclear aggregates (M53L125A) and fibrous structures (M53K128A, Fig. 26) which did not co-localize with M50/p35. In the absence of M50/p35 the intra-nuclear distribution of the mutants was indistinguishable from that of wt M53/p38.

### 7.2 Distinct M53/p38 point mutants showed reduced binding to M50/p35 and resulting viruses were strongly attenuated

Next, 293 cells were co-transfected with M50ST and the set of alanine scanning M53/p38 mutants. Strep-Tactin Sepharose pull-down was performed to analyze the binding capacity of the M53 point mutants to M50ST. Remarkably, despite the different distribution phenotypes, all M53 point mutants could still be retrieved by M50ST pull-down, including those that did not show a detectable interaction in the co-localization assay (Fig. 27A). Notably, the binding was found significantly reduced for the mutants M53L112A, M53L125A, M53Y129A and M53M133A.

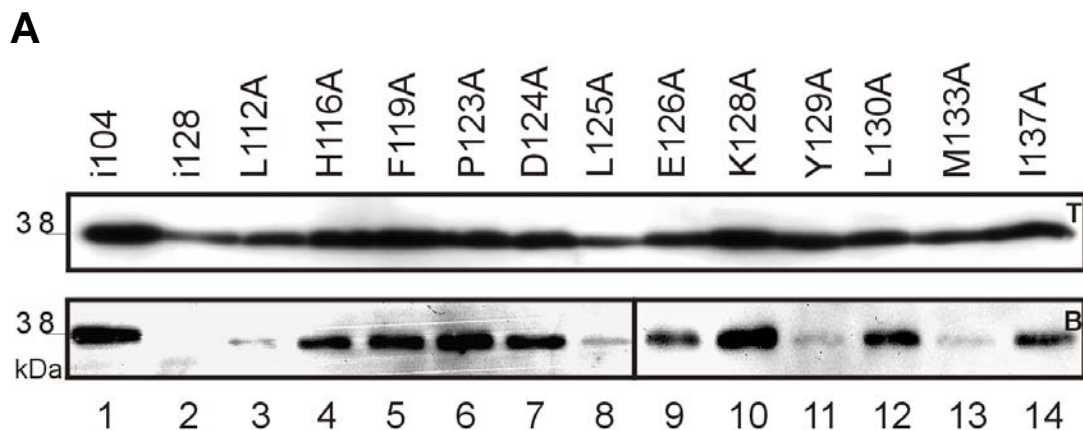


**Figure 27A. Pull down analysis of 12 M53 point mutants with Strep-tagged M50/p35.** 293 cells were co-transfected with the indicated M53 point mutants and M50ST. Total cell lysates were analyzed to test the protein expression by Western blot using specific antiserum against M53/p38 (upper panel, T). Proteins complexed with M50ST were precipitated by Strep-Tactin Sepharose. Desthiobiotin eluates were analyzed by SDS-PAGE and blotted on membranes. Signals for M53 point mutants were visualized by Western blot with M53/p38 specific antiserum (lower panel, B). As positive control for precipitation functional insertion mutant M53i104 was used (lane 1) and M53 insertion mutant M53i128 served as negative control (lane 2).

## D. Results

Since there was a substantial degree of variability in the co-localization assay and certain heterogeneity of interactions detectable by the pull-down assay, we tested the M53 point mutants for functionality in the viral context. Interestingly, the null phenotype of  $\Delta$ M53FRT-BAC could be reverted by all M53 point mutants. Usually about 11 days are required to detect the first virus plaques after transfection of the ectopically complemented deletion genome. Remarkably, virus reconstitution time and plaque formation was significantly delayed to three weeks for mutants M53K128A and M53L130A. Virus reconstitution from the BAC carrying M53Y129A required even six weeks.

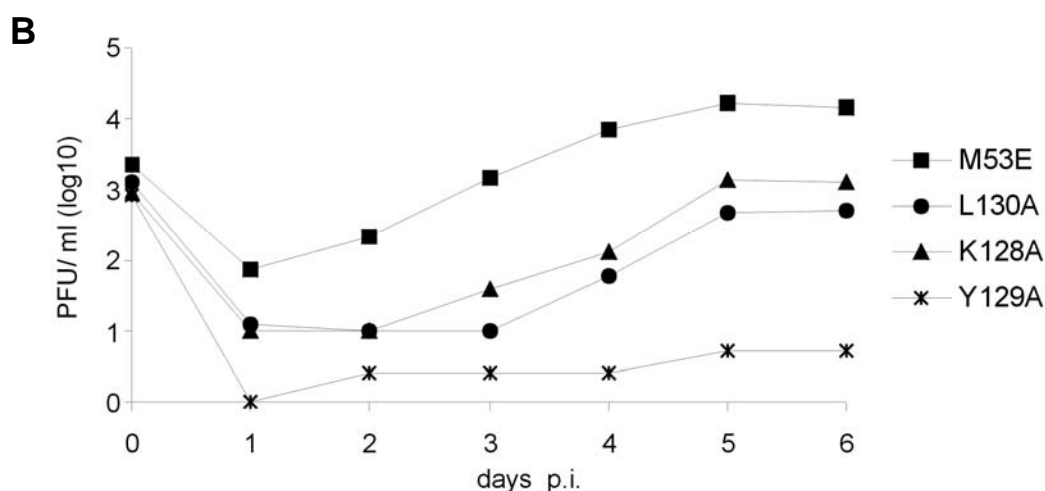


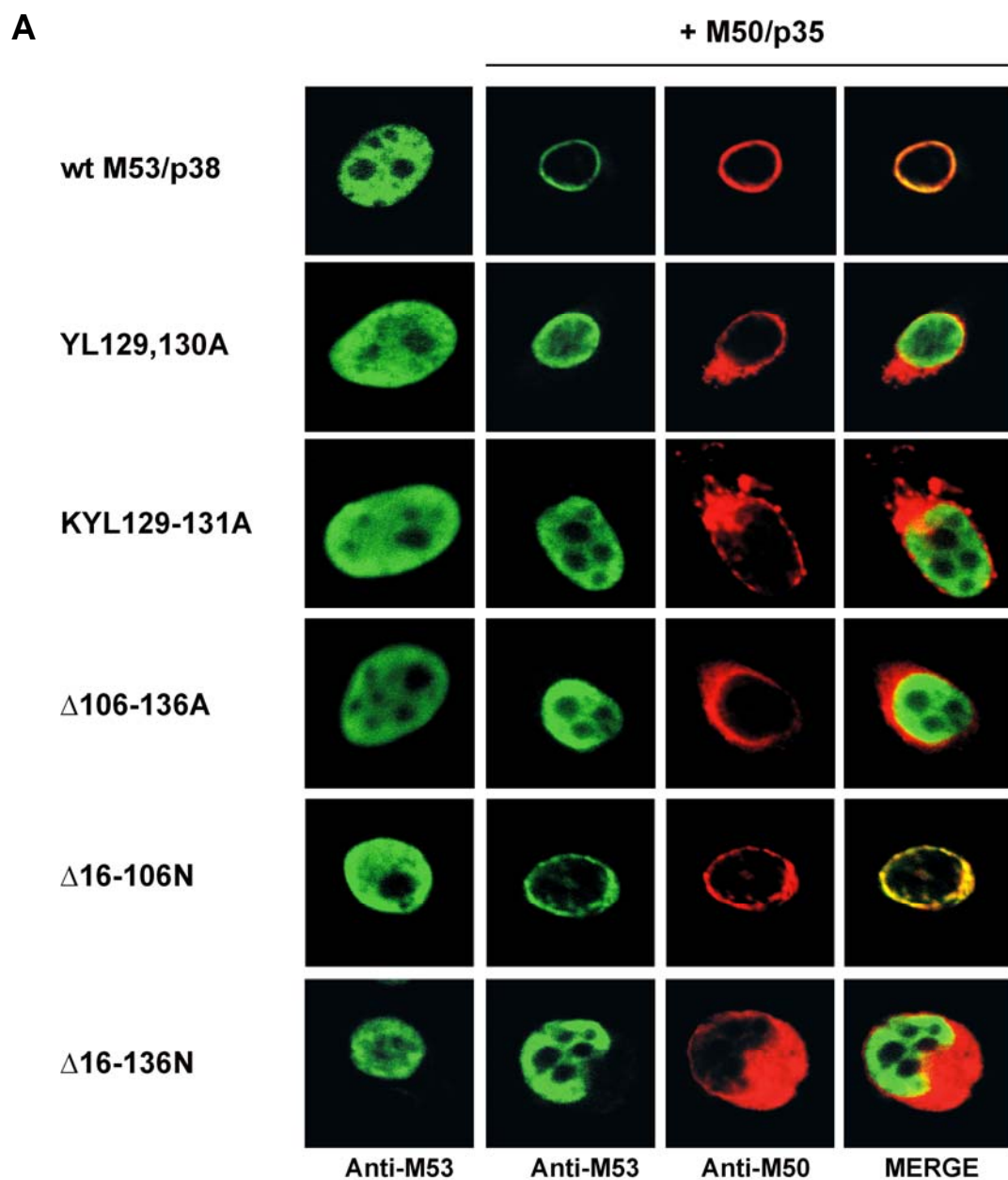
**Figure 27B. Rescue of  $\Delta$ M53-BAC by M53 point mutants K128A, Y129A and L130A.** Growth kinetics of the viruses derived from pM53E or pM53K128AE, pM53Y129AE and pM53L130AE. NIH 3T3 cells were infected with the respective viruses. Supernatants of the infected cells were harvested on the indicated days, and virus titers were determined by plaque assay.

Accordingly, the growth of mutants M53K128A and M53L130A was reduced by one order and M53Y129A was attenuated more than 3 orders of magnitude in comparison with a genome complemented by wt M53 ORF (Fig. 27B). These data show that already the exchange of a single aa within the binding region of M53/p38 can strongly affect M50/p35 binding but cannot completely abolish a functional M50/p35-M53/p38 interaction.

## D. Results

### 7.3 Exchange of only two aminoacids abolishes M50-M53 interaction and rescue of the M53 null phenotype

To rigorously test the binding site we replaced either two adjacent critical amino acids (M53YL129-130A) or three adjacent amino acids by alanine (M53KYL128-130A). In addition, we deleted the sequences aa 108-136 of M53 (M53 $\Delta$ 106-136). As expected, each of these mutants completely failed to co-localize with M50/p35 (Fig. 28A), failed to interact with M50ST in the pull-down assay (Fig. 28B) and also failed to rescue the M53 null phenotype.



## D. Results

**Figure 28A. Functional analysis of M53 point-and deletion mutants.** Sub-cellular localization of M53 point-and deletion mutants. NIH 3T3 cells were transfected alone with M53 point- and deletion mutants M53YL129-130A, M53KYL128-130A,  $\Delta$ 16-136A,  $\Delta$ 16-106N and  $\Delta$ 16-136N (first vertical row) or co-transfected with wt M50/p35 (second to fourth vertical rows). Single transfected cells were stained with rat specific antiserum against M53/p38. For detection a fluorescein-conjugated secondary antibody was used (green). Co-transfected cells were treated as described above and co-stained with an M50/p35 specific rabbit serum, which was detected by Texas red coupled secondary antibody (red).

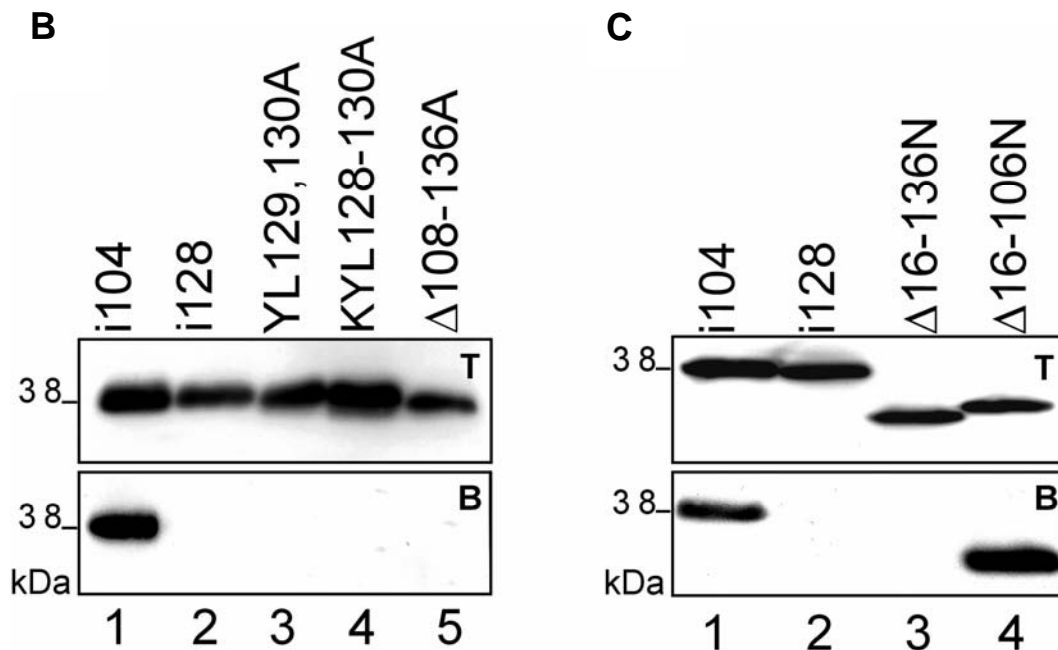


**Figure 28B and C. Analysis of the interaction of M50/p35 with M53 point- and N-terminal deletion mutants. (B)** Pull down analysis of M53 point mutants YL129,130A, KYL 128-130A and M53- $\Delta$ 108-136 with Strep-tagged M50. 293 cells were co-transfected with M53 point mutants and M50ST. Expression of the constructs was tested by SDS-PAGE of total cell lysates and Western blot using specific M53/p38 antiserum (upper panel, T). Proteins complexed with M50ST were precipitated by Strep-Tactin Sepharose. Desthiobiotin eluates were analyzed by SDS-PAGE and blotted on membranes. Signals for M53 point mutants were visualized by Western blot with M53/p38 specific antiserum (lower panel, B). As a positive control a functional insertion mutant, M53i104, was used (lane 1) and M53i128, which failed to bind to M50/p35 served as negative control (lane 2). **(C) Pull down analysis of N-terminal deletion mutants of M53/p38.** 293 cells were co-transfected with M53 N-terminal deletion mutants M53- $\Delta$ 16-106NLS or M53- $\Delta$ 16-136NLS and M50ST. Analysis of total cell lysates (upper panel, T) and protein complex formation (lower panel, B) was performed as described above.

The N-terminal deletion mutant of M53- $\Delta$ 16-106NLS carrying deletions of aa 16 to aa 106 and an artificial NLS rescued the M53 deletion after ectopic re-insertion into the mutant MCMV-BAC indicating that this mutant can interact with the M50/p35. To confirm the M50/p35 interaction site mapping data, the N-terminal deletion was increased to aa 16 to aa 136 (M53- $\Delta$ 16-136NLS). As

## D. Results

expected, the M53- $\Delta$ 16-106NLS did interact with M50ST in the pull-down assay whereas M53- $\Delta$ 16-136NLS did not (Fig. 28C). Also, in contrast to M53- $\Delta$ 16-106NLS the N-terminal deletion mutant M53- $\Delta$ 16-136NLS was not able to rescue the M53 null phenotype upon insertion into the deletion BAC.

### 8. Homo-oligomerization of M53/p38

So far we could show, that the N-terminal domain of M53/p38 possesses a nuclear targeting sequence as functional element. The N-terminal 1/3 of the protein is crucial for M50/p35 interaction. Next, we wanted to investigate, if M53/p38 is able to interact with itself. Therefore, 293 cells were co-transfected with expression plasmids containing Ig-tagged M53 construct and pM53 expressing wt M53/p38. Controls were mock transfected or transfected with plasmids expressing wt M53 or Ig-tagged M53 alone. In total cell lysates the M53/p38 specific signal at 38 kDa or at 62 kDa for Ig-tagged M53/p38 became detectable for all analyzed probes but was missing for mock transfected 293 cells (Fig. 29, T, lanes 1-4).

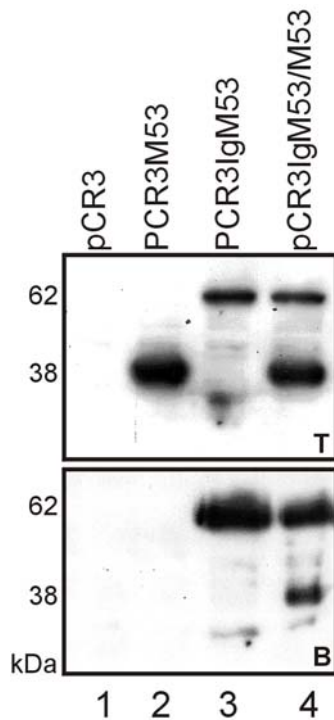


**Figure 29. Analysis of oligomerization of M53/p38.** Pull down analysis of wt M53 with Ig-tagged M53. 293 cells were transfected with wt M53 or Ig-tagged M53 or co-transfected with wt M53 and IgM53. Expression of the constructs was tested by SDS-PAGE of total cell lysates and Western blot using specific M53/p38 antiserum (upper panel, T). Proteins complexed with Ig M53 were precipitated by protein-A sepharose. Eluates were analyzed by SDS-PAGE and blotted on membranes. Signals for M53 were visualized by Western blot with M53/p38 specific antiserum (lower panel, B).

## D. Results

Next, cell lysates were precipitated by addition of protein G-sepharose (Pharmacia). M53/p38 signals were visualized by Western-blot using rat antiserum specific to the N-terminal 15 amino acids (aa) of the M53/p38 ORF (Bubeck, 2004). As expected, the Ig-tagged M53/p38, could be precipitated directly by the G-sepharose beads as indicated by presence of the specific 62 kDa band (Fig. 29, B, lane 3), whereas the wt M53/p38 did not bind when expressed alone (Fig.29, B, lane 2). However, the wt M53/p38 could be co-precipitated in the presence of Ig-tagged M53/p38, indicated by an additional specific signal at 38 kDa (Fig. 29, B, lane 4). Therefore, beside interaction with M50/p35, M53/p38 is able to oligomerize.

### **9. Cellular interaction partners of M53/p38 and M50/p35**

Next, we wanted to target functions that can be assigned to the C-terminal 2/3 of M53/p38. For the  $\alpha$ -herpesvirus herpes simplex virus type 1 (HSV-1) it has been described recently that the M53/p38- and M50/p35 homologues UL31 and UL34 can induce conformational changes in the nuclear lamina (Reynolds, 2004). Both gene products have been assumed to bind to lamin A/C thereby promoting the late maturation of viral replication compartments to the nuclear periphery (Simpson-Holley, 2004). Furthermore, UL34- and UL31-gene products from HSV-1 seem to be involved in alteration of the nuclear architecture (Simpson-Holley, 2005). The M53/p38- and M50/p35 homologues BFLF2 and BFRF1 of  $\gamma$ -herpesvirus EBV were shown to interact as complex with lamin B (Farina, 2005; Gonnella, 2005). Moreover, for human cytomegalovirus (HCMV) it has been described that the viral kinase pUL97 is recruited to the nuclear lamina by the cellular protein p32, thereby inducing conformational changes there (Marschall, 2005). Herpesvirus nucleocapsid formation is followed by a complex process of nucleocapsid transitions through cellular membranes. Most interestingly, co-transfected UL31 and UL34 of the  $\alpha$ -herpesvirus pseudorabies virus (PrV) seem to be sufficient for formation of budding membrane vesicles from the inner nuclear membrane in absence of any other viral proteins (Klupp, 2006). These data indicate that a number of host cell proteins might be involved in function of the NEC either as a target or as a



## D. Results

partner for function. Therefore, we wanted to analyze, which cellular proteins can be found that are associated with the NEC of MCMV.

### 9.1 Identification of the M50/p35-M53/p38 complex in post nuclear fractions

The nuclear lamina is on the one hand connected with integral membrane proteins of the INM and on the other hand connected with the chromatin (Östlund, 2006, Foisner, 2001, Gruenbaum, 2005). This makes the nuclear matrix components difficult to analyze. In order to study interaction of matrix components with M53/p38 or M50/p35, the NEC, extraction conditions had to be set up in a fashion that the matrix is disrupted but that NEC formation is maintained. Matrix proteins can be solubilized using mild detergents and high salt conditions (salt out effect; Montes de Oca, 2005). Therefore, first we tested the effect of increasing salt concentration on complex formation by M53/p38 and M50p35. To that end, 293 cells were either mock transfected, transfected with pM53 or pM50, expressing wtM53 or wtM50, or co-transfected with pM53 and pM50.

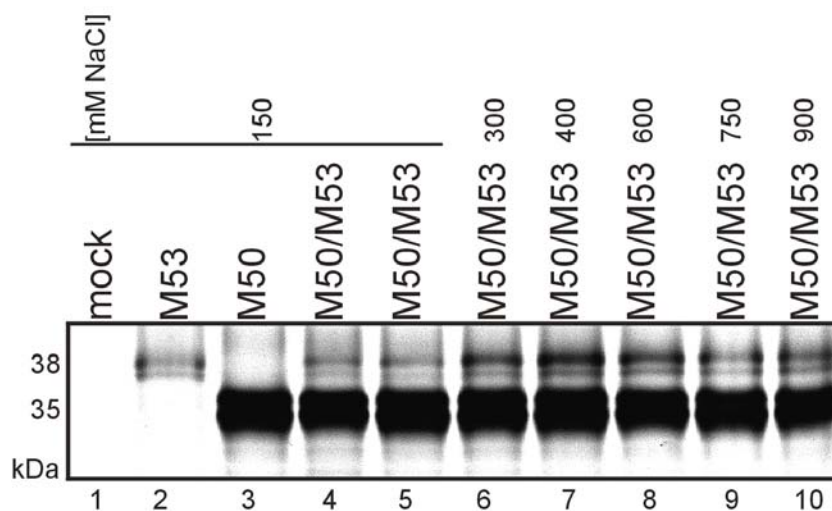


**Figure 30. Co-immunoprecipitation of M53/p38 and M50/p35 under increasing salt conditions.** Plasmids expressing wt M53/p38 (lane 2), wt M50/p35 (lane 3) were transfected into 293 cells. In parallel wt M53/p38 was co-transfected with wt M50/p35 (lanes 4-10). Cells were radioactively labeled, lysed at NaCl concentrations 150 mM, 300 mM, 400 mM, 600 mM, 750 mM and 900 mM and single transfected probes were precipitated with anti-M53/p38 specific rat serum on protein-G sepharose or with anti-M50/p35 specific sera from rabbit on protein-A sepharose. Protein complexes with wt M50 were precipitated with protein-A

## D. Results

sepharose using anti-M50/p35 specific rabbit serum. Samples were analyzed by SDS-PAGE followed by autoradiography.

Cell lysates were prepared at different salt concentrations and co-immunoprecipitation was performed. Lysates of mock and pM50 transfected cells or lysates of cells co-transfected with M50/p35 and M53/p38 were precipitated with specific rabbit anti-M50/p35 sera and protein A-sepharose (Fig. 30, lanes 1,2 and 4-10). M53/p38 was precipitated with specific rat anti-M53/p38 sera (Fig. 30, lane 2). As described previously, using anti-M50/p35 sera M50/p35 was precipitated indicated by a specific band at 35 kDa (Fig. 30, lanes 1,2 and 4-10). M53/p38 could be precipitated and co-precipitated at all tested salt concentrations indicated by a specific band at 38 kDa (Fig. 30, lane 2 and 4-10). The amount of co-precipitated M53/p38 increased by addition of 300 mM NaCl to the lysis buffer and reached its maximum at 400 mM NaCl (Fig. 30, lanes 5 and 6). M53/p38 co-precipitation at higher salt concentrations was slightly less efficient than at 400 mM NaCl (Fig. 30, lanes 8-10). Therefore, to guarantee complex stability of M53/p38 and M50/p35 in further experiments for protein extraction the NaCl concentration was limited to 400 mM.

### **9.2 Cellular lamins and M53/p38 are retained in a salt resistant compartment of the cell: the nuclear matrix**

Next, we determined the effect of different salt concentrations on solubilization of nuclear matrix proteins such as lamin B and A/C and M53/p38 after MCMV-infection. To that end, NIH 3T3 fibroblasts were infected with wt MCMV at an MOI of 0.5 and cells were lysed at different salt concentrations 24 hours after infection and separated by SDS-PAGE. Proteins retained in the pelleted cellular debris were re-solubilized and analyzed, too. The M53/p38 signals in different fractions were visualized by Western-blot using rat antiserum specific to the N-terminal 15 amino acids (aa) of the M53/p38 ORF at a dilution of 1:2000 (Bubeck, 2004).



## D. Results

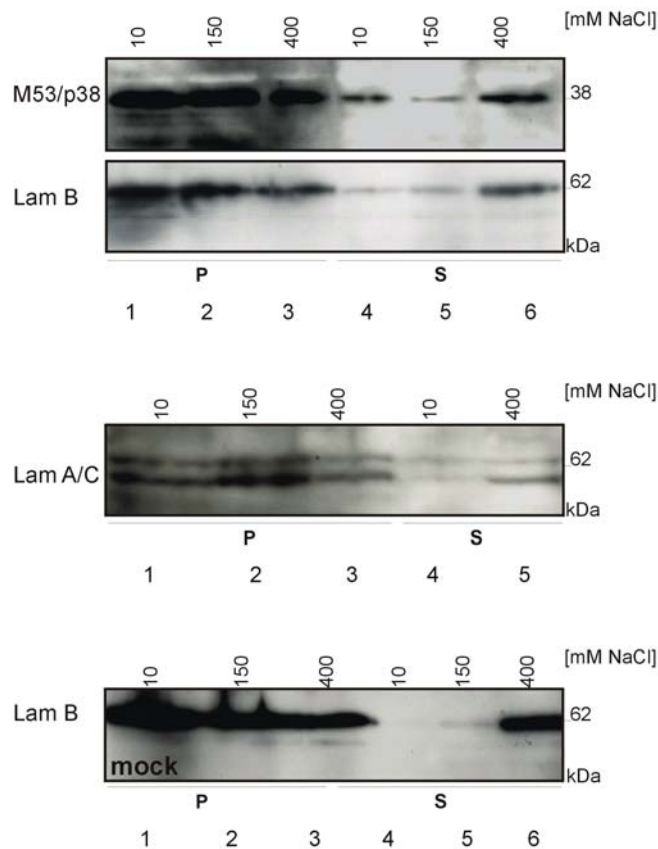


**Figure 31. Cellular lamins and M53/p38 are retained in a salt resistant compartment of the cell.** 3T3 cells were infected with wt MCMV at an MOI of 0.5. 24 hours post infection cells were lysed at different salt concentrations. Pelleted debris from cell lysates (lanes 1-3) and supernatants (lanes 4-6) were analyzed by Western blot using specific antiserum against M53/p38, lamin B or lamin A/C. Control cell lysates from uninfected NIH3T3 cells were probed for lamin B.

The specific M53/p38 band at 38 kDa was detectable for all analyzed probes of the pelleted cellular debris after low-, moderate- and high salt protein extraction, indicating that the majority of M53/p38 was still retained in the matrix (Fig. 31, lanes 1-3). At high salt extraction the M53/p38 signal strength was slightly reduced for the pelleted cellular debris (Fig. 31, lane 3). Accordingly, the M53/p38 signal intensity in the supernatant increased after high salt protein extraction (Fig. 31, lanes 6). In contrast low-or moderate salt extraction did not increase the M53/p38-signal intensity in the supernatants. Here, using low-or moderate salt protein extraction M53/p38 was hardly solubilized (Fig. 31, lanes 4, 5). High salt protein extraction could improve M53/p38 solubilization after infection (Fig. 31, lane 6).

The same conditions were applied for lamins B and A/C which were visualized by Western-blot using specific antibodies at a dilution of 1:300. Interestingly, in contrast to lamin C the lamin A was not efficiently solubilized after low- or high salt protein extraction. Control cell lysates from uninfected NIH 3T3 cells were

## D. Results

processed as described above and probed for lamin B. Also lamin B could be detected only after high salt protein extraction. Therefore, M53/p38 and cellular proteins lamin B and A/C are retained in the same salt resistant nuclear compartment of the cell designated as nuclear matrix. Proteins can be efficiently solubilized using high salt conditions for extraction. Apparently, in contrast to uninfected cells after MCMV infection some lamin B is already solubilized using low salt extraction conditions.

### **10. The lamin B receptor complex (LBR) interacts with STM50 alone or STM50 complexed with M53/p38**

Next, we wanted to analyze interactions between nuclear matrix proteins and the viral NEC. There are two main matrix residents of the INM: The lamin B receptor complex (LBR) and the LEM domain proteins (LEMs), such as emerin, MAN1 or LAPs (see introduction: 4.2.1 and 4.2.2). First, we tested the lamin B receptor complex (LBR) for interaction with the MCMV NEC proteins.

Binding was tested by pull down assay after isolated expression of pM50ST expressing Strep-II tagged M50/p35 or after co-expression with wt M53. As control for specificity of the assay 293 cells were either mock transfected or transfected with pM53, expressing wt M53 alone. As control for protein load and expression total cell lysates were separated by SDS-PAGE and subjected to Western-blot analysis using LBR specific antibody at a dilution of 1:300.

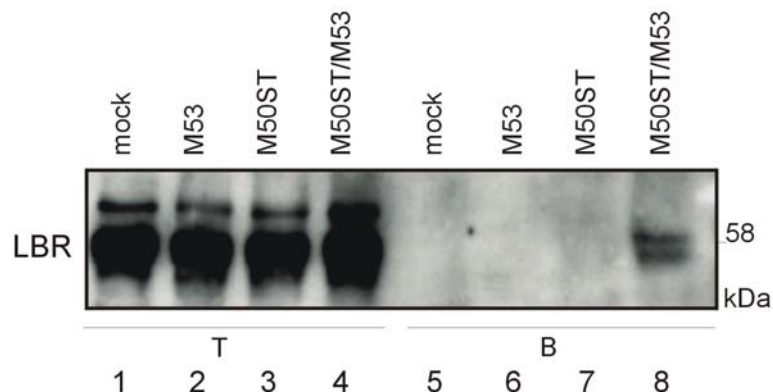


**Figure 32. Pull down of LBR with Strep tagged M50/p35.** 293 cells were transfected with wt M53/p38 and M50ST. Furthermore 293 cells were co-transfected with M50ST and wt M53. Total cell lysates were analyzed to test the protein expression by Western blot using specific antiserum against LBR (T, lanes 1-4). Proteins complexed with M50ST were precipitated by Strep-Tactin sepharose. Desthiobiotin eluates were analyzed by SDS-PAGE and blotted on membranes. LBR was detected by Western blot with LBR specific antiserum (B, lanes 5-8).

## D. Results

The specific LBR-band at 58 kDa became detectable in total cell lysates of all probes (Fig. 32, T, lanes 1-4). Proteins bound to M50ST were recovered by Strep-Tactin sepharose beads from cell lysates of 293 cells transfected with pM50ST or cell lysates after co-expression of pM50ST and pM53.

Bound proteins were eluted from the beads by desthiobiotin, separated by SDS-PAGE and subjected to Western-blot analysis using LBR specific antibody. The LBR specific band at 58 kDa was missing in mock-, M53- and M50ST transfected cells. But there was a LBR specific band detectable after co-expression of M50ST and wt M53 (Fig. 32, B, lane 8). Thus, the LBR complex p58 interacts with the NEC.

However, the efficiency of the Strep-tag pull down was poor for the LBR. Moreover, interaction of M53/p38 with cellular proteins could only be addressed in complex with M50ST and not in isolation. Therefore, new pull down assays needed to be established for further analysis of cellular interaction partners of M53 and M50.

### **11. Both, Flag-tagged M53/p38 and HA-tagged M50/p35 can efficiently pull down LBR**

In order to further improve the efficiency of the pull down assay to identify cellular interaction partners of M50/p35 and M53/p38 additional pull down systems were established: The HA-tag pull down and the Flag-tag pull down.

To test the specificity of HA-pull down 293 cells were either mock transfected, transfected with pM53, expressing wt M53, transfected with pHAM50, expressing HA-tagged M50 or co-transfected with pHAM50 and pM53. As controls for protein load- and expression total cell lysates were separated by SDS-PAGE and subjected to Western-blot analysis using M53- and M50-specific antisera at dilutions of 1:2000 (Fig. 33A, T, upper- and middle panel).

The specific M53-band at 38 kDa became detectable for total cell lysates after isolated expression of M53/p38 and after co-expression of wt M53 and HA-tagged M50 (Fig. 33A, upper panel, T, lanes 2, 4). The specific M50-band at 35 kDa was present in total cell lysates after isolated expression of HAM50 and

## D. Results

after co-expression of wt M53 and HA-tagged M50 (Fig. 33A, middle panel, T, lanes 3, 4).

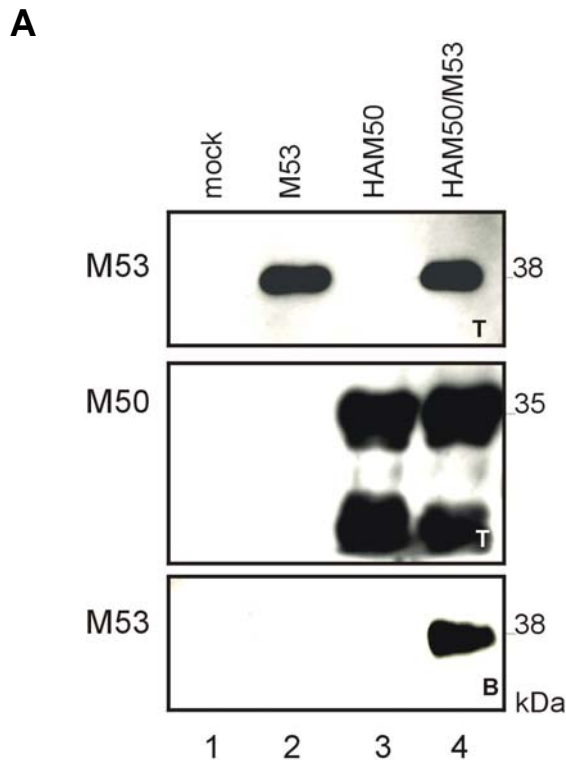


**Figure 33A. HA-pull down analysis.** 293 cells were mock transfected, transfected with HAM50, transfected with wt M53 or co-transfected with HAM50 and wt M53. Total cell lysates were analyzed by SDS-PAGE and Western blot using specific M53/p38 antiserum (upper panel, M53, T) or specific M50/p35 antiserum (middle panel, M50, T). Proteins complexed with HAM50 were precipitated with HA-matrix sepharose beads and eluted by specific IP loading buffer. Next, proteins were separated by SDS-PAGE and signals for M53/p38 were visualized by Western blot using specific antiserum against M53/p38 (lower panel, M53, B).

In the HA- tag pull down assay only proteins bound to M50 should be recovered by HA-matrix sepharose beads from lysates of 293 cells transfected with pHAM50 or lysates of co-expressed pHAM50 and pM53. Bound proteins were eluted from the HA-matrix by SDS-sample buffer, separated by SDS-PAGE and subjected to Western-blot analysis using M53-specific antisera. The M53/p38 specific band at 38 kDa was clearly detectable only after co-expression of M53 with HA-tagged M50, but was missing for the other controls (Fig. 33A, B, lanes 5-8). No signals for unspecific bound proteins were detectable, indicating the high specificity of this assay.

Next, the Flag-tag pull down assay was tested. To test the specificity of the Flag-tag pull down 293 cells were either mock transfected, transfected with pFlagM53, expressing Flag-tagged M53 or co-transfected with pFlagM53 and pM50. To control protein load- and expression the total cell lysates were separated by SDS-PAGE and subjected to Western-blot analysis using M50-specific antisera at a dilution of 1:2000. Here, the specific M50-band at 35 kDa and signals for M50-processing products became detectable in total cell lysates

## D. Results

after co-expression of wt M50 and Flag-tagged M53 (Fig. 33B, upper panel, T, lane 3). As a further control for protein load- and expression total cell lysates were separated by SDS-PAGE and subjected to Western-blot analysis using M53-specific antisera at a dilution of 1:2000. The specific M53-band at 38 kDa was seen only in total cell lysates after isolated expression of Flag-tagged M53 or after co-expression of wt M50 and Flag-tagged M53 (Fig. 33B, middle panel, T, lanes 2, 3).

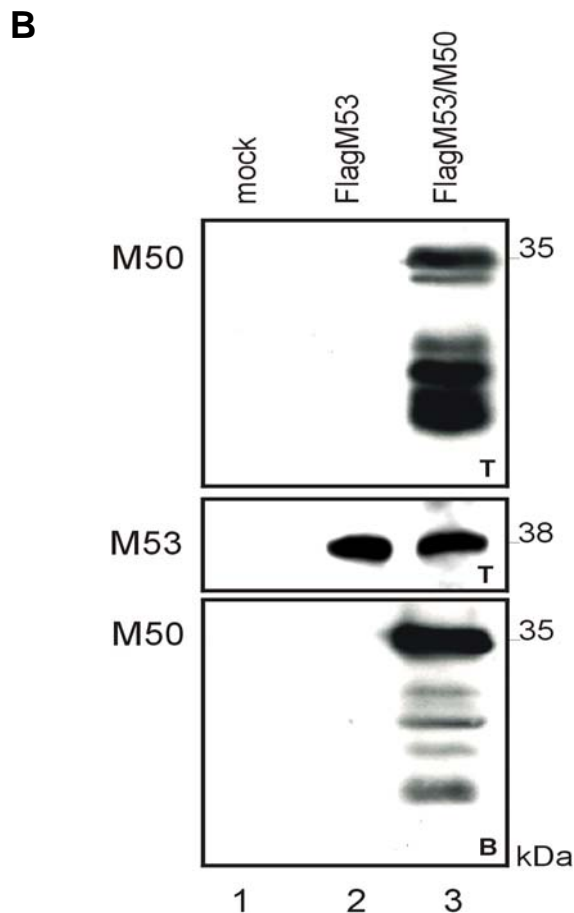


**Figure 33B. Flag-tag pull down analysis.** 293 cells were mock transfected, transfected with FlagM53, or co-transfected with FlagM53 and wt M50. Total cell lysates were analyzed by SDS-PAGE and Western blot using specific M50/p35 antiserum (upper panel, M50, T) or specific M53/p38 antiserum (middle panel, M53, T). Proteins complexed with FlagM53 were precipitated with Flag-matrix sepharose beads and eluted by specific IP loading buffer. Next, proteins were separated by SDS-PAGE and signals for M50/p35 were visualized by Western blot using specific antiserum against M50/p35 (lower panel, M50, B).

Flag-tag pull down should only reveal proteins bound to Flag-tagged M53. Bound proteins were eluted from the Flag-matrix by SDS-sample buffer, separated by SDS-PAGE and subjected to Western-blot analysis using M50-specific antisera. M50/p35 and processing products were only detectable after co-expression with Flag-tagged M53/p38, indicating the high specificity of the assay (Fig. 33B, lower panel, B, lane 3).

Next, the interaction of LBR with M50/p35 or M53/p38 alone or with the M50/p35-M53/p38 complex was re-analyzed. For the HA-tag pull down 293 cells were mock transfected, transfected with pHAM50 or co-transfected with

## D. Results

pHAM50 and pM53. For Flag-tag pull down 293 cells were mock transfected, transfected with pFlagM53 or co-transfected with pM50 and pFlagM53. As control for protein load- and expression total cell lysates were separated by SDS-PAGE and subjected to Western-blot analysis using LBR- specific antibody at a dilution of 1:300.

**C**

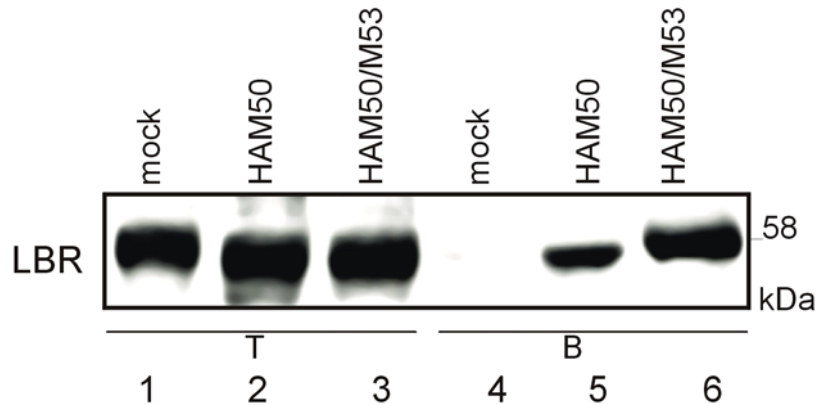


**Figure 33C. LBR pull down using HA-tagged M50/p35.** 293 cells were mock transfected, transfected with HAM50 or co-transfected with HAM50 and wt M53. Total cell lysates were analyzed by SDS-PAGE (12% SDS-gel) and Western blot using specific LBR antibody (T; lanes 1-3). Proteins complexed with HAM50 were precipitated with HA-matrix sepharose beads and eluted proteins were separated by SDS-PAGE (12% SDS-gel). Signals for LBR were visualized by Western blot using specific antibody against LBR (B; lanes 4-8).

The LBR band at 58 kDa was present in all total cell lysates of both sets (Fig. 33C, D, lanes 1-3). Due to a higher resolution of the SDS-PAGE for total cell lysates of the Flag set an additional LBR band was detectable (Fig. 33D, lanes 1-3). Proteins bound to Flag-or HA-matrix were eluted from the respective sepharose beads by SDS-sample buffer, separated by SDS-PAGE and subjected to Western-blot analysis using LBR-specific antibody at a dilution of 1:300.

The signal at 58 kDa, characteristic for the LBR complex major component p58, was detectable after Flag-pull down assay with the lysate of isolated expressed Flag-tagged M53. Due to the higher efficiency compared to the Strep-tag pull down assay p58 was also detectable after HA-pull down with the lysate of isolated expressed HA-tagged M50, indicating direct interaction with both NEC proteins (Fig. 33C, D, lanes 5). The lower LBR complex band was not detectable after Flag-pull down, suggesting two LBR isoforms.

## D. Results

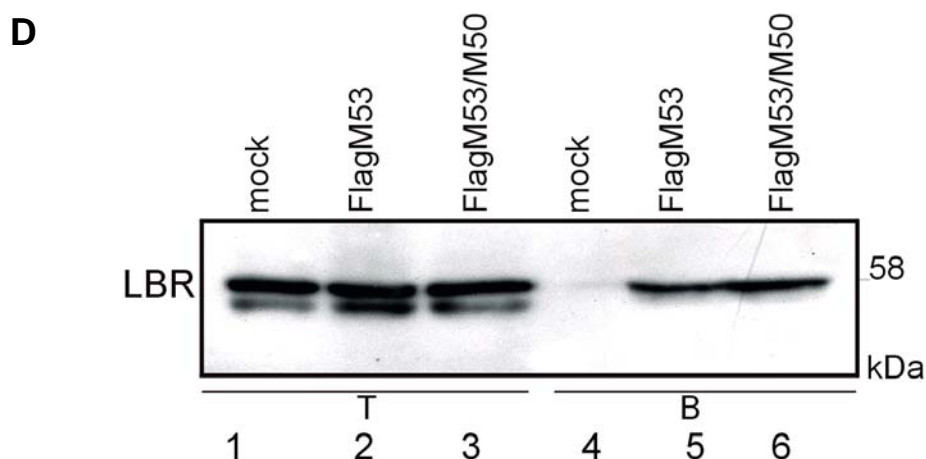


**Figure 33D. LBR pull down using Flag-tagged M53/p38.** 293 cells were mock transfected, transfected with FlagM53 or co-transfected with FlagM53 and wt M50. Total cell lysates were analyzed by SDS-PAGE (15% SDS-gel) and Western blot using specific LBR antibody (T; lanes 1-3). Proteins complexed with FlagM53 were precipitated with Flag-matrix sepharose beads and eluted proteins were separated by SDS-PAGE (15% SDS-gel). Signals for LBR were visualized by Western blot using specific antibody against LBR (B; lanes 4-8).

In the HA-pull down, the intensity of the LBR signal was increased for co-expressed HAM50 and wt M53 (Fig. 33C, lane 6). The LBR signal intensity was not increased after pull down with co-expressed FlagM53 and wt M50, suggesting a more prominent role of M50/p35 in LBR interaction (Fig. 33D, lane 6).

### **12. Both M53/p38 and M50/p35 specifically interact with nuclear matrix proteins**

Next, we tested other nuclear matrix proteins for interaction with M53/p38 and M50/p35. Total lysates were separated by SDS-PAGE and subjected to Western-blot analysis using specific antibodies for cellular matrix proteins at a dilution of 1:300 to control protein load and expression (Fig. 34A and B, T, lanes 1-3). All tested cellular proteins were expressed and protein load was comparable for all analyzed samples. After pull down p32, a component of the LBR, binds to M53/p38 and M50/p35 and can be detected by a doubled band at 32/34 kDa (Fig. 34A and B, lanes 5). Interestingly, after pull down with isolated expressed FlagM53 or HAM50 only the lower p32 band is detectable.



D. Results

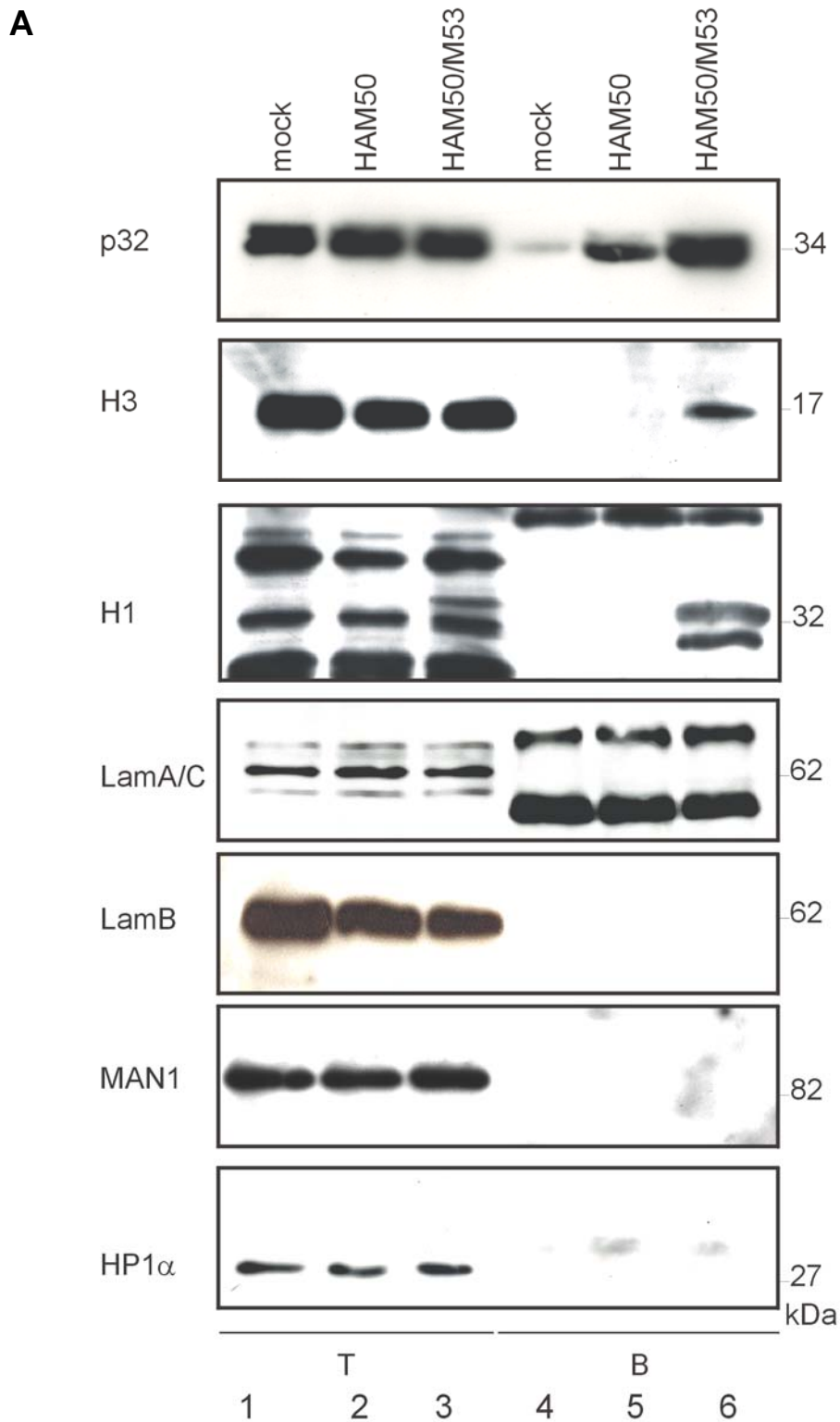


**Figure 34A. Pull down analysis of cellular interaction partners using HA-tagged M50/p35.** 293 cells were mock transfected, transfected with HAM50, transfected with wt M53 or co-transfected with HAM50 and wt M53. Total cell lysates were analyzed by SDS-PAGE and Western blot using antibodies specific for the tested Cellular proteins. (T; lanes 1-3). Proteins complexed with HAM50 were precipitated with HA-matrix sepharose beads and eluted by 2x SDS sample buffer. Next, proteins were separated by SDS-PAGE and signals for cellular interaction partners were visualized by Western blot using specific antibodies (B; lanes 4-6).



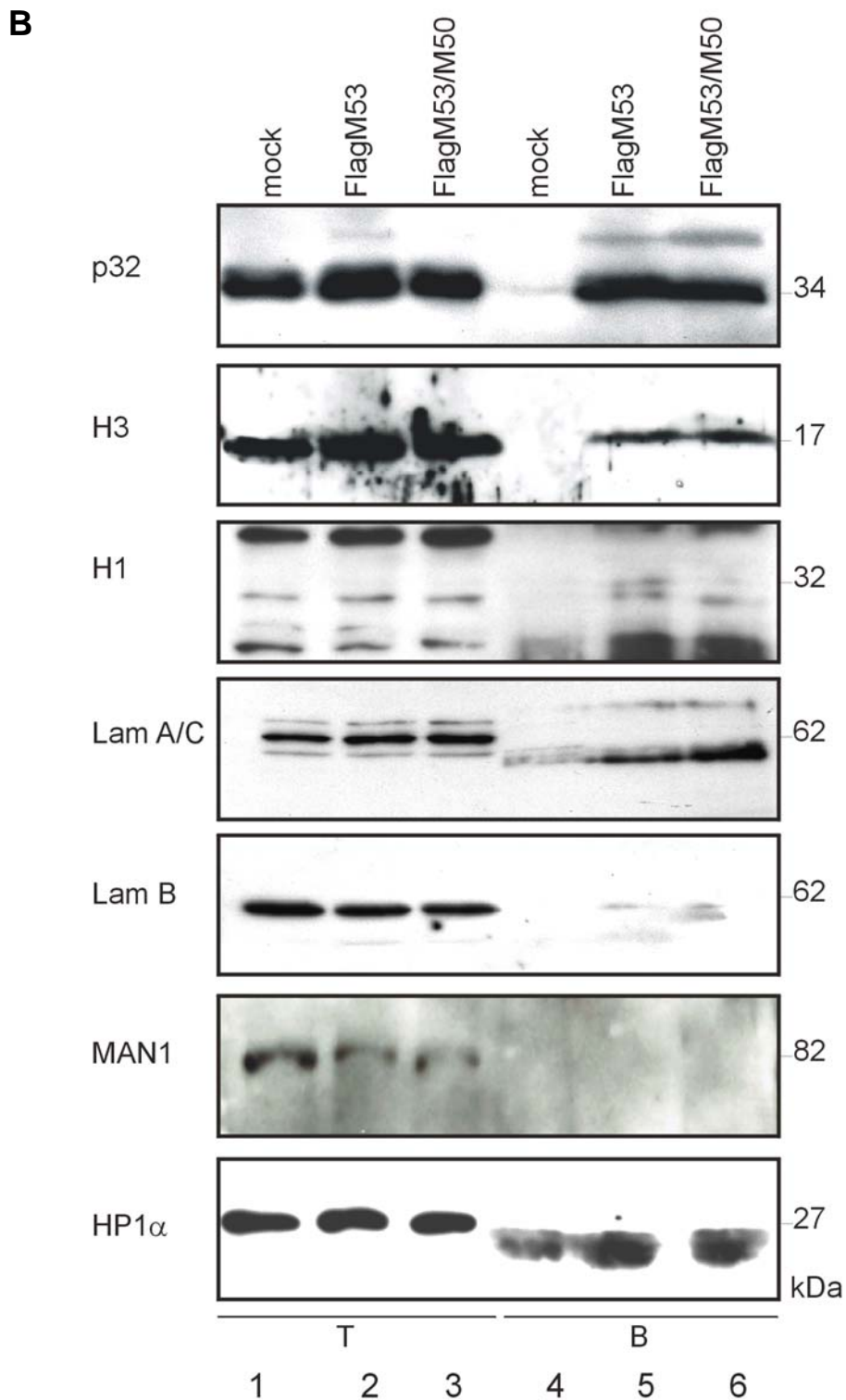


**Figure 34B. Pull down analysis of cellular interaction partners using Flag-tagged M53/p38.** 293 cells were mock transfected, transfected with FlagM53 or co-transfected with FlagM53 and wt M50. Total cell lysates were analyzed by SDS-PAGE and Western blot using antibodies specific for the tested proteins (T; lanes 1-3). Proteins complexed with FlagM53 were precipitated with Flag-matrix sepharose beads and eluted proteins were separated by SDS-PAGE. Signals for cellular proteins were visualized by Western blot using specific antibodies (B; lanes 4-8).

## D. Results

The upper p32 band was only detectable to some extent, suggesting two modified p32 isoforms of which one is bound preferentially to isolated expressed M50/p35 or M53/p38. Both p32 bands were equally induced in lysates after co-expression of HAM50 and wt M53. This was not the case after Flag-tag pull down with lysates from co-expressed FlagM53 and wt M50 (Fig. 34A and B, lanes 6), suggesting a more prominent role of M50/p35 in binding p32 isoforms.

Linker histone 1 (H1) and histone 3 (H3) are connected with the LBR and the lamina (Gruenbaum, 2005; Montes de Oca, 2005; Bártoová, 2005; Poliodaki, 2001). They were seen in pull downs only after isolated expression of FlagM53, co-expression of FlagM53 and wt M50 or co-expression of HAM50 and wt M53, indicating that histone interaction is a function of M53/p38 (Fig. 34A and B, lanes 5, 6). Furthermore, interaction of M53/p38 and M50/p35 with HP1 $\alpha$ , which bridges LBR and chromatin, with the LEM-domain protein MAN1 and with lamins B and A/C was analyzed by pull down assays. Neither after pull down of isolated expressed M53/p38 or M50/p35 nor after pull down of co-expressed M53/p38 and M50/p35 specific signals for these cellular proteins were detectable, indicating no specific interaction (Fig. 34A and B, lanes 4-6).

In conclusion, after isolated expression both M53/p38 and M50/p35 react very specific with cellular residents of the inner nuclear membrane. Only M53/p38 binds to histone 1 and- 3, whereas M50/p35 does not. Using HA-tag sepharose beads for pull down of LBR and p32 after co-expression of the viral proteins additive effects could be observed which may be linked to different specificity of the respective matrix or may be due to conformational changes of the cellular matrix.

### **13. Proteomics on the MCMV NEC**

To verify the pull down results we analyzed isolated proteins by mass-spectrometry.

To that end, two sets of 293 cells were mock transfected, transfected with pHAM50, transfected with pFlagM53 or co-transfected with pHAM50 and pFlagM53. Cell lysates were prepared 24 hours post transfection. Next, HA-tag

## D. Results

pull down was performed with one set, and proteins bound to the HA-matrix sepharose beads were eluted from the beads by IP-sample buffer. With the second set of lysates Flag-tag pull down was performed and proteins bound to Flag-matrix sepharose beads were recovered by SDS-sample buffer. Eluted proteins were separated by SDS-PAGE on a gradient gel and silver staining was performed. Using both Flag- or HA-matrices for pull down distinct bands became visible after isolated expression of HAM50, FlagM53 and co-expression of FlagM53 and HAM50 that were missing in mock controls (Fig. 35, black arrowheads).

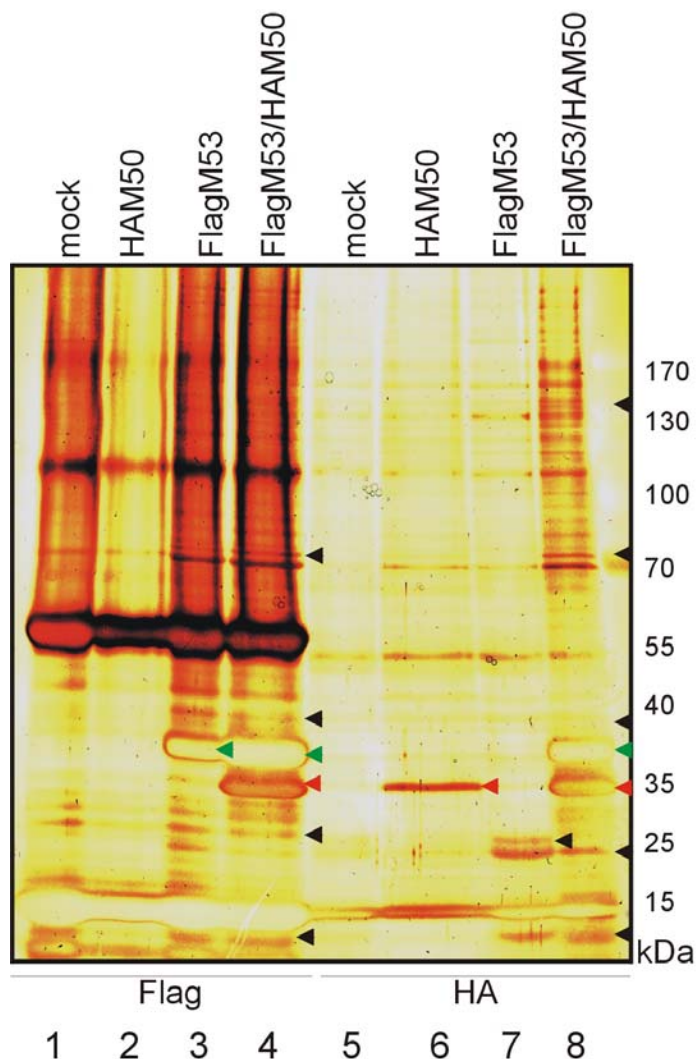


**Figure 35. Analysis of cellular interaction partners of M53/p38 and M50/p35 by silver staining and mass-spectrometry.** 293 cells were transfected with pHAM50, pFlagM53 or co-transfected with pHAM50 and pFlagM53. Cells were lysed and either HA- and Flag-tag pull down was performed. Eluted proteins were analyzed by SDS-PAGE on an 8-16% gradient gel. Silver staining was performed and protein bands (arrowheads) were isolated from the gel and analyzed by mass-spectrometry. Silver staining indicates numerous putative interactors (black arrowheads) of M53 (green arrowheads), M50 (red arrowheads) or the complex of M53 and M50.

## D. Results

---

Furthermore, the pattern was different to some extent between isolated expressed HAM50 and FlagM53 and the co-expressed viral NEC proteins. At 15 kDa, 25 kDa, 35 kDa, 38 kDa, 40 kDa and 65 kDa bands became visible using both matrices for pull-down of co-expressed HAM50 and FlagM53.

Using the Flag-tag pull down after transfection with FlagM53, bands at around 15 kDa, 25 kDa, 38 kDa and 40 kDa became visible. Using the HA-tag pull down after transfection with HAM50 only an additional band at around 35 kDa became visible that differed from the mock control. Therefore we suggested, that either M53 and M50 or complexed M53-M50 share cellular interaction partners but may also have unique ones. Next, a set of bands was isolated from the gel and analyzed by mass-spectrometry, that only appeared after pull down of lysates from isolated expressed FlagM53 or HAM50 or from lysates of co-expressed FlagM53 and HAM50 but were missing for mock control. Mass-spectrometry was performed in cooperation with Arnd Kieser and Thomas Knöfel (GSF, Hämatologikum, München). We could identify both viral interaction partners. Unfortunately the amount of recovered protein was too low for further identification of cellular interaction partners. To increase recovery proteins bound to Flag-matrix or HA-matrix were competed out by specific Flag-or HA-peptide. The advantage of this elution strategy is, that eluted proteins can be analyzed as a pool and that proteins can be eluted under native conditions. The specificity of this assay is shown in figure 36 A and B.

For the identification of cellular interaction partners of M53/p38 and M50/p35 by mass-spectrometry in the future the system needs to be up-scaled, since mass-spectrometry is less sensitive than Western-blot analysis and proteins are often expressed only at low levels.

D. Results

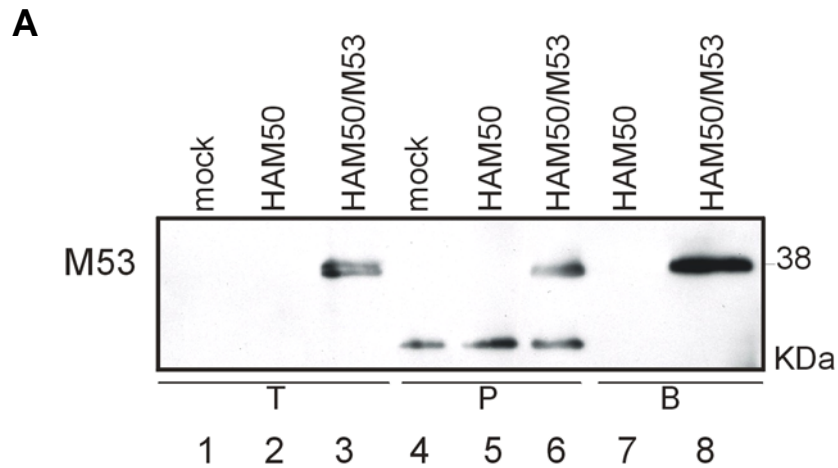


**Figure 36A. Peptide elution after pull down analysis using HA-tagged M50/p35.** 293 cells were mock transfected, transfected with HAM50 or co-transfected with HAM50 and wt M53. Total cell lysates and pelleted debris from the lysates were analyzed by SDS-PAGE and Western blot using specific M53/p38 antiserum (T, P; lanes 1-6). Proteins complexed with HAM50 were precipitated with HA-matrix sepharose beads and proteins eluted by specific HA-peptide were separated by SDS-PAGE. Signals for M53/p38 were visualized by Western blot using specific antiserum against M53/p38 (B; lanes 7, 8).

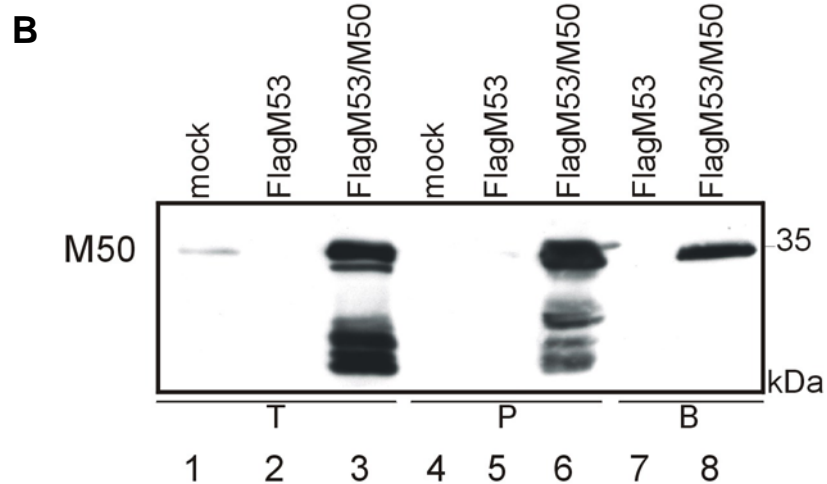


**Figure 36B. Peptide elution after pull down analysis using Flag-tagged M53.** 293 cells were mock transfected, transfected with FlagM53 or co-transfected with FlagM53 and wt M50. Total cell lysates and debris from the lysates were analyzed by SDS-PAGE and Western blot using specific M50/p35 antiserum (T, P; lanes 1-6). Proteins complexed with FlagM53 were precipitated with Flag-matrix sepharose beads and proteins eluted by specific Flag-peptide were separated by SDS-PAGE. Signals for M50/p35 were visualized by Western blot using specific antiserum against M50/p35 (B; lanes 7, 8).

## **E. Discussion**

### **1. The UL31- and UL34 homologues and their function during virus replication**

We owe our basic knowledge on the herpes-common proteins governing the egress of the herpesvirus nucleocapsid from the cell nucleus to pioneering studies in alpha-herpesviruses. To achieve nucleocapsid egress the UL31- and UL34-proteins need to form a complex at the nuclear membrane. Deletion of either protein severely compromises virus replication but still gives rise to progeny (Bubic, 2004; Fuchs, 2002; Liang, 2004; Reynolds, 2001, 2002; Ye, 2000). For beta- and gamma-herpesviruses the conditions are even more stringent. The lack of either protein abolishes virus replication (Bubeck, 2004, Farina, 2005; Gonella, 2005). Therefore, these studies could only be initiated after cloning and mutagenesis of complete infectious herpesvirus genomes as BAC in *E. coli* (Messerle, 1997; Wagner, 2002). Published work and data presented in this study converge to the conclusion that UL31- and UL34-homologues of alpha-, beta- and gamma-herpesviruses have to interact at the inner nuclear membrane to execute their function as nuclear egress complex (NEC) (Bubeck, 2004; Chang, 1997; Reynolds, 2004; Gonnella, 2005; Lake, 2004, Liang, 2004; Muranyi, 2002; Reynolds, 2002; Simpson-Holley, 2004; Ye, 2000). This must involve contacts with several other unknown cellular and viral proteins. The mutual binding sites need to be determined to address the question, which functions of these proteins are conducted in isolation and which are executed subsequent to NEC formation.

### **2. M53/p38, an essential MCMV protein, which is expressed by late kinetics**

M50 is an essential MCMV gene. The M50 gene product p35 is expressed by early late kinetics upon MCMV infection and is involved in the egress of the

## E. Discussion

---

MCMV capsid from the nucleus. M53/p35 can be co-precipitated with M50/p35, indicating functional interaction between both gene products (Bubeck, 2004). When the M53 ORF is deleted from the MCMV-BAC reconstitution of infectious virus in cell culture is not possible. The null-phenotype is reverted by reinsertion of the M53 ORF at an ectopic position of the  $\Delta$ M53-MCMV-BAC. Thus, the inability to gain infectious virus is solely due to the deletion of the M53 gene and not an effect of neighboring genes. Growth of the reconstituted virus is slightly attenuated. Probably this attenuation is connected to altered expression kinetics of the ectopic M53/p38, which is controlled by the immediate early (ie) promoter of HCMV and not by its endogenous promoter. These findings were also confirmed by a trans-complementation assay. Here, a trans-complemented M53 deletion virus was unable to produce viral progeny under non-complementing conditions (Lötzerich, 2006).

M53/p38 is detectable after 18 hours and accumulated gradually over time in MCMV infected cells. The accumulation of M53/p38 after 24 hours can be related to a second replication cycle of MCMV. PAA treatment, which blocks DNA replication, could prevent gene expression of late MCMV major capsid protein (M86) and also of M53/p38. Therefore M53/p38 expression is following true late kinetics. We showed recently that M50/p35 follows early-late expression kinetics upon MCMV infection (Bubeck, 2004). Like M53/p38, expression of UL31 homologues of  $\alpha$ -herpesviruses follows late kinetics (Liang, 2004; Fuchs, 2002). Interestingly, the M53/p38- and M50/p35- homologues BFLF2 and BFRF1 of  $\gamma$ -herpesvirus EBV are already expressed at the early late stage of infection (Farina, 2005; Gonnella, 2005). Although M53/p38 and M50/p35 can be co-precipitated and therefore assumingly functionally interact, expression of M50/p35 follows early late kinetics. One can speculate whether M50/p35 has an M53/p38 independent function early in infection.

### **3. Exploring M53/p38 by transposon mutagenesis of the M53 ORF**

Viral functions that are involved in morphogenesis are preferably studied in the context of viral replication where the relevant genes are expressed in



## E. Discussion

---

operational conditions. Random transposon mutagenesis procedures described so far for herpesviruses create null-mutants of the respective gene in order to analyze non-essential genes or to define essentiality (Brune, 2001; Hobom, 2000; Menard, 2003; Smith, 1999). These insertion libraries cannot be used for a detailed functional characterization of a gene. The type of transposon cannot be removed from the genome and most of the insertions destroy the target gene completely. Furthermore, the number of insertions within a given gene in these libraries is far below the requirements of a comprehensive or even saturating analysis. Comprehensive mutant pools for cloned viral genes can be obtained through random mutagenesis procedures creating small insertions or deletions (Biery, 2000). Due to the genome size of large DNA viruses, simple approaches using traditional molecular cloning techniques are not feasible. In a previous paper we reported on the comprehensive mutagenesis of M50/p35, the UL34 homologue of beta-herpesvirus MCMV (Bubeck, 2004). After mutagenesis the mutated M50-gene was re-introduced into the viral genome (Menard, 2003). However, due to frequent insertions into the rescue vector backbone the efficiency of random insertion mutagenesis of the M50 ORF was less than 20% and required laborious screening.

In this study we improved the transposon mediated random mutagenesis technique. Several transposon- donor and- acceptor combinations were analyzed. To that end, we excluded vector insertions by sub-cloning the primary pool of transposon labeled M53-ORFs into the rescue vector. Furthermore, background signals originating from the transposon donor vector were minimized by means of a temperature sensitive transposon donor. Both, sub-cloning of the primary pool of transposon labeled M53-ORFs and selection against the transposon donor after transposition at non-permissive temperature raised the successful insertion frequency to 55%, which was almost five times more efficient than the method we published earlier. Actually, we had expected a higher insertion frequency. It turned out that by sub-cloning of the M53 ORF also sequences originating from the multiple cloning sites were transferred to the new rescue vector. Since the transposon preferentially inserts to GC-rich sequences the multiple cloning sites with inserted transposons led to insertion frequency numbers that are far below 100 %. In the future the efficiency could



be improved by selection of adequate multiple cloning sites with a low GC content. Altogether, we created a library of about 28,000 insertion/stop mutants in the M53-ORF, screened 986 by PCR and sequenced 498 PCR-positive clones. A total of 54 random mutants (46 M53-insertion- and 8 truncation-mutants) were tested both at the level of isolated expression and for complementation of the M53 null phenotype in the viral context. In addition, a total of 18 targeted mutants were tested also in the genomic context.

#### **4. Analysis of M53/p38 mutants**

The analysis of M53/p38 transposon- and targeted mutants lead to the following conclusions:

i) Sequence comparison of 36 known members of the UL31 family of herpesvirus proteins revealed an N-terminal variable region and 4 conserved regions (CR) located within the C-terminal 2/3 of the sequences.

ii) For the less conserved N-terminal part of M53/p38 a bi-parted nuclear localization signal (NLS) was predicted. We could confirm this by co-localization- and co-precipitation experiments and also by testing functionality of the respective N-terminal deletion mutants.

iii) Within CR1 (aa 115-174 in MCMV M53/p38) we found the binding motif for M50/p35. This motif is represented by aa 115-137 which is necessary for binding to M50/p35.

iv) Mutation of all conserved amino acids of this region into alanines resulted in different phenotypes with regard to NEC formation, revealing a prominent role for the residues K128, Y129, and L130. Nevertheless, all single point mutants were able to bind to M50/p35 and to rescue the M53 null phenotype of the genome. Only when two or three of the critical residues were replaced the mutants failed to bind to M50/p35 and did not rescue the M53 null phenotype.

v.) The C-terminal conserved regions two to four (CR2-4) bear yet unidentified essential function(s). Insertion mutants in these regions could bind to M50/p35 but lack functionality.

### **4.1. The N-terminal part of M53/p38 harbors a NLS as functional element**

Alignment of M53 to members of the UL31 family demonstrated a conserved central and C-terminal region whereas the N-terminal region was variable. The results of the functional analysis of the M53-insertion mutants were in line with the *in silico* prediction. Non-functional insertion mutants accumulated only within the conserved regions of the M53 ORF. Within the N-terminal variable region of M53/p38 two overlapping nuclear localization signals (NLS) were predicted between aa 24 and 42. The deletion mutant of M53/p38 lacking the region from aa 16 to 106 failed to rescue the virus growth in absence of the wt M53 gene, however, introduction of an artificial 9 aa SV40 NLS rescued the functionality of the mutant. Thus, the variable N-terminal domain of M53/p38 contains an NLS as functional element. The consensus sequence for a nuclear targeting signal (Dingwall, 1991) is present only in 14 out of 36 members of UL31 family. For instance, the type bi-parted NLS is not predicted for the N-terminal part of HCMV UL53. However, if an NLS is predicted it is always located within the N-terminal variable region. All analyzed members of the UL31 protein family are localized exclusively in the nucleus upon isolated expression indicating that they possess an active NLS and we believe that this is the function of the N-terminal variable domain. The presence of one N-terminal NLS for UL53 or other UL31 family members remains to be elucidated.

### **4.2. The interaction of M50/p35 and M53/p38**

Binding between M50/p35 homologues (UL34) and M53/p38 homologues (UL31) is a conserved feature in all herpesviruses. A stop mutant suggested that the N-terminal 136 aa of M53/p38 are sufficient for M50/p35 binding. The

## E. Discussion

---

N-terminal sequences aa16 to aa106 could be replaced without loss of functionality, which placed the M50/p35 binding region between aa 106 and 136. The non-functional insertion mutants M53i115 and i131 further located sequences necessary for M50/p35 binding within aa 115-131 of M53/p38. The alanine scanning mutagenesis for the 12 conserved aa of this essential region confirmed and extended these observations. All point mutants showed wt nuclear distribution upon isolated expression. No difference in protein stability compared to wild type M53/p38 was traceable. Analysis of total lysates by western blot displayed no degradation of the produced proteins. However, a variety of phenotypes occurred in the presence of M50/p35, including those which formed intranuclear aggregates (M53L125A) or filamentous structures (M53K128A). Since these structures were only seen in the presence of the M50/p35 we assume that at least a transient M50/p35-M53/p38 interaction is responsible for the observed phenotypic changes. M50/p35 binding may initiate M53/p38 processing, thereby inducing conformational changes in different mutants. Furthermore, this transient interaction was apparently sufficient to cause aggregation of M53/p38 alone or in complex with so far unknown cellular partners. Surprisingly, all tested point mutants could bind to M50/p35 to some extent in the pull-down assay and more importantly all rescued the M53 null phenotype in the viral context including those without apparent co-localization. This indicates that using only one assay to study a protein-protein interaction might not be sufficient to define a function. Co-localization studies show only the major steady state phenotype. Residual low affinity interactions may be overlooked and protein-protein interaction or functionality of the virus are not addressed. Co-IP reveals the potential to bind. But a confirmed protein-protein interaction does not implicate functionality. Furthermore, testing M53-mutants for functionality enables to map essential domains of the protein but not to identify protein-protein interaction domains. Thus, to produce reliable results, the application of various assays was indicated.

The growth of reconstituted viruses was poor for mutants M53K128A, M53Y129A and M53L130A. These data imply that wt M50/p35-M53/p38 complexes are required for efficient productive infection, and that a small number of complexes or transient complex formations suffice for virus

## E. Discussion

---

production. However, if two or more aa within the predicted binding region were exchanged the mutants neither co-localized with nor bound to M50/p35 and were not able to rescue the M53 null phenotype. Loss of M53/p38-binding to M50/p35 is associated with the inability to replicate. However, M50/p35-binding is not the only function of CR1. Notably there are M53-insertion mutants within the identified binding motif (i115 and i131) which bind to M50/p35 but are nevertheless lethal. Interestingly, the M50/p35 binding region of M53/p38 is strictly conserved only in beta-herpesviruses. The homology of alpha- or gamma-herpesvirus UL31 family members to the beta-herpesvirus sequence (aa 115-136) is lower than the average similarity of the conserved regions and is presumably determined more by the character of the amino acids than by sequence. Only within sub-families the sequence conservation is considerably high. We could show that M53 can be replaced by its HCMV homologue UL53. UL53, expressed at an ectopic position of the  $\Delta$ M53-MCMV-BAC could rescue the M53-null phenotype, implicating that M50/p35 can interact with M53/p38 homologues from different species within  $\beta$ -herpesviruses. The same phenomenon could be observed within other subfamilies (Schnee, 2006). The divergence is already experimentally proven for the binding region for UL34 members from the alpha- and beta-herpesvirus subfamilies. In MCMV M50/p35 aa 53-57 and aa 114 are important for M53/p38 binding (Bubeck, 2004). Using a set of 9 HSV-1 UL34 mutants, one of which was introduced into the genomic context, the binding region was located to a different region, namely to aa 137-181 of UL34 (which corresponds to region aa 129-173 of M50/p35) (Liang, 2004). Therefore, it can be expected that sequences in the conserved regions but not necessarily the same sequences in CR1 functionally define the binding region in alpha- and gamma-herpesvirus homologues.

### **4.3. The C-terminal 2/3 of M53/p38 bears essential MCMV functions**

The C-terminal regions CR2 to CR4 are conserved in the UL31-family and several insertion mutants have a null phenotype, although they bind to M50/p35. This indicates that the C-terminal half of M53/p38 bears yet

unidentified essential functions. Under certain conditions HSV-1 UL31 interacts with lamins A/C and is involved in chromatin reorganization (Reynolds, 2001; Scott, 2001; Simpson-Holley, 2004). M50/p35 and BFRF1 have indirect effects on the nuclear lamina (Farina, 2005; Muranyi, 2002) and in EBV the complex of BFLF2 and BFRF1 interacts with lamin B (Gonnella, 2005). These features but also oligomerization, capsid recruitment and regulation of the subsequent budding event may involve the CR2-4 of the UL31 family proteins. Experimental approaches, such as testing mutants for dominant negative effects (Rupp, 2005) or protein pull-downs using a functional or a non-functional NEC may pave the way to the elucidation of the other herpesvirus NEC functions.

### **5. Homo-oligomerization of M53/p38**

In this study we could show, that at least after isolated expression M53/p38 is able to form homo-dimer or –oligomers. It may be that M53/p38 dimers are built by interaction within the same binding region of CR1 as M50/p35. Oligomerization may contribute to stabilization of NEC formation and therefore could be an essential process. As suggested for lamins, BAF and certain LEM domain proteins (e.g. LAP2 $\alpha$ ) M53/p38 oligomers may also exhibit a scaffolding function for multi-protein complexes (Gruenbaum, 2005). However, whether the oligomerization is required for a function of the MCMV NEC remains to be determined. But at the moment no suitable technique is available to address this question.

### **6. Interaction of M53/p38 and M50/p35 with nuclear matrix proteins**

A critical step of herpesvirus morphogenesis is the nucleocapsid egress from the nucleus. A well accepted model suggests that nucleocapsid penetration of the nuclear envelope involves a budding process through the inner nuclear membrane (INM) (Mettenleiter, 2002, 2004, 2006). This is not simply accessible, since the INM is stabilized by a filamentous nuclear lamina layer.

## E. Discussion

---

The lamina represents a physical barrier for capsid budding and is only dissolved during mitotic events due to phosphorylation of lamins by cellular protein kinase C (PKC) (Gerace, 1980; Ottaviano, 1985; Otto, 2001; Peter, 1990; Dessev, 1988; Buenida, 2001; Muranyi, 2002). Also upon infection with  $\beta$ -herpesvirus MCMV- or  $\alpha$ -herpesvirus HSV-1- cellular PKC is recruited to the nuclear envelope. This is accompanied by lamin B phosphorylation (Muranyi, 2002; Park, 2006). The HCMV kinase UL97, which is not essential but critical for viral replication also was shown to be involved in lamin phosphorylation. (Prichard, 1999, 2005; Krosky, 2003; Azzeh, 2006; Marschall, 2005).

The M53/p38- and M50/p35 homologues UL31 and UL34 of  $\alpha$ -herpesvirus HSV-1 are involved in nuclear egress processes of viral nucleocapsids. Both proteins induce alterations of the nuclear architecture. Under certain conditions UL31 interacts with lamins A and C and is suggested to be involved in chromatin reorganization (Simpson-Holley, 2004, 2005; Reynolds, 2004; Scott, 2001). Also, in  $\gamma$ -herpesvirus EBV the UL31- and UL34 homologues BFLF2 and BFRF1 interact with lamin B (Gonella, 2005). Furthermore, BFRF1 is presumably involved in transport of nucleocapsids across the nuclear membrane (Farina, 2005).

M53/p38 and/ or M50/p35 probably have similar functions. As a first hint here we showed that M53/p38 and M50/p35 are retained with lamin B in the same salt resistant compartment of the nucleus, the nuclear matrix. To maintain the M50/p35-M53/p38 complex stability the NaCl concentration was limited to a maximum of 400 mM. Only at these high-salt conditions for extraction also several matrix proteins became soluble. Interestingly, although the majority of lamin B but also of M53/p38 was found soluble under high salt extraction conditions, upon MCMV infection already a small amount of lamin B and M53/p38 was already detectable under low salt protein extraction conditions. We therefore assumed, that MCMV infection increases the solubility of lamin B. In contrast, lamin A/C was not solubilized under low salt protein extraction conditions upon MCMV infection. Moreover, high salt protein extraction upon infection with MCMV only solubilized lamin C but had no effect on lamin A extraction. We therefore concluded that MCMV infection has no effect on A-type lamin solubilization.

## E. Discussion

Next, we studied interactions of M50/p35 and M53/p38 with proteins residing in the inner nuclear matrix. For HCMV capsid egress from the nucleus an involvement of cellular lamin B receptor-complex (LBR) and p32 is indicated. Viral UL97 kinase phosphorylates p32 *in vitro*. The UL97-p32 complex is recruited to the nuclear envelope and interacts with the LBR complex. *In vitro* this is accompanied by lamin phosphorylation (Marschall, 2005). Moreover, LBR was suggested to be involved in disruption of the nuclear lamina after  $\alpha$ -herpesvirus HSV-1 infection (Scott, 2001). The lamin B receptor (LBR) is one of the best characterized lamin- but also chromatin- binding membrane proteins. It is widely expressed in cells of higher eukaryotes and the human gene is already characterized (Schuler, 1994).

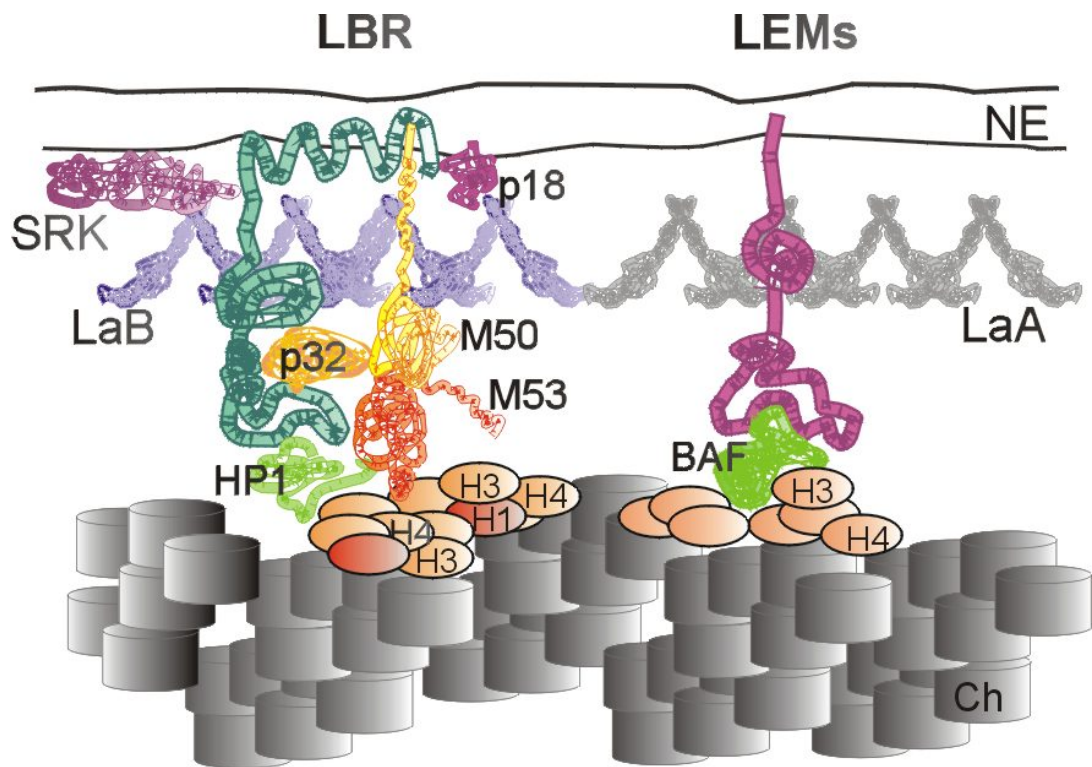


**Figure 37. Schematic diagram of possible cellular interaction partners of M50/p35 and M53/p38.** INM protein complexes LBR and LEM domain proteins with associated cellular and viral proteins, nuclear envelope (NE), nuclear lamina and chromatin structures (Ch) are depicted: Lamin B receptor (LBR/ p58) as complex with SR-kinase (SRK), p18, p32, lamin B (LaB), heterochromatin protein-1 (HP1), histone 1 (H1), histone 3 (H3) and histone 4 (H4); LEMs with barrier to autointegration factor (BAF), lamin A/C (LaA) and histones H3 and H4.

The human LBR or p58 comprises of an amino-terminal nucleoplasmic domain and a hydrophobic C-terminal domain with eight putative transmembrane



## E. Discussion

---

segments that integrate the protein into the INM (Chu, 1998; Worman, 1990; Ye, 1994; Fig. 37). LBR forms a multimeric-protein complex with p32, a polypeptide p18 of yet unknown function, a LBR kinase that phosphorylates LBR and associated proteins and with nuclear A- and B-type lamins (Simos, 1996; Nikolakaki, 1997, Deb, 1996). LBR also binds to lamin B. Furthermore, LBR was shown to interact with (ds) DNA, histone H3-H4 tetramers, HA95 and heterochromatin protein-1 (HP1) (for review: Chu, 1998; Foisner, 2001; Gruenbaum, 2005).

By Strep-II tag pull down assay we showed that the major component of the LBR complex p58 interacts with the NEC. In presence of M53/p38 this interaction was intensified, indicating that p58 may also interact with M53/p38. Since this interaction was hardly detectable we assumed that the Strep-II tag pull down assay is not recommended for a reliable screen of cellular interaction partners of M50/p35 and M53/p38. Furthermore, interaction of M53/p38 with cellular proteins only could be analyzed in complex with M50ST. Therefore, two efficient pull down assays were established: the HA-tag- and the Flag-tag pull down assay.

We showed after isolated expression of Flag-tagged M53 or HA-tagged M50 that both NEC proteins directly interact with the LBR complex major component p58. In the HA-pull down, the intensity of the LBR signal was increased for co-expressed HAM50 and wt M53. This was not the case after pull down with co-expressed FlagM53 and wt M50. Although there may be differences in efficiency of the two pull down systems a more prominent role of M50/p35 in the LBR interaction can be suggested.

Furthermore, similar results for interaction of M50/p35 and M53/p38 were obtained with LBR complex component p32 (Fig. 37). The p32 protein localizes to the mitochondrial matrix as well as to the nucleus and forms homo-trimers. It was shown to be involved in different cellular-but also viral processes and therefore may have multifunctional properties (Simos, 1994, Jiang, 1999; Sunayama, 2004; Muta 1997; Krainer, 1991; Luo, 1994; Matthews, 1998; Hall, 2002). A phosphorylation of p32 by cellular and viral kinases is indicated (Simos, 1994; Marschall, 2005). Interestingly, we detected for p32 after pull down with Flag-tagged M53 or HA-tagged M50 a doubled band at 32/34 kDa for



## E. Discussion

---

p32. The lower p32-band was strongly induced using both pull down systems after isolated expression of the tagged viral MCMV egress proteins or co-expression with the respective non-tagged partner. In contrast, the upper p32-band was detectable only to some extent and remained uninduced in both assays after isolated expression of HAM50- or FlagM53 constructs. Moreover, HA-pull down after co-expression of HA-tagged M50 and wt M53 revealed an equal and strong induction of both p32-bands. After Flag-tag pull down of co-expressed FlagM53 and wt M50 an induction of the upper p32 band could not be observed. Perhaps two modified isoforms of p32 exist that are able to interact with M53/p38 or M50/p35. As already mentioned, p32 can be phosphorylated. We therefore suggest that the induced upper p32-band represents the phosphorylated p32-isoform, which may interact with the NEC proteins M53/p38 and M50/p35 preferentially by binding to M50/p35. However, phosphorylation of p32 and its involvement in NEC formation need to be addressed in further experiments.

In addition, several other cellular matrix proteins were tested for interaction with M50/p35 and M53/p38. Recently, it was shown that the human polyomavirus agnoprotein interacts with HP1 and presumably is responsible for HP1 dissociation from the LBR and perturbation of the NE. This enables polyomavirus virions to egress from the nucleus (Okada, 2005). Like MCMV, the polyomavirus is a DNA virus. Therefore a similar nuclear egress mechanism for DNA viruses may exist. HP1 links LBR complex and chromatin by H3-H4 interaction (Bartova, 2005; Gruenbaum, 2005). Furthermore, HP1 interacts with subtypes of linker-histone H1 (Daujatz, 2005). But here we could show that HP1 $\alpha$  neither binds to M50/p35 or M53/p38 nor to the M50-M53 complex. Therefore both MCMV proteins fulfill functions different from that of polyomavirus agnoprotein during nuclear egress.

Next we tested the interaction of M50/p35 or M50-M53 complex with the LEM domain protein MAN1. All yet identified LEM domain proteins in vertebrates exhibit direct interaction with A- and/or B-type lamins and are important for nuclear integrity (Fig. 37). Therefore, like the LBR complex, LEM domain proteins are possible targets of the MCMV egress machinery. They are variable in length and the majority is anchored in the INM. Besides binding to lamins all

## E. Discussion

---

LEM domain proteins directly bind to BAF dimers (barrier to autointegration factor) (Lee, 2001; Shumaker, 2001; Lin, 2000; Furukawa, 1999; Chu, 1998; Mansharamani, 2005; Dechat, 2004). Furthermore, LEM domain proteins exhibit binding to chromatin, which is mediated by BAF (Margalit, 2005; Tiffit, 2006, Haraguchi, 2001; Segura-Totten, 2002). BAF was shown to interact with histone H3 and linkerhistone H1 (Bengtsson, 2006; Montes De Oca, 2005). Therefore, an inter-connection of LBR complex and LEM domain proteins can be assumed. But to that end, using both pull down systems after isolated expression of HAM50 and FlagM53 or co-expression of the tagged proteins with the corresponding partners no interaction of MAN1 with the viral proteins was detectable. Other LEM domain- or LEM associated proteins, e.g. emerin, LAP2 $\alpha$ , LAP2 $\beta$  and BAF are of further interest and need to be analyzed.

For HSV-1 it was shown, that under certain conditions the M53/p38 homologue UL31 interacts with A-type lamins A and C (Simpson-Holley, 2004, 2005; Reynolds, 2004; Scott, 2001). Also for  $\gamma$ -herpesvirus EBV the UL31- and UL34 homologues BFLF2 and BFRF1 were shown to interact with lamin B (Gonnella, 2005). Therefore, the interaction of M53/p38 and M50/p35 with A-and B-type lamins was tested. In both pull down systems no direct interaction of lamin B or lamin A/C with the MCMV-NEC proteins was detectable. Thus, the results for the MCMV-NEC proteins could not confirm the lamin interactions described for  $\alpha$ -herpesvirus HSV-1 and of  $\gamma$ -herpesvirus EBV. A divergent development of herpesviruses during evolution might be the reason for the variable results. We presume technical reasons since insufficient solubilization of matrix proteins can easily result in a non specific interaction.

Next, the interaction of M53/p38 and M50/p35 with linker-histone H1 and histone H3 was tested. We could show that both histones are unable to bind to HAM50. In contrast, both, H3 and H1, directly interacted with FlagM53 and furthermore bound to the M53-M50 complex using both pull down systems. Moreover, in presence of the M53-M50 complex or isolated expressed pFlagM53 an additional protein co-precipitated with H1, which was missing for the controls. Histones H1 and H3 both interact via HP1 with the LBR complex and via BAF with the LEM domain proteins. Therefore, a critical role of M53/p38

or M53/p38 in complex with M50/p35 in chromatin re-organization can be assumed.

The interaction of M53/p38 or M50/p35 with nuclear matrix proteins was only tested upon isolated expression of the NEC proteins. For the M53/p38- and M50/p35- homologues UL31 and UL34 of  $\alpha$ -herpesvirus pseudorabies virus (PrV) it has been demonstrated that the expression of only the PrV-NEC proteins is apparently sufficient for formation of primary envelopment structures (Klupp, 2006). Nevertheless, the interactions of M53/p38 and M50/p35 with cellular matrix proteins need to be analyzed upon MCMV infection to confirm the results during infection conditions.

Altogether, we could identify for the first time four interaction partners of the MCMV-NEC proteins: LBR, p32, H3 and H1. The complex of M53/p38 and M50/p35 was able to bind the listed cellular proteins, whereas in isolation only FlagM53 bound to H1 and H3. Therefore, as described for UL31 from HSV-1, also M53/p38 might be involved in chromatin reorganization (Reynolds, 2004).

### **7. Basic proteomics to identify MCMV- and cellular NEC proteins**

We tried to confirm indicated cellular interaction partners of M53/p38 and M50/p35 by mass-spectrometric analysis. Therefore, cells transfected with pHAM50, pFlagM53 or co-transfected with HAM50 and FlagM53 were lysed and Flag-tag- or HA-tag pull down assay was performed. Proteins bound to the two matrices were eluted, separated by SDS-PAGE and analyzed by silver staining. Numerous interaction partners of M53/p38 and M50/p35 were indicated. Protein bands were isolated from the gel and analyzed by mass-spectrometry, which was performed in cooperation with Arnd Kieser and Thomas Knöfel (GSF, Hämatologikum, München). We could identify both viral interaction partners. However, the amount of recovered protein was too low for a more detailed and specific analysis and reliable identification of the less prominent members of the protein complexes. The system needs to be improved and to be scaled up in future experiments.

## F. References

1. **Ahn, K., A. Angulo, P. Ghazal, P. A. Peterson, Y. Yang, and K. Fruh.** 1996. Human cytomegalovirus inhibits antigen presentation by a sequential multistep process. *Proc. Natl. Acad. Sci. U. S. A.* **93**:10990-10995.
2. **Ahn, K. A. Gruhler, B. Galocha, T. R. Jones, E. J. Wiertz, H. L. Ploegh, P. A. Peterson, Y. Yang, and K. Fruh.** 1997. The ER-luminal domain of the HCMV glycoprotein US6 inhibits peptide translocation by TAP. *Immunity* **6**:613-621.
3. **Alcami, A., and U. H. Koszinowski.** 2000. Viral mechanisms of immune evasion. *Immunol. Today* **21**:447–455.
4. **Arase, H., E. S. Mocarski, A. E. Campbell, A. B. Hill, and L. L. Lanier.** 2002. Direct recognition of cytomegalovirus by activating and inhibitory NK cell receptors. *Science* **296**:1323–1326.
5. **Azzeh, M., A. Honigman, A. Taraboulos, A. Rouvinski, and D. G. Wolf.** 2006. Structural changes in human cytomegalovirus cytoplasmic assembly sites in the absence of UL97 kinase activity. *Virology* **354**:69-79.
6. **Baldick, C. J., and T. Shenk.** 1996. Proteins associated with purified human cytomegalovirus particles. *J. Virol.* **70**:6097–6105.
7. **Bártová, E., J. Pacherník, A. Harnicarová, A. Kovarík, M. Kovaríková, J. Hofmanová, M. Skalníková, M. Kozubek, and S. Kozubek.** 2005. Nuclear levels and patterns of histone H3 modification and HP1 proteins after inhibition of histone deacetylases. *J. Cell Sci.* **118**:5035-5046.
8. **Bateman, A., L. Coin, R. Durbin, R. D. Finn, V. Hollich, S. Griffiths-Jones, A. Khanna, M. Marshall, S. Moxon, E. L. Sonnhammer, D. J. Studholme, C. Yeats, and S. R. Eddy.** 2004. The Pfam protein families database. *Nucleic Acids Res.* **32**:D138-D141.
9. **Bengtsson, L., and K. L. Wilson.** 2006. Barrier-to autointegration factor phosphorylation on Ser-4 regulates emerlin binding to lamin A in vitro and emerlin localization in vivo. *Mol. Biol. Cell* **17**:1154-1163.
10. **Biery, M. C., F. J. Stewart, A. E. Stellwagen, E. A. Raleigh, and N. L. Craig.** 2000. A simple in vitro Tn7-based transposition system with low target site selectivity for genome and gene analysis. *Nucleic Acids Res.* **28**:1067-1077.
11. **Bjerke, S. L., and R. J. Roller.** 2006. Roles for herpes simplex virus type 1 UL34 and US3 proteins in disrupting the nuclear lamina during herpes simplex virus type 1 egress. *Virology* **347**:261–276.

## F. References

---

12. **Bogner, E.** 2002. Human cytomegalovirus terminase as a target for antiviral chemotherapy. *Rev. Med. Virol.* **12**:115–127.
13. **Boehmer, P. E., and I. R. Lehman.**1997. Herpes simplex virus DNA replication. *Annu. Rev. Biochem.* **66**:347-384.
14. **Boehmer, P. E., and A. V. Nimonkar.** 2003. Herpes virus replication. *IUBMB Life* **55**:13-22.
15. **Boppana, S. B., R. F. Pass, W. J. Britt, S. Stagno, and C. A. Alford.** 1992. Symptomatic congenital cytomegalovirus infection: neonatal morbidity and mortality. *Pediatr. Infect. Dis. J.* **11**:93-99.
16. **Brachner, A., S. Reipert, R. Foisner, and J. Gotzmann.** 2005. LEM2 is a novel MAN1-related inner nuclear membrane protein associated with A-type lamins. *J. Cell Sci.* **118**:5797-5810.
17. **Bresnahan, W. A., and T. Shenk.** 2000. A subset of viral transcripts packaged within human cytomegalovirus particles. *Science* **288**:2373–2376.
18. **Britt, W. J., and C.A. Alford.** 1996. Cytomegalovirus. In *Fields Virology*. Fields, B. N., D. M. Knipe, and P. M. Howley (eds.). Philadelphia: Lippincott-Raven publishers:2493-2523.
19. **Brune, W., C. Menard, J. Heesemann, and U. H. Koszinowski.** 2001. A ribonucleotide reductase homolog of cytomegalovirus and endothelial celltropism. *Science* **291**:303–305.
20. **Bubeck, A., M. Wagner, Z. Ruzsics, M. Lötzerich, M. Iglesias, I. R. Singh, and U. H. Koszinowski.** 2004. Comprehensive mutational analysis of a herpesvirus gene in the viral genome context reveals a region essential for virus replication. *J. Virol.* **78**:8026-8035.
21. **Bubic, I., M. Wagner, A. Krmpotic, T. Saulig, S. Kim, W. M. Yokoyama, S. Jonjic, and U. H. Koszinowski.** 2004. Gain of virulence caused by loss of a gene in murine cytomegalovirus. *J. Virol.* **78**:7536-7544.
22. **Buendia, B., J.-C. Courvalin, and P. Collas.** 2001. Dynamics of the nuclear envelope at mitosis and during apoptosis. *Cell. Mol. Life Sci.* **58**:1781-1789.
23. **Chang, Y. E., C. Van Sant, P. W. Krug, A. E. Sears, and B. Roizman.** 1997. The null mutant of the U(L)31 gene of herpes simplex virus 1: construction and phenotype in infected cells. *J. Virol.* **71**:8307-8315.

## F. References

24. **Chee, M. S., A. T. Bankier, S. Beck, R. Bohni, C. M. Brown, R. Cherry, T. Horsnell, C. A. Hutchinson, T. Kouzarides, J. A. Martignetti, and a. et.** 1990. Analysis of the protein-coding content of the sequence of human cytomegalovirus strain AD169. *Curr. Top Microbiol. Immunol.* **154**:125-169.
25. **Chee, M.S., G.L. Lawrence, and B.G. Barrell.** 1989. Alpha-, beta- and gamma-herpesviruses encode a putative phosphotransferase. *J. Gen. Virol.* **70**:1151–1160.
26. **Cherepanov, P. P., and W. Wackernagel.** 1995. Gene disruption in *Escherichia coli*: TcR and KmR cassettes with the option of Flp-catalyzed excision of the antibiotic-resistance determinant. *Gene* **158**:9-14.
27. **Chong, K. T., and C. A. Mims.** 1981. Murine cytomegalovirus particle types in relation to sources of virus and pathogenicity. *J. Gen. Virol.* **57**:415-419.
28. **Chu, A., R. Rassadi, and U. Stochaj.** 1998. Velcro in the nuclear envelope: LBR and LAPs. *FEBS letters* **441**:165-169.
29. **Coen, D. M., and P. A. Schaffer.** 2003. Antiherpesvirus drugs: a promising spectrum of new drugs and drug targets. *Nat. Rev. Drug Discovery* **2**:278-288.
30. **Courvalin, J. C., N. Segil, G. Blobel, and H. J. Worman.** 1992. The lamin B receptor of the inner nuclear membrane undergoes mitosis-specific phosphorylation and is substrate for a p34<sup>cdc2</sup>-type protein kinase. *J. Biol. Chem.* **267**:19035-19038.
31. **Dal Monte, P., S. Pignatelli, N. Zini, N. M. Maraldi, E. Perret, M. C. Prevost, and M. P. Landini.** 2002. Analysis of intracellular and intraviral localization of the human cytomegalovirus UL53 protein. *J. Gen. Virol.* **83**:1005–1012.
32. **D'Angelo, M.A., and M.W. Hetzer.** 2006. The role of the nuclear envelope in cellular organization. *Cell. Mol. Life Sci.* **63**:316–332.
33. **Daujat, S., U. Zeissler, T. Waldmann, N. Happel, and R. Schneider.** 2005. HP1 binds specifically to Lys<sup>26</sup>-methylated histone H1.4, whereas simultaneous Ser<sup>27</sup> phosphorylation blocks HP1 binding. *J. Biol. Chem.* **280**:38090–38095.
34. **Deb, T. B., and K. Datta.** 1996. Molecular cloning of human fibroblast hyaluronic acid-binding protein confirms its identity with P-32, a protein co-purified with splicing factor SF2. Hyaluronic acid-binding protein as P-32, co-purified with splicing factor SF2. *J. Biol. Chem.* **271**:2206-2212.

## F. References

35. **Dechat, T., A. Gajewski, B. Korbei, D. Gerlich, N. Daigle, T. Haraguchi, K. Furukawa, J. Ellenberg and R. Foisner.** 2004. LAP2a and BAF transiently localize to telomeres and specific regions on chromatin during nuclear assembly. *J. Cell Sci.* **117**:6117-6128.
36. **Dessev, G., C. Iovcheva, B. Tasheva, and R. Goldman.**1988. Protein kinase activity associated with the nuclear lamina. *Proc. Natl. Acad. Sci. U.S.A.* **85**:2994-2998.
37. **Dijke, P. ten, and C. S. Hill.** 2004. New insights into TGF- $\beta$ -Smad signalling. *Trends Biochem. Sci.* **29**:265-273.
38. **Dingwall, C. and R. A. Laskey.** 1991. Nuclear targeting sequences--a consensus? *Trends Biochem. Sci.* **16**:478-481.
39. **Dohner, K., and B. Sodeik.** 2004. The role of the cytoplasm during viral infection. *Curr. Top. Microbiol. Immunol.* **285**:67-108.
40. **Enquist, L. W., P. J. Husak, B. W. Banfield, and G. A. Smith.** 1998. Infection and spread of alphaherpesviruses in the nervous system. *Adv. Virus Res.* **51**:237-247.
41. **Farina, A., R. Feederle, S. Raffa, R. Gonnella, R. Santarelli, L. Frati, A. Angeloni, M. R. Torrisi, A. Faggioni, and H. J. Delecluse.** 2005. BFRF1 of Epstein-Barr virus is essential for efficient primary viral envelopment and egress. *J. Virol.* **79**:3703-3712.
42. **Farina, A., R. Santarelli, R. Gonnella, R. Bei, R. Muraro, G. Cardinali, S. Uccini, G. Ragona, L. Frati, A. Faggioni, and A. Angeloni.** 2000. The BFRF1 gene of Epstein-Barr virus encodes a novel protein. *J. Virol.* **74**:3235-3244.
43. **Flint, S. J., L. W. Enquist, R. M. Krug, V. R. Racaniello, and A. M. Skalka.** 2000. Principles of virology: molecular biology, pathogenesis, and control. First edition. ASM press; Washington, DC 20036; ISBN 1-55581-127-2.
44. **Foisner, R.** 2001. Inner nuclear membrane proteins and the nuclear lamina. *J. Cell Science* **114**:3791-3792.
45. **Forest, T., S. Barnard, and J. D. Baines.** 2005. Active intranuclear movement of herpesvirus capsids. *Nat. Cell Biol.* **7**:429-431.
46. **Fuchs, W., B. G. Klupp, H. Granzow, N. Osterrieder, and T. C. Mettenleiter.** 2002. The interacting UL31 and UL34 gene products of pseudorabies virus are involved in egress from the host-cell nucleus and represent components of primary enveloped but not mature virions. *J. Virol.* **76**:364-378.



## F. References

47. **Furukawa, K.** 1999. LAP2 binding protein 1 (L2BP1/BAF) is a candidate mediator of LAP2-chromatin interaction. *J. Cell Sci.* **112**:2485-2492.
48. **Furukawa, K., et al.** 2003. Barrier-to-autointegration factor plays crucial roles in cell cycle progression and nuclear organization in *Drosophila*. *J. Cell Sci.* **116**:3811-3823.
49. **Gerace, L., and G. Blobel.** 1980. The nuclear envelope lamina is reversibly depolymerized during mitosis. *Cell* **19**:277-287.
50. **Gershburg, E., D. Scheswohl, S. Raffa, M. R. Torrasi, and J. S. Pagano.** 2006. Role of the viral protein kinase BGLF4 in Epstein-Barr virus nuclear egress. Oral presentation: 31<sup>st</sup> international herpesvirus workshop. University of Washington; Seattle, Washington USA. Abstract:**11.07**.
51. **Gershon, A. A., D. L. Sherman, Z. Zhu, C. A. Gabel, R. T. Ambron, and M. D. Gershon.** 1994. Intracellular transport of newly synthesized varicella-zoster virus: final envelopment in the trans-Golgi network. *J. Virol.* **68**:6372-6390.
52. **Gold, M. C., M. W. Munks, M. Wagner, U. H. Koszinowski, A. B. Hill, and S. P. Fling.** 2002. The murine cytomegalovirus immunomodulatory gene m152 prevents recognition of infected cells by M45-specific CTL but does not alter the immunodominance of the M45-specific CD8 T cell response in vivo. *J Immunol.* **169**:359-365.
53. **Gonnella, R., A. Farina, R. Santarelli, S. Raffa, R. Feederle, R. Bei, M. Granato, A. Modesti, L. Frati, H. J. Delecluse, M. R. Torrasi, A. Angeloni, and A. Faggioni.** 2005. Characterization and intracellular localization of the Epstein-Barr virus protein BFLF2: interactions with BFRF1 and with the nuclear lamina. *J. Virol.* **79**:3713-3727.
54. **Gossen, M. and H. Bujard.** 1992. Tight control of gene expression in mammalian cells by tetracycline-responsive promoters. *Proc. Natl. Acad. Sci. U S A* **89**:5547-5551.
55. **Gruenbaum, Y., A. Margalit, R. D. Goldman, D. K. Shumaker, and K. L. Wilson.** 2005. The nuclear lamina comes of age. *Mol. Cell Biol.* **6**:21-31.
56. **Hahn, G., R. Jores, and E.S. Mocarski.** 1998. Cytomegalovirus remains latent in a common precursor of dendritic and myeloid cells. *Proc. Natl. Acad. Sci. USA* **95**:3937-3942.
57. **Hall, K. T., M. S. Giles, M. A. Calderwood, D. J. Goodwin, D. A. Matthews, and A. Whitehouse.** 2002. The herpesvirus saimiri open reading frame 73 gene product interacts with the cellular protein p32. *J. Virol.* **76**:11612-11622.

## F. References

---

58. **Haraguchi, T., T. Koujin, M. Segura-Totten, K. K. Lee, Y. Matsuoka, Y. Yoneda, K. L. Wilson and Y. Hiraoka.** 2001. BAF is required for emerin assembly into the reforming nuclear envelope. *J. Cell Sci.* **114**:4575-4585.
59. **Hengel, H., U. Reusch, A. Gutermann, H. Ziegler, S. Jonjic, P. Lucin, and U. H. Koszinowski.** 1999. Cytomegaloviral control of MHC class I function in the mouse. *Immunol. Rev.* **168**:167-176.
60. **Herrmann, H. and R. Foisner.** 2003. Intermediate filaments: novel assembly models and exciting new functions for nuclear lamins. *Cell. Mol. Life Sci.* **60**:1607-1612.
61. **Holaska, J. M., and K. L. Wilson.** 2006. Multiple roles for emerin: implications for Emery-Dreifuss muscular dystrophy. *Anat. Rec. Part A* **288A**:676–680.
62. **Holmer, L., A. Pezhman, and H. J. Worman.** 1998. The human lamin B receptor/sterol reductase multigene family. *Genomics* **54**:469–476.
63. **Hobom, U., W. Brune, M. Messerle, G. Hahn, and U. H. Koszinowski.** 2000. Fast screening procedures for random transposon libraries of cloned herpesvirus genomes: mutational analysis of human cytomegalovirus envelope glycoprotein genes. *J. Virol.* **74**:7720–7729.
64. **Hudson, J. B.** 1979. The murine cytomegalovirus as a model for the study of viral pathogenesis and persistent infection. *Arch. Virol.* **62**:1-29.
65. **Irmiere, A., and W. Gibson.** 1983. Isolation and characterization of a noninfectious virion-like particle released from cells infected with human strains of cytomegalovirus. *Virology* **130**:118-133.
66. **Jackson, S. A., and N. A. DeLuca.** 2003. Relationship of herpes simplex virus genome configuration to productive and persistent infections. *Proc. Natl. Acad. Sci. U. S. A.* **100**:7871-7876.
67. **Jacque, J. M., and M. Stevenson.** 2006. The inner-nuclear-envelope protein emerin regulates HIV-1 infectivity. *Nature* **441**:641-645.
68. **Jiang, J., Y. Zhang, A. R. Krainer, and R. M. Xu.** 1999. Crystal structure of the human p32, a doughnut-shaped acidic mitochondrial matrix protein. *Proc. Natl. Acad. Sci. USA* **96**:3572-3577.
69. **Jones, T. R., and L. Sun.** 1997. Human cytomegalovirus US2 destabilizes major histocompatibility complex class I heavy chains. *J. Virol.* **71**:2970-2979.

## F. References

70. **Jones, T. R., E. J. Wiertz, L. Sun, K. N. Fish, J. A. Nelson, and H. L. Ploegh.** 1996. Human cytomegalovirus US3 impairs transport and maturation of major histocompatibility complex class I heavy chains. *Proc. Natl. Acad. Sci. U. S. A.* **93**:11327-11333.
71. **Jonjic, S., I. Pavic, P. Lucin, D. Rukavina, and U. H. Koszinowski.** 1990. Efficacious control of cytomegalovirus infection after long-term depletion of CD8<sup>+</sup> T lymphocytes. *J. Virol.* **64**:5457-5464.
72. **Kato, A., M. Yamamoto, T. Ohno, H. Kodaira, Y. Nishiyama, and Y. Kawaguchi.** 2005. Identification of proteins phosphorylated directly by the Us3 protein kinase encoded by herpes simplex virus 1. *J. Virol.* **79**:9325–9331.
73. **Kato, A., M. Yamamoto, T. Ohno, M. Tanaka, T. Sata, Y. Nishiyama, and Y. Kawaguchi.** 2006. Herpes simplex virus 1-encoded protein kinase UL13 phosphorylates viral Us3 protein kinase and regulates nuclear localization of viral envelopment factors UL34 and UL31. *J. Virol.* **80**:1476-1486.
74. **Kawaguchi, Y., K. Kato, M. Tanaka, M. Kanamori, Y. Nishiyama, and Y. Yamanashi.** 2003. Conserved protein kinases encoded by herpesviruses and cellular protein kinase cdc2 target the same phosphorylation site in eukaryotic elongation factor 1d. *J. Virol.* **77**:2359–2368.
75. **Kleijnen, M. F., J. B. Huppa, P. Lucin, S. Mukherjee, H. Farrell, A. E. Campbell, U. H. Koszinowski, A. B. Hill, and H. L. Ploegh.** 1997. A mouse cytomegalovirus glycoprotein, gp34, forms a complex with folded class I MHC molecules in the ER which is not retained but transported to the cell surface. *EMBO J.* **16**:685-694.
76. **Klupp, B. G., H. Granzow, G. M. Keil, and T. C. Mettenleiter.** 2006. The capsid-associated UL25 protein of the alphaherpesvirus pseudorabies virus is nonessential for cleavage and encapsidation of genomic DNA but is required for nuclear egress of capsids. *J. Virol.* **80**:6235-6246.
77. **Klupp, B. G., H. Granzow, G. M. Keil, and T. C. Mettenleiter.** 2006. Nuclear egress of herpesvirus capsids. Oral presentation on 31<sup>st</sup> international herpesvirus workshop. University of Washington; Seattle, Washington USA. Abstract:**11.02**.
78. **Klupp, B. G., H. Granzow, and T. C. Mettenleiter.** 2001. Effect of the pseudorabies virus US3 protein on nuclear membrane localization of the UL34 protein and virus egress from the nucleus. *J. Gen. Virol.* **82**:2363–2371.
79. **Klupp, B. G., H. Granzow, and T. C. Mettenleiter.** 2000. Primary envelopment of pseudorabies virus at the nuclear membrane requires the UL34 gene product. *J. Virol.* **74**:10063–10073.

## F. References

80. **Kondo, K., J. Xu, and E. S. Mocarski.** 1996. Human cytomegalovirus latent gene expression in granulocyte-macrophage progenitors in culture and in seropositive individuals. *Proc. Natl. Acad. Sci. U. S. A.* **93**:11137-11142.
81. **Koszinowski, U. H., and H. Hengel. (eds.).** 2002. *Viral proteins counteracting host defenses.* Springer-Verlag Berlin Heidelberg. ISBN:3-540-43261-2.
82. **Kotsakis, A., L. E. Pomeranz, A. Blouin, and J. A. Blaho.** 2001. Microtubule reorganization during herpes simplex virus type 1 infection facilitates the nuclear localization of VP22, a major virion tegument protein. *J. Virol.* **75**:8697–8711.
83. **Krainer, A. R., A. Mayeda, D. Kozak, and G. Binns.** 1991. Functional expression of cloned human splicing factor SF2: homology to RNA-binding proteins, U1 70K, and Drosophilla splicing regulators. *Cell* **66**:383–394.
84. **Krmpotic, A., I. Bubic, B. Polic, P. Lucin, and S. Jonjic.** 2003. Pathogenesis of murine cytomegalovirus infection. *Microbes and Infection* **5**:1263–1277.
85. **Krosky, P. M., M.-C. Baek, and D. M. Coen.** 2003. The human cytomegalovirus UL97 protein kinase, an antiviral drug target, is required at the stage of nuclear egress. *J. Virol.* **77**:905–914.
86. **Lake, C. M., and L. M. Hutt-Fletcher.** 2004. The Epstein-Barr virus BFRF1 and BFLF2 proteins interact and coexpression alters their cellular localization. *Virology* **320**:99-106.
87. **Landolfo, S., M. Gariglio, G. Gribaudo, and D. Lembo.** 2003. The human cytomegalovirus. *Pharmacology & Therapeutics* **98**:269– 297.
88. **Lee, K. K., T. Haraguchi, R. S. Lee, T. Koujin, Y. Hiraoka, and K. L. Wilson.** 2001. Distinct functional domains in emerin bind lamin A and DNA bridging protein BAF. *J. Cell Sci.* **114**:4567-4573.
89. **Leeuwen, H. C. van, and P. O'Hare.** 2001. Retargeting of the mitochondrial protein p32/gC1Qr to a cytoplasmic compartment and the cell surface. *J. Cell Sci.* **114**:2115-2123.
90. **Leung, G. K., W. K. Schmidt, M. O. Bergo, B. Gavino, D. H. Wong, A. Tam, M. N. Ashby, S. Michaelis, and S. G. Young.** 2001. Biochemical studies of Zmpste24-deficient mice. *J. Biol. Chem.* **276**:29051-29058.
91. **Leuzinger, H., U. Ziegler, E. M. Schraner, C. Fraefel, D. L. Glauser, I. Heid, M. Ackermann, M. Mueller, and P. Wild.** 2005. Herpes simplex virus type 1 envelopment follows two diverse pathways. *J. Virol.* **79**:13047–13059.

## F. References

---

92. **Liang, L., and J. D. Baines.** 2005. Identification of an essential domain in the herpes simplex virus 1 UL34 protein that is necessary and sufficient to interact with UL31 protein. *J. Virol.* **79**:3797-3806.
93. **Liang, L., M. Tanaka, Y. Kawaguchi, and J. D. Baines.** 2004. Cell lines that support replication of a novel herpes simplex virus 1 UL31 deletion mutant can properly target UL34 protein to the nuclear rim in the absence of UL31. *Virology* **329**:68-76.
94. **Lin, F., D. L. Blake, I. Callebaut, I. S. Skerjanc, L. Holmer, M. W. McBurney, M. Paulin-Levasseur, and H. J. Worman.** 2000. MAN1, an inner nuclear membrane protein that shares the LEM domain with lamina associated polypeptide 2 and emerin. *J. Biol. Chem.* **275**:4840-4847.
95. **Lötzerich, M., Z. Ruzsics, and U. H. Koszinowski.** 2006. Functional domains of murine cytomegalovirus nuclear egress protein M53/p38. *J. Virol.* **80**:73-84.
96. **Luo, Y., H. Yu, and B. M. Peterlin.** 1994. Cellular protein modulates effects of human immunodeficiency virus type 1. *Rev. J. Virol.* **68**:3850-3856.
97. **Malone, C. J. et al.** 2003. The *C. elegans* hook protein, ZYG-12, mediates the essential attachment between the centrosome and nucleus. *Cell* **115**:825-836.
98. **Mansharamani, M., and K. L. Wilson.** 2005. Direct binding of nuclear membrane protein MAN1 to emerin in vitro and two modes of binding to barrier-to-autointegration factor. *J. Biol. Chem.* **280**:13863–13870.
99. **Margalit, A., M. Segura-Totten, Y. Gruenbaum, and K. L. Wilson.** 2005. Barrier-to-autointegration factor is required to segregate and enclose chromosomes within the nuclear envelope and assemble the nuclear lamina. *PNAS* **102**:3290–3295.
100. **Marschall, M., A. Marzi, P. aus dem Siepen, R. Jochmann, M. Kalmer, S. Auerochs, P. Lischka, M. Leis, and T. Stamminger.** 2005. Cellular p32 recruits cytomegalovirus kinase pUL97 to redistribute the nuclear lamina. *J. Biol. Chem.* **280**:33357-33367.
101. **Marschall, M., J. Milbrandt, S. Auerochs, R. Jochmann, A. Marzi, and T. Stamminger.** 2006. The nuclear capsid export complex (NEC) of human cytomegalovirus consists of viral and cellular lamina associated proteins and protein kinases. Oral presentation: 31<sup>st</sup> international herpesvirus workshop. University of Washington; Seattle, Washington USA. Abstract:11.08.
102. **Matthews, D. A., and W. C. Russell.** 1998. Adenovirus core protein V interacts with p32- a protein which is associated with both the mitochondria and the nucleus. *J. General Virol.* **79**:1677-1685.

## F. References

---

103. **Mattout, A., T. Dechat, S. A. Adam, R. D. Goldman, and Y. Gruenbaum.** 2006. Nuclear lamins, diseases and aging. *Curr. Opin. Cell Biol.* **18**:335–341.
104. **Mayo, D. R., J. A. Armstrong, and M. Ho.** 1977. Reactivation of murine cytomegalovirus by cyclophosphamide. *Nature* **267**:721-723.
105. **McVoy, M.A., and S.P.Adler.**1994. Human cytomegalovirus DNA replicates after early circularization by concatemer formation, and inversion occurs within the concatemer. *J. Virol.* **68**:1040–1051.
106. **Meier, J. and S.D. Georgatos.** 1994. Type B lamins remain associated with the integral nuclear envelope protein p58 during mitosis: implications for nuclear reassembly. *EMBO J.* **13**:1888-1898.
107. **Menard, C., M. Wagner, Z. Ruzsics, K. Holak, W. Brune, A. E. Campbell, and U. H. Koszinowski.** 2003. Role of murine cytomegalovirus US22 gene family members in replication in macrophages. *J. Virol.* **77**:5557-5570.
108. **Messerle, M., I. Crnkovic, W. Hammerschmidt, H. Ziegler, and U. H. Koszinowski.** 1997. Cloning and mutagenesis of a herpesvirus genome as an infectious bacterial artificial chromosome. *Proc. Natl. Acad. Sci. U. S. A* **94**:14759-14763.
109. **Mettenleiter, T. C..** 2002. Herpesvirus assembly and egress. *J. Virol.* **76**:1537-1547.
110. **Mettenleiter, T. C..** 2004. Budding events in herpesvirus morphogenesis. *Virus Res.* **106**:167-180.
111. **Mettenleiter, T. C..** 2006. Intriguing interplay between viral proteins during herpesvirus assembly or: The herpesvirus assembly puzzle. *Vet. Microbiol.* **113**:163–169.
112. **Mettenleiter, T. C..** 2006. Letter to the editor. Egress of alphaherpesviruses. *J. Virol.* **80**:1610-1612.
113. **Mettenleiter, T. C..** 2006. Letter to the editor. The egress of herpesviruses from cells: the unanswered questions. *J. Virol.* **80**:6716-6719.
114. **Mettenleiter, T. C., B. G. Klupp, and H. Granzow.** 2006. Herpesvirus assembly: a tale of two membranes. *Curr. Opin. Microbiol.* **9**:1–7.
115. **Mocarski, E. S.** 2002. Immunomodulation by cytomegaloviruses: manipulative strategies beyond evasion. *Trends Microbiol.* **10**:332–339.



## F. References

116. **Mocarski, E. S.** 2006. In Human herpesviruses: Biology, therapy and immunoprophylaxis.(A. M. Arvin, G. Campadielli-Fiume, P. S. Moore, E. S. Mocarski, B. Roizman, R. Whitley, and K. Yamanishi, eds.). Cambridge University Press. ISBN-13:9780521827140, available from Dec 2006.
117. **Mocarski, E. S., Jr., and C. T. Courcelle.** 2001. Cytomegaloviruses and their replication. Fourth edition, ed. in "Fields Virology" (D. M. Knipe, P. M. Howley, D. E. Griffin, R. A. Lamb, M. A. Martin, B. Roizman, and S. E. Straus, eds.). Lippincott Williams & Wilkins, Philadelphia. **2**:2629-2673.
118. **Mocarski, E. S., G. W. Kemble, J. M. Lyle, and R. F. Greaves.** 1996. A deletion mutant in the human cytomegalovirus gene encoding IE1 (491aa) is replication defective due to a failure in autoregulation. Proc. Natl.Acad. Sci. U. S. A. **94**:11321–11326.
119. **Moir, R. D., M. Yoon, S. Khuon, and R. D. Goldman.** 2000. Nuclear lamins A and B1. Different pathways of assembly during nuclear envelope formation in living cells. J. Cell Biol. **151**:1155-1168.
120. **Montes de Oca, R., K. K. Lee, and K. L. Wilson.** 2005. Binding of barrier to autointegration factor (BAF) to histone H3 and selected linker histones including H1.1. J. Biol. Chem. **280**:42252–42262.
121. **Muchir, A. and H. J. Worman.** 2004. The nuclear envelope and human disease. Physiology **19**:309-314.
122. **Muranyi, W., J. Haas, M. Wagner, G. Krohne, and U. H. Koszinowski.** 2002. Cytomegalovirus recruitment of cellular kinases to dissolve the nuclear lamina. Science **297**:854-857.
123. **Muta, T., D. Klang, S. Kitajima, T. Fujiwara, and N. Hamasaki.** 1997. p32 protein, a splicing factor 2-associated protein, is localized in mitochondrial matrix and is functionally important in maintaining oxidative phosphorylation. J. Biol. Chem. **272**:24363-24370.
124. **Neubauer, A., J. Rudolph, C. Brandmuller, F. T. Just, and N. Osterrieder.** 2002. The equine herpesvirus 1 UL34 gene product is involved in an early step in virus egress and can be efficiently replaced by a UL34-GFP fusion protein. Virology **300**:189–204.
125. **Nikolakaki, E., G. Simos, S. D. Georgatos, and T. Giannakouros.** 1996. A nuclear envelope-associated kinase phosphorylates arginine-serine motifs and modulates interaction between the lamin B receptor and other nuclear proteins. J. Biol. Chem. **271**:8365-8372.
126. **Nikolakaki, E., M. Meier, G. Simos, S. D. Georgatos, and T. Giannakouros.** 1997. Mitotic phosphorylation of the lamin B receptor by a serine/arginine kinase and p34<sup>cdc2</sup>. J. Biol. Chem. **272**:6208-6213.



## F. References

---

127. **Öhrmalm, C., and G. Akusjärvi.** 2006. Cellular splicing and transcription regulatory protein p32 represses adenovirus major late transcription and causes hyperphosphorylation of RNA polymerase II. *J. Virol.* **80**:5010-5020.
128. **Östlund, C., T. Sullivan, C. L. Stewart, and H. J. Worman.** 2006. Dependence of diffusional mobility of integral inner nuclear membrane proteins on A-type lamins. *Biochemistry* **45**:1374-1382.
129. **Okada, Y., T. Suzuki, Y. Sunden, Y. Orba, S. Kose, N. Imamoto, H. Takahashi, S. Tanaka, W. W. Hall, K. Nagashima, and H. Sawa.** 2005. Dissociation of heterochromatin protein 1 from lamin B receptor induced by human polyomavirus agnoprotein: role in nuclear egress of viral particles. *EMBO reports* **6**:452-457.
130. **Osada, S., S. Y. Ohmori, and M. Taira.** 2003. XMAN1, an inner nuclear membrane protein, antagonizes BMP signalling by interacting with Smad1 in *Xenopus* embryos. *Development* **130**:1783-1794.
131. **Ottaviano, Y., and L. Gerace.** 1985. Phosphorylation of the nuclear lamins during interphase and mitosis. *J. Biol. Chem.* **260**:624-632.
132. **Otto, H., M. Dreger, L. Bengtsson, and F. Hucho.** 2001. Identification of tyrosine-phosphorylated proteins associated with the nuclear envelope. *Eur. J. Biochem.* **268**:420-428.
133. **Padgett, K. A. and J. A. Sorge.** 1996. Creating seamless junctions independent of restriction sites in PCR cloning. *Gene* **168**:31-35.
134. **Park, R., and J. D. Baines.** 2006. Herpes simplex virus type 1 infection induces activation and recruitment of protein kinase C to the nuclear membrane and increased phosphorylation of lamin B. *J. Virol.* **80**:494-504.
135. **Peter, M., J. Nakagawa, M. Doree, J. C. Labbe, and E. A. Nigg.** 1990. In vitro disassembly of the nuclear lamina and phase-specific phosphorylation of lamins by cdc2 kinase. *Cell* **61**:591-602.
136. **Polioudaki, H., N. Kourmouli, V. Drosou, A. Bakou, P. A. Theodoropoulos, P. B. Singh, T. Giannakouros, and S. D. Georgatos.** 2001. Histones H3/H4 form a tight complex with the inner nuclear membrane protein LBR and heterochromatin protein 1. *EMBO rep.* **2**:920-925.
137. **Posfai, G., M. D. Koob, H. A. Kirkpatrick, and F. R. Blattner.** 1997. Versatile insertion plasmids for targeted genome manipulations in bacteria: isolation, deletion, and rescue of the pathogenicity island LEE of the *Escherichia coli* O157:H7 genome. *J. Bacteriol.* **179**:4426-4428.

## F. References

138. **Prichard, M. N., N. Gao, S. Jairath, G. Mulamba, P. Krosky, D. M. Coen, B. O. Parker, and G. S. Pari.** 1999. A recombinant human cytomegalovirus with a large deletion in UL97 has a severe replication deficiency. *J. Virol.* **73**:5663–5670.
139. **Prichard, M.N., W. J. Britt, S. L. Daily, C. B. Hartline, and E. R. Kern.** 2005. Human cytomegalovirus UL97 kinase is required for the normal intranuclear distribution of pp65 and virion morphogenesis. *J. Virol.* **79**:15494–15502.
140. **Radsak, K. M. Eickmann, T. Mockenhaupt, E. Bogner, H. Kern, A. Eishubinger, and M. Reschke.** 1996. Retrieval of human cytomegalovirus glycoprotein B from the infected cell surface for virus envelopment. *Arch. Virol.* **141**:557-572.
141. **Rawlinson, W. D., H. E. Farrell, and B. G. Barrell.** 1996. Analysis of the complete DNA sequence of murine cytomegalovirus. *J. Virol.* **70**:8833-8849.
142. **Rawlinson, W. D., F. Zeng, H. E. Farrell, A. L. Cunningham, A. A. Scalzo, T. W. M. Booth, and G. M. Scott.** 1997. The murine cytomegalovirus (MCMV) homolog of the HCMV phosphotransferase (UL97(pk)) gene. *Virology* **233**:358–363.
143. **Reddehase, M. J., F. Weiland, K. Munch, S. Jonjic, A. Luske, and U. H. Koszinowski.** 1985. Interstitial murine cytomegalovirus pneumonia after irradiation: characterization of cells that limit viral replication during established infection of the lungs. *J. Virol.* **55**:264-273.
144. **Reddehase, M. J., M. Balthesen, M. Rapp, S. Jonjic, I. Pavic, and U. H. Koszinowski.** 1994. The conditions of primary infection define the load of latent viral genome on organs and the risk of recurrent cytomegalovirus disease. *J. Exp. Med.* **179**:185-193.
145. **Reddehase, M. J., S. Jonjic, F. Weiland, W. Mutter, and U. K. Koszinowski.** 1988. Adoptive immunotherapy of murine cytomegalovirus adrenalitis in the immunocompromised host: CD4-helper-independent antiviral function of CD8-positive memory T lymphocytes derived from latently infected donors. *J. Virol.* **62**:1061-1065.
146. **Reed, I. J., and H. A. Muench.** 1938. A simple method of estimating 50% endpoints. *Am. J. Hyg.* **27**:493-497.
147. **Regenmortel, M. H. V. van, and B. W. J. Mahy.** 2004. Emerging issues in virus taxonomy. *Emerg. Inf. Dis.* **10**:8-13.
148. **Reusch, U., W. Muranyi, P. Lucin, H. G. Burgert, H. Hengel, and U. H. Koszinowski.** 1999. A cytomegalovirus glycoprotein re-routes MHC class I complexes to lysosomes for degradation. *EMBO J.* **18**:1081-1091.

## F. References

149. **Reynolds, A. E., B. J. Ryckman, J. D. Baines, Y. Zhou, L. Liang, and R. J. Roller.** 2001. U(L)31 and U(L)34 proteins of herpes simplex virus type 1 form a complex that accumulates at the nuclear rim and is required for envelopment of nucleocapsids. *J. Virol.* **75**:8803-8817.
150. **Reynolds, A. E., E. G. Wills, R. J. Roller, B. J. Ryckman, and J. D. Baines.** 2002. Ultrastructural localization of the herpes simplex virus type 1 UL31, UL34, and US3 proteins suggests specific roles in primary envelopment and egress of nucleocapsids. *J. Virol.* **76**:8939-8952.
151. **Reynolds, A. E., L. Liang, and J. D. Baines.** 2004. Conformational changes in the nuclear lamina induced by herpes simplex virus type 1 require genes U(L)31 and U(L)34. *J. Virol.* **78**:5564-5575.
152. **Roizman, B., and P. E. Pellet.** 2001. The family herpesviridae: A brief introduction. Fourth edition ed. in "Fields Virology" (D. M. Knipe, P. M. Howley, D. E. Griffin, R. A. Lamb, M. A. Martin, B. Roizman, and S. E. Straus, Eds.). **2**:2221-2230. Lippincott Williams & Wilkins, Philadelphia.
153. **Roller, R. J., Y. Zhou, R. Schnetzer, J. Ferguson, and D. DeSalvo.** 2000. Herpes simplex virus type 1 U(L)34 gene product is required for viral envelopment. *J. Virol.* **74**:117-129.
154. **Rupp, B., Z. Ruzsics, T. Sacher, and U. H. Koszinowski.** 2005. Conditional cytomegalovirus replication in vitro and in vivo. *J. Virol.* **79**:486-494.
155. **Sambrook, J. and D. W. Russel.** 2001. Molecular cloning - a laboratory manual. Cold Spring Harbor laboratory press, Cold Spring Harbor, New York.
156. **Schirmer, E. C., and L. Gerace.** 2005. The nuclear membrane proteome: extending the envelope. *Trends Biochem. Sci.* **30**:551-558.
157. **Schnee, M., R. Ruzsics, A. Bubeck, and U. H. Koszinowski.** 2006. Common and specific properties of herpesvirus UL34/UL31 protein family members revealed by protein complementation assay. *J. Virol.* **80**:11658-11666.
158. **Schuler, E., F. Lin, and H. J. Worman.** 1994. Characterization of the human gene encoding LBR, an integral protein of the nuclear envelope inner membrane. *J. Biol. Chem.* **269**:11312-11317.
159. **Schynts, F., M. A. McVoy, F. Meurens, B. Detry, A. L. Epstein, and E. Thirya.** 2003. The structures of bovine herpesvirus 1 virion and concatemeric DNA: implications for cleavage and packaging of herpesvirus genomes. *Virology* **314**:326-335.
160. **Scott, E. S. and P. O'Hare.** 2001. Fate of the inner nuclear membrane protein lamin B receptor and nuclear lamins in herpes simplex virus type 1 infection. *J. Virol.* **75**:8818-8830.

## F. References

161. **Segura-Totten, M., A.M. Kowalski, R. Craigie, K. L. Wilson.** 2002. Barrier to-autointegration factor: major roles in chromatin decondensation and nuclear assembly. *J. Cell. Biol.* **158**:475–485.
162. **Serrano, M., A. W. Lin, M. E. McCurrach, D. Beach, and S. W. Lowe.** 1997. Oncogenic ras provokes premature cell senescence associated with accumulation of p53 and p16INK4a. *Cell* **88**:593-602.
163. **Shumaker, D. K., K. K. Lee, Y. C. Tanhehco, R. Craigie, and K. L. Wilson.** 2001. LAP2 binds to BAF-DNA complexes: requirement for the LEM-domain and modulation by variable regions. *EMBO J.* **20**:1754-1764.
164. **Simos, G., C. Maison, and S. D. Georgatos.** 1996. Characterization of p18, a component of the lamin B receptor complex and a new integral membrane protein of the avian erythrocyte nuclear envelope. *J. Biol. Chem.* **271**:12617-12625.
165. **Simos, G., and S. D. Georgatos.** 1992. The inner nuclear membrane protein p58 associates in vivo with a p58 kinase and the nuclear lamins. *EMBO J.* **11**:4027-4036.
166. **Simos, G., and S. D. Georgatos.** 1994. The lamin B receptor-associated protein p34 shares sequence homology and antigenic determinants with the splicing factor 2-associated protein p32. *FEBS Lett.* **346**:225-228.
167. **Simpson-Holley, M., J. Baines, R. Roller, and D. M. Knipe.** 2004. Herpes simplex virus 1 U(L)31 and U(L)34 gene products promote the late maturation of viral replication compartments to the nuclear periphery. *J. Virol.* **78**:5591-5600.
168. **Simpson-Holley, M., R. C. Colgrove, G. Nalepa, J. W. Harper, and D. M. Knipe.** 2005. Identification and functional evaluation of cellular and viral factors involved in the alteration of nuclear architecture during herpes simplex virus 1 infection. *J. Virol.* **79**:12840-12851.
169. **Skepper, J. N., A. Whiteley, H. Browne, and A. Minson.** 2001. Herpes simplex virus nucleocapsids mature to progeny virions by an envelopment- deenvelopment- reenvelopment pathway. *J. Virol.* **75**:5697-5702.
170. **Smith, G. A., and L. W. Enquist.** 1999. Construction and transposon mutagenesis in *Escherichia coli* of a full-length infectious clone of pseudorabies virus, an alphaherpesvirus. *J. Virol.* **73**:6405–6414.
171. **Smith, G. A., and L. W. Enquist.** 2002. Break ins and break outs: viral interactions with the cytoskeleton of Mammalian cells. *Annu. Rev. Cell Dev. Biol.* **18**: 135-61.

## F. References

---

172. **Soderberg-Naucler, C., K. N. Fish, and J. A. Nelson.** 1997. Reactivation of latent human cytomegalovirus by allogeneic stimulation of blood cells from healthy donors. *Cell* **91**:119-126.
173. **Spann, T. P., A. E. Goldman, C. Wang, S. Huang, and R. D. Goldman.** 2002. Alteration of nuclear lamin organization inhibits RNA polymerase II-dependent transcription. *J. Cell Biol.* **156**:603-608.
174. **Spear, P. G.** 2004. Herpes simplex virus: receptors and ligands for cell entry. *Cell Microbiol.* **6**:401-410.
175. **Spear, P. G., and R. Longnecker.** 2003. Herpesvirus entry: an update. *J. Virol.* **77**:10179-85.
176. **Stagno, S., R. F. Pass, G. Cloud, W. J. Britt, R. E. Henderson, P. D. Walton, D. A. Veren, F. Page, and C. A. Alford.** 1986. Primary cytomegalovirus infection in pregnancy. Incidence, transmission to fetus, and clinical outcome. *JAMA* **256**:1904-1908.
177. **Stagno, S., R. F. Pass, M. E. Dworsky, and C. A. Alford.** 1982. Maternal cytomegalovirus infection and perinatal transmission. *Clin. Obstet. Gynecol.* **25**:563-576.
178. **Stoddart, C. A., R. D. Cardin, J. M. Boname, W. C. Manning, G.B. Abenes, and E. S. Mocarski.** 1994. Peripheral blood mononuclear phagocytes mediate dissemination of murine cytomegalovirus. *J. Virol.* **68**:6243-6253.
179. **Sullivan, T. D. Escalante-Alcalde, H. Bhatt, M. Anver, K. Nagashima, C. L. Stewart, and B. Burke.** 1999. Loss of A-type lamin expression compromises nuclear envelope integrity leading to muscular dystrophy. *J. Cell Biol.* **147**:913-920.
180. **Sunayama, J., Y. Ando, N. Itoh, A. Tomiyama, K. Sakurada, A. Sugiyama, D. Kang, F. Tashiro, Y. Gotoh, Y. Kuchino, and C. Kitanaka.** 2004. Physical and functional interaction between BH3-only protein Hrk and mitochondrial pore-forming protein p32. *Cell Death Diff.* **11**:771-781.
181. **Tang, Q., E. A. Murphy, and G. Maul.** 2006. Experimental confirmation of the global murine cytomegalovirus open reading frames by transcriptional detection and partial characterization of newly described gene products. *J. Virol.* **80**:6873-6882.
182. **Thale, R., U. Szepan, H. Hengel, G. Geginat, P. Lucin, and U. H. Koszinowski.** 1995. Identification of the mouse cytomegalovirus genomic region affecting major histocompatibility complex class I molecule transport. *J. Virol.* **69**:6098-6105.

## F. References

183. **Tifft, K. E., M. Segura-Totten, K. K. Lee, K. L. Wilson.** 2006. Barrier-to-autointegration factor-like (BAF-L): A proposed regulator of BAF. *Exp. Cell Res.* **312**: 478 – 487.
184. **Tran, E. J., and S. R. Wentz.** 2006. Dynamic nuclear pore complexes: life on the edge. *Cell* **125**:1041-1053.
185. **Varnum, S. M., D. N. Streblow, M. E. Monroe, P. Smith, K. J. Auberry, L. Pasa-Tolic, D. Wang, D. G. Camp, K. Rodland, S. Wiley, W. Britt, T. Shenk, R. D. Smith, and J. A. Nelson.** 2004. Identification of proteins in human cytomegalovirus (HCMV) particles: the HCMV proteome. *J. Virol.* **78**:10960-10966.
186. **Vlcek, S. B. Korbei, and R. Foisner.** 2002. Distinct functions of LAP2 $\alpha$ 's unique C-terminus in cell proliferation and nuclear assembly. *J. Biol. Chem.* **277**:18898-18907.
187. **Wagner, M., S. Jonjic, U. H. Koszinowski, and M. Messerle.** 1999. Systematic excision of vector sequences from the BAC-cloned herpesvirus genome during virus reconstitution. *J. Virol.* **73**:7056-7060.
188. **Wagner, M.** 2000. Entwicklung von Mutageneseverfahren für klonierte Cytomegalovirusgenome. Dissertation.
189. **Wagner, M., A. Gutermann, J. Podlech, M.J. Reddehase, U.H. Koszinowski.** 2002. Major histocompatibility complex class I allele-specific cooperative and competitive interactions between immune evasion proteins of cytomegalovirus, *J. Exp. Med.* **196**:805–816.
190. **Wagner, M., D. Michel, P. Schaarschmidt, B. Vaida, S. Jonjic, M. Messerle, T. S. Mertens, and U. H. Koszinowski.** 2000. Comparison between human cytomegalovirus pUL97 and murine cytomegalovirus (MCMV) pM97 expressed by MCMV and vaccinia virus: pM97 does not confer ganciclovir sensitivity. *J. Virol.* **74**: 10729–10736.
191. **Wagner, M. and U. H. Koszinowski.** 2004. Mutagenesis of viral BACs with linear PCR fragments (ET recombination). *Methods Mol. Biol.* **256**:257-268.
192. **Wagner, M., Z. Ruzsics, and U. H. Koszinowski.** 2002. Herpesvirus genetics has come of age. *Trends Microbiol.* **10**:318-324.
193. **Weber, K., U. Plessmann, and P. Traub.** 1989. Maturation of nuclear lamin A involves a specific carboxy-terminal trimming, which removes the polyisoprenylation site from the precursor; implications for the structure of the nuclear lamina. *FEBS Lett.* **257**:411-414.
194. **Welte, M. A.** 2004. Bidirectional transport along microtubules. *Curr. Biol.* **14**:R525-37.



## F. References

195. **Wild, P., M. Engels, C. Senn, K. Tobler, U. Ziegler, E. Schranker, E. Loepfe, M. Ackermann, M. Mueller, and P. Walther.** 2005. Impairment of nuclear pores in bovine herpesvirus 1-infected MDBK cells. *J. Virol.* **79**:1071–1083.
196. **Wilhelmsen, K., S. H. M. Litjens, I. Kuikman, N. Tshimbalanga, H. Janssen, I. van den Bout, K. Raymond, and A. Sonnenberg.** 2006. Nesprin-3, a novel outer nuclear membrane protein, associates with the cytoskeletal linker protein plectin. *J. Cell Biol.* **171**:799-810.
197. **Wilkie, G. S., and E. C. Schirmer.** 2006. Guilt by association: the nuclear envelope proteome and disease. MCP papers in press. Published on June 21, 2006 as manuscript R600003-MCP200.
198. **Wilkinson, D. E., and S. K. Weller.** 2004. Recruitment of cellular recombination and repair proteins to sites of herpes simplex virus type 1 DNA replication is dependent on the composition of viral proteins within prereplicative sites and correlates with the induction of the DNA damage response. *J. Virol.* **78**:4783-96.
199. **Wilkinson, D. E., and S. K. Weller.** 2003. The role of DNA recombination in herpes simplex virus DNA replication. *IUBMB Life* **55**:451-458.
200. **Wolfstein, A., C. H. Nagel, K. Radtke, K. Döhner, V. J. Allan, and B. Sodeik.** 2006. The inner tegument promotes herpes simplex virus capsid motility along microtubules in vitro. *Traffic* **7**:227–237.
201. **Worman, H. J.** 2005. Inner nuclear membrane and signal transduction. *J. Cell. Biochem.* **96**:1185–1192.
202. **Worman, H. J., C. D. Evans, and G. Blobel.** 1990. The lamin B receptor forms the nuclear envelope inner nuclear membrane: a polytopic protein with eight potential transmembrane domains. *J. Cell Biol.* **111**:1535-1542.
203. **Worman, H. J., and J. C. Courvalin.** 2002. The nuclear lamina and inherited disease. *TRENDS Cell Biol.* **12**:591-598.
204. **Ye, G. J. and B. Roizman.** 2000. The essential protein encoded by the UL31 gene of herpes simplex virus 1 depends for its stability on the presence of UL34 protein. *Proc. Natl. Acad. Sci. U. S. A.* **97**:11002-11007.
205. **Ye, Q., and H. J. Worman.** 1994. Primary structure analysis and lamin B and DNA binding of human LBR, an integral protein of the nuclear envelope inner membrane. *J. Biol. Chem.* **269**:11306-11311.
206. **Zastrow, M. S., S. Vlcek, and K. L. Wilson.** 2004. Proteins that bind A-type lamins: integrating isolated clues. *J. Cell Sci.* **117**:979-987.



## F. References

---

207. **Zhen, Y. Y., T. Libotte, M. Munck, A. A. Noegel, and E. Korenbaum.** 2002. NUANCE, a giant protein connecting the nucleus and cytoskeleton. *J. Cell Sci.* **115**:3207-3222.
208. **Ziegler, H. W. Muranyi, H. G. Burgert, E. Kremmer, and U. H. Koszinowski.** 2000. The luminal part of the murine cytomegalovirus glycoprotein gp40 catalyzes the retention of MHC class I molecules. *EMBO J.* **19**:870-881.
209. **Ziegler, H. R. Thale, P. Lucin, W. Muranyi, T. Flohr, H. Hengel, H. Farrell, W. Rawlinson, and U. H. Koszinowski.** 1997. A mouse cytomegalovirus glycoprotein retains MHC class I complexes in the ERGIC/cis-Golgi compartments. *Immunity* **6**:57-66.

## G. Supplementary information

### 1. Abbreviations

A	adenine
aa	amino acid(s)
Ab	antibody
Amp	ampicillin
APS	ammonium persulfate
$\beta$ -ME	$\beta$ -mercapto-ethanol
BAC	Bacterial artificial chromosome
BAF	barrier-to autointegration factor
bp	base pair(s)
BSA	bovine serum albumin
$^{\circ}$ C	degree celsius
C	cytosine
Cam	chloramphenicol
Ci	curie
cm	centimeter
CMV	cytomegalovirus
Co-IP	co-immuno precipitation
CR	conserved region
Croma	Croatia monoclonal antibody
Da	Dalton
dd	deionized distilled
DMEM	Dulbecco's modified Eagle medium
DMSO	dimethylsulfoxid
DN	dominant negative
DNA	desoxyribonucleid acid
dNTP	desoxynucleotide
DTT	1,4 dithiotreitol
E. coli	Escherichia coli
e.g.	exempli gratia (Lat.=for instance)

## G. Supplementary information

---

EBV	Epstein-Barr virus
EDTA	ethylenediamine tetraacetic acid
EGFP	enhanced green fluorescent protein
ER	endoplasmic reticulum
et al.	Et alii (Lat.=and others)
EtOH	ethanol
FCS	fetal calf serum
Fig	figure
FITC	fluoresceinisocyanat
FLP	flippase
FRT	FLP recognition target
G	guanine
GFP	green fluorescent protein
gp	glycoprotein
h	hour(s)
HA	hemagglutinin-tag
HCMV	human CMV
HSV	herpes simplex virus
i	insertion mutant(s)
INM	inner nuclear membrane
kan	kanamycine
kb	kilo bases
kg	kilogram
l	liter
LB	Luria-Bertani medium
lg	logarithm with basis 10
M	molarity
MCMV	mouse CMV
MEF	murine embryonal fibroblasts
min	minute(s)
ml	milliliter
mM	millimolar
MOI	multiplicity of infection

## G. Supplementary information

---

n.a.	not applicable
NE	nuclear envelope
NEC	nuclear egress complex
NLS	nuclear localization signal
N	nanometer
OD	optical density
ON	over night
ONM	outer nuclear membrane
ORF	open reading frame
p.i.	post infection
PAA	phosphonoacetic acid
PAGE	polyacrylamide-gel electrophoresis
PBS	phosphate buffered saline
PCR	polymerase chain reaction
Pen./ Strep.	penicillin/ streptomycin
PFU	plaque forming unit
PrV	pseudorabies virus
RNA	ribonucleic acid
rpm	rounds per minute
RPMI	Roswell Park Memorial Institute
RT	room temperature
s	stop mutant(s)
SDS	sodiumdodecylsulfate
ST	strep-II-tag
SV40	simian virus 40
T	thymine
tab.	Table
TAE	Tris-acetate-EDTA
TBST	Tris buffered saline with Tween 20
TE	Tris/EDTA
TEMED	N, N, N', N'-tetramethylenediamine
TCID	tissue culture infective dose
TM	transmembrane region

## G. Supplementary information

---

TR	texas red
Tris	Tris(hydroxymethyl)aminomethan
U	unit(s), enzyme activity
V	volt
v/v	volume/ volume
VZV	Varicella Zoster virus
w/v	weight/ volume
wt	wild type
μ	micro (10 <sup>-6</sup> )
μg	microgram
μl	microliter
μm	micrometer
zeo	zeocin

### Amino acids

A, Ala	alanine
C, Cys	cysteine
D, Asp	aspartic acid
E, Glu	glutamic acid
F, Phe	phenylalanine
G, Gly	glycine
H, His	histidine
I, Ile	isoleucine
K, Lys	lysine
L, Leu	leucine
M, Met	methionine
N, Asn	asparagine
P, Pro	proline
Q, Gln	glutamine
R, Arg	arginine
S, Ser	serine
T, Thr	threonine
V, Val	valine
W, Trp	tryptophan
Y, Tyr	tyrosine

## G. Supplementary information

### 2. List of figures

<b>Figure 1.</b> Structure of a herpesvirus virion.....	6
<b>Figure 2.</b> Herpesvirus replication.....	9
<b>Figure 3.</b> Schematic diagram of the nuclear envelope showing nuclear membranes, nuclear pore complex, nuclear lamina and chromatin structures.....	10
<b>Figure 4.</b> Herpesvirus assembly and egress from the nucleus.....	16
<b>Figure 5.</b> Schematic diagram of the M50/p35 and M53/p38 localization within the MCMV genome.....	17
<b>Figure 6.</b> Proposed working model for egress of MCMV capsids from the nucleus-the MCMV-nuclear egress complex (NEC).....	19
<b>Figure 7.</b> Analysis of the essential MCMV gene M53.....	20
<b>Figure 8.</b> Schematic representation of M53 inserted into the expression vector pO6R6k-zeo-ie.....	28
<b>Figure 9.</b> General principle of a random mutagenesis of an essential viral gene.....	47
<b>Figure 10.</b> Re-insertion of mutated plasmids into the viral genome.....	50
<b>Figure 11.</b> Virus-reconstitution.....	51
<b>Figure 12.</b> Determination of proper MOI for infection experiments.....	69
<b>Figure 13A.</b> Expression kinetics of M53/p38.....	70
<b>Figure 13B.</b> Expression kinetics of M53/p38.....	70
<b>Figure 14A.</b> Sub-cellular localization of M53/p38 and M50/p35.....	71
<b>Figure 14B.</b> Subcellular localization of M53/p38 and M50/p35.....	72
<b>Figure 15.</b> Co-immunoprecipitation of M53/p38 and M50/p35.....	73
<b>Figure 16.</b> Pull down assay of M53/p38 with Strep tagged M50/p35.....	75
<b>Figure 17.</b> Ectopic rescue of the M53 deletion mutant.....	77
<b>Figure 18A-D.</b> Construction of an insertion mutant library of the M53 ORF.....	80
<b>Figure 18E.</b> Principle of random transposon insertion mutagenesis.....	81
<b>Figure 19.</b> Analysis of 498 M53 insertion mutants.....	82
<b>Figure 20.</b> Analysis of M53 insertion mutants by ectopic cis-complementation of $\Delta$ M53-BAC..	83
<b>Figure 21.</b> M53 mutants and their ability to rescue virus growth of the $\Delta$ M53 genome.....	84
<b>Figure 22.</b> Functional analysis of N-terminal deletion mutants of M53.....	86
<b>Figure 23A.</b> Analysis of the interaction of M53 stop mutants with M50/p35.....	88
<b>Figure 23B and C.</b> Analysis of the interaction of M53 stop- and N-terminal deletion mutants with M50/p35.....	89
<b>Figure 24A.</b> Co-immunoprecipitation of M53 stop mutants and M50/p35.....	91
<b>Figure 24B and C.</b> (B) Co-immunoprecipitation of M53 N-terminal deletion mutants and M50/p35 (C) Pull down assay of M53 stop mutants with Strep tagged M50/p35.....	92
<b>Figure 25A.</b> Analysis of the interaction of M53 insertion mutants with M50/p35.....	93
<b>Figure 25B.</b> Pull down analysis of M53 insertion mutants with Strep tagged M50/p35.....	94
<b>Figure 26.</b> Functional analysis of M53 point mutants.....	96

## G. Supplementary information

<b>Figure 27A.</b> Pull down analysis of 12 M53 point mutants with Strep-tagged M50/p35.....	97
<b>Figure 27B.</b> Rescue of $\Delta$ M53-BAC by M53 point mutants K128A, Y129A and L130A.....	98
<b>Figure 28A.</b> Functional analysis of M53 point-and deletion mutants .....	100
<b>Figure 28B and C.</b> Analysis of the interaction of M50/p35 with M53 point- and N-terminal deletion mutants .....	100
<b>Figure 29.</b> Analysis of oligomerization of M53/p38 .....	101
<b>Figure 30.</b> Co-immunoprecipitation of M53/p38 and M50/p35 under increasing salt conditions. ....	103
<b>Figure 31.</b> Cellular lamins and M53/p38 are retained in a salt resistant compartment of the cell. ....	105
<b>Figure 32.</b> Pull down of LBR with Strep tagged M50/p35 .....	106
<b>Figure 33A.</b> HA-pull down analysis .....	108
<b>Figure 33B.</b> Flag-tag pull down analysis. ....	109
<b>Figure 33C.</b> LBR pull down using HA-tagged M50/p35 .....	110
<b>Figure 33D.</b> LBR pull down using Flag-tagged M53/p38 .....	111
<b>Figure 34A.</b> Pull down analysis of cellular interaction partners using HA-tagged M50/p35 ....	112
<b>Figure 34B.</b> Pull down analysis of cellular interaction partners using Flag-tagged M53/p38 ..	113
<b>Figure 35.</b> Analysis of cellular interaction partners of M53/p38 and M50/p35 by silver staining and mass-spectrometry.....	115
<b>Figure 36A.</b> Peptide elution after pull down analysis using HA-tagged M50/p35 .....	117
<b>Figure 36B.</b> Peptide elution after pull down analysis using Flag-tagged M53 .....	117
<b>Figure 37.</b> Schematic diagram of possible cellular interaction partners of M50/p35 and M53/p38. ....	127

### 3. List of tables

<b>Table 1.</b> BACs constructed during this study.....	30
<b>Table 2.</b> Cell lines used during this work.....	48
<b>Table 3.</b> Transposon donor- and acceptor combinations used in this study.....	78



G. Supplementary material

**4. Primers used in this study**

<sup>a</sup>The recognition sequences of restriction endonuclease are underlined.

<b>Primer name</b>	<b>5' to 3' sequence<sup>a</sup></b>
<b>ieST1</b>	TCGAGCGCTTGGTCCCACCCCCAGTTCGAGAAGTAGGG GCC
<b>ieST2</b>	CCTACTTCTCGAACTGGGGGTGGGACCAAGCGC
<b>M50Strep</b>	GTGT <u>GCTCGAG</u> GGGATGACCCGCCGAACG
<b>5'-M53del</b>	AGCCCGGAGGGAGAGGAACGGGACGCCGCCGACCGAG AAGAGGACGATTTATTCAACAAAGCCACG
<b>3'-M53del</b>	TATCAATAAAATACAACGTTGAACGACAGTCTCACACTGT GTGCCTCGTCAGCCAGTGTTACAACCAATTAACC
<b>5'-AB6-02</b>	CGC <u>GGTACC</u> ATGTTTAGGAGC
<b>3'-AB7-02</b>	CGC <u>GGATCCT</u> CACAACGAGTA
<b>5'-SapI-delIN</b>	TCTCGCTCTT <u>CCTTCTT</u> CTTGGGCACACCGGTTCCGGTCG GCGGCGTCCCGT
<b>3'-NdeI-SapI</b>	GTGTGGCTCTT <u>CAGA</u> AAGAGGAAAGTCTCCACCGGTGAGT ATCTGAACGTGAAGC
<b>Flag1</b>	CATGGATTACAAGGATGACGACGATAAGTTTAGGAGCCC GGAGGGAGAGGAACGGGACGCCGCCGA
<b>Flag2</b>	CGGTCGGCGGGCGTCCCGTTCCTCTCCCTCCGGGCTCCT AACTTATCGTCGTCATCCTTGTAATCCATGGTAC
<b>NLS21</b>	CCGGTGTGCCCAAGAAGAAGAGGAAAGTCTCCACCGGC AT
<b>NLS22</b>	CATGATGCCGGTGGAGACTTTCCTCTTCTTCTTGGGCAC A
<b>Mutfor-</b>	
<b>-5'L112A</b>	GGGGG <u>GCTCTTCCG</u> CCCATGACGTGTTTCAGAGACAT
<b>-5'H116A</b>	GGGGG <u>GCTCTTCCG</u> CCGACGTGTTTCAGAGACA
<b>-5'F119A</b>	GGGGG <u>GCTCTTCCG</u> CTCAGAGACATCCCGACCTC
<b>-5'P123A</b>	GGGGG <u>GCTCTTCCG</u> CCGACCTCGAACAGAAGTAC

G. Supplementary material

<b>Primer name</b>	<b>5' to 3' sequence<sup>a</sup></b>
-5'D124A	GGGGG <u>CTCTTCC</u> GCTCTCGAACAGAAGTACCTC
-5'L125A	GGGGG <u>CTCTTCC</u> GCCGAACAGAAGTACCTCAAG
-5'E126A	GGGGG <u>CTCTTCC</u> GCGCAGAAGTACCTCAAGATC
-5'K128A	GGGGG <u>CTCTTCC</u> GCCTACCTCAAGATCATGAAG
-5'Y129A	GGGGG <u>CTCTTCC</u> CAGCGCTCAAGATCATGAAGCT
-5'L130A	GGGGG <u>CTCTTCC</u> GCCAAGATCATGAAGCTAC
-5'YL129,130A	GGGGG <u>CTCTTCC</u> GCCAAGATCATGAAGCTACCG
-5'KYL128-130A	GGGGG <u>CTCTTCC</u> GCGGCCAAGATCATGAAGCTACCG
-5' Delmo108-136	GGGGG <u>CTCTTCC</u> GCCAAGATCATGAAGCTACCG
-5'M133A	GGGGG <u>CTCTTCC</u> GCCAAGCTACCGATCACGGGC
-5'I137A	GGGGG <u>CTCTTCC</u> CACCGGTAAGGAGTCGATCCGACTC
<b>Mutrev-</b>	
-3'L112A	GGGGG <u>CTCTTCC</u> GGCCTCAGAGAGCTTCACGTT
-3'H116A	GGGGG <u>CTCTTCC</u> GCGAGCTCAGAGAGCTTCACG
-3'F119A	GGGGG <u>CTCTTCC</u> CAGCCACGTCGTGAAGCTCAGA
-3'P123A	GGGGG <u>CTCTTCC</u> GGCATGTCTCTGAAACACGTC
-3'D124A	GGGGG <u>CTCTTCC</u> CAGCGGGATGTCTCTGAAACAC
-3'L125A	GGGGG <u>CTCTTCC</u> GCGGTCCGGATGTCTCTGAAACACG
-3'E126A	GGGGG <u>CTCTTCC</u> GCAAGGTCGGGATGTCTCTG
-3'K128A	GGGGG <u>CTCTTCC</u> GGCCTGTTGAGGTCGGGATG
-3'Y129A	GGGGG <u>CTCTTCC</u> GCTTTCTGTTGAGGTCGGGA
-3'L130A	GGGGG <u>CTCTTCC</u> GCGTACTTCTGTTGAGGTC
-3'YL129,130A	GGGGG <u>CTCTTCC</u> GCGGCTTTCTGTTGAGGTC

G. Supplementary material

<b>Primer name</b>	<b>5' to 3' sequence<sup>a</sup></b>
-3' KYL128-130A	GGGGG <u>CTCTT</u> CCGCGGCCTGTTTCGAGGTCTGGGATG
-3' Delmo108-136	GGGGG <u>CTCTT</u> CCGGCCTCAGAGAGCTTCACGTT
-3' M133A	GGGGG <u>CTCTT</u> CCGGCGATCTTGAGGTA
-3' 1137A	GGGGG <u>CTCTT</u> CCGGTGGCCGGTAGCTTCATGATCTT
<b>AB6-SpAs</b>	GGG <u>ACTAGTGGCGCGCC</u> GGTACCATGTTTAGGAGC
<b>M53rev</b>	AGAGGTCCAGGCACGTGTG

## **5. Publications**

Parts of this work were already published or prepared for publication:

**Mark Lötzerich, Zolt Ruzsics and Ulrich H. Koszinowski.**

Functional domains of murine cytomegalovirus nuclear egress protein M53/p38.  
J. Virol., Jan. 2006, Vol. **80** (1):73-84.

**Anja Bubeck, Markus Wagner, Zsolt Ruzsics, Mark Lötzerich, Margot Iglesias, R. Singh, and Ulrich H. Koszinowski.**

Comprehensive mutational analysis of a herpesvirus gene in the viral genome context reveals a region essential for virus replication.  
J. Virol., Aug. 2004, Vol. **78** (15):8026-8035.

**Brigitte Rupp, Christopher Buser, Mirela Popa, Anja Bubeck, Mark Lötzerich, Paul Walther, and Ulrich H. Koszinowski.**

A screen for dominant-negative mutants of essential viral genes.  
2006, in preparation.

### Other publications

**Löms Ziegler-Heitbrock, Mark Lötzerich, Annette Schaefer, Thomas Werner, Marion Frankenberger, and Elke Benkhart.**

IFN- $\alpha$  induces the human IL-10 gene by recruiting both IFN regulatory factor 1 and Stat3.  
J. Immunol., 2003, **171**:285–290.

**6. Posters and oral presentations**

**28th International Herpesvirus Workshop 2003, Madison, USA.**

*Poster presentation:* Characterization of the essential murine cytomegalovirus protein M53/p38.

**2nd Workshop study group in the society for virology The cell biology of viral infections 2003, Zeilitzheim, Germany.**

*Oral presentation:* Characterization of the essential murine cytomegalovirus protein M53/p38.

**Annual Meeting of the “Gesellschaft für Virologie”, 2004, Tübingen, Germany.**

*Poster presentation:* Comprehensive mutagenesis of the essential murine cytomegalovirus protein M53/p38.

**Annual Meeting of the “Gesellschaft für Virologie”, 2005, Hannover, Germany.**

*Poster presentation:* Comprehensive mutagenesis of the essential mouse CMV protein M53/p38.

**30th International Herpesvirus Workshop 2005, Turku, Finland**

*Oral presentation:* Mapping functional domains of the murine cytomegalovirus nuclear egress protein M53/p38.

**Annual Meeting of the “Gesellschaft für Virologie”, 2006, München, Germany**

*Poster presentation:* Screening for dominant-negative mutants of the nuclear egress protein M53/p38.

## **7. Acknowledgements**

This work was supported by the Deutsche Forschungsgemeinschaft through SFB 455 "Viral functions and immune modulation".

I would like to thank some persons who made this work possible:

First of all I want to thank Prof. Ulrich Koszinowski for giving me the possibility to join his research group, for his supervision and for his constructive criticism and motivation.

I would like to thank PD Dr. Bettina Kempkes for outstanding supervision and helpful discussions all over the time.

Special thanks for my supervisor Dr. Zolt Ruzsics for his brilliant ideas and enthusiasm, motivation, lots of productive discussions and his extraordinary patience.

Moreover, I want to thank our cooperation partners Dr. Arnd Kieser and especially Dr. Thomas Knöfel for helping me with the mass-spectrometric analysis of the NEC complex.

Furthermore, I want to thank Simone Boos for the excellent technical assistance.

I further want to thank all my colleagues of the AG Koszinowski and AG Conzelmann and the colleagues (present and ex-) from the Gene Center for the nice scientific and social environment.

Special thanks to Dr. Zolt Ruzsics and Dr. Detlef Apelt, who have patiently helped me by critically reading and correcting this thesis.

A big "THANK YOU" to all my friends who were next to me during the years of my PhD work and their support.

Finally, I thank my parents, my brother and Kerstin for their care, support, encouragement and love.

**8. Ehrenwörtliche Versicherung**

Hiermit versichere ich, dass ich die vorliegende Arbeit selbstständig angefertigt habe. Es wurden keine anderen als die angegebenen Hilfsmittel und Quellen verwendet. Ich habe weder anderweitig versucht, eine Dissertation einzureichen oder eine Doktorprüfung durchzuführen, noch habe ich diese Dissertation oder Teile derselben einer anderen Prüfungskommission vorgelegt.

München, 28. März 2007



---

Mark Lötzerich



## **9. Curriculum vitae**

### **Personal data:**

Name: Mark Lötzerich

Date of birth: 31.08.1972

Place of birth: Kassel, Germany

Nationality: German

### **Education:**

06/2002-present: **Max von Pettenkofer Institute, LMU, Munich, Germany.**  
Doctoral thesis, "Analysis of the nuclear egress complex of mouse cytomegalovirus". Supervisors: Prof. Dr. U.H. Koszinowski and PD. Dr. B. Kempkes.

11/1999-08/2000: **Institute for Immunology, LMU, Munich, Germany.**  
Diploma thesis, "The role of IRF-1 and Stat3 for the regulation of the human interleukin 10-promotor". Supervisors: Prof. Dr. L. H. W. Ziegler-Heitbrock and Prof. Dr. E. Weiss.

10/1993-08/2000: **Ludwig-Maximilians-University, Munich, Germany.**  
Study of biology. Degree: Diplom Biologe Univ. (Certified-biologist univ.), Subjects: Molecular biology, biochemistry, pharmacology/ toxicology, microbiology.

07/1992: **Gymnasium Geretsried, Geretsried, Germany.**  
Abitur (equivalent to A-levels) with the main subjects chemistry and history.

## G. Supplementary material

---

### Practical trainings and work experience:

- 05/2001-10/2001: **Institute for Neuropathology, LMU, Munich, Germany.**  
Scientific assistant in the group of Prof. Dr. H. A. Kretzschmar.
- 09/2000-04/2001: **Institute for Immunology, LMU, Munich, Germany and Institute for Inhalation biology, GSF, Gauting, Germany.**  
Scientific assistant in the group of Prof. Dr. L. H. W. Ziegler-Heitbrock.
- 05/1999-07/1999: **Max-Planck-Institute for evolutionary anthropology, Leipzig, Germany.**  
Practical work experience in the group of Prof. Dr. S. Pääbo.
- 04/1999: **Institute for Human genetics, University of Würzburg, Würzburg, Germany.**  
Practical course of cell analytics: FACS analysis.  
Supervisor: Prof. Dr. M Kubbies.
- 12/1998-04/1999: **Institute for Pharma-onkology of Roche diagnostics GmbH, Penzberg, Germany.**  
Practical work experience in the group of Prof. Dr. M. Kubbies.
- 09/1997-11/1997: **Max-Planck-Institute for Biochemistry, Munich, Germany.**  
Practical work experience in different groups (protein research, virology, molecular biology, neurology and cell biology). Supervisor: Prof. Dr. Dr. W. J. Neubert.